CORRELATION AND PREDICTION OF THE PHYSICAL AND EXCESS PROPERTIES OF THE IONIC LIQUID 1-BUTYL-3-METHYLIMIDAZOLIUM METHYL SULPHATE WITH SEVERAL ALCOHOLS AT *T* = (298.15 TO 313.15) K.

SANGEETA SINGH

Submitted in fulfilment of the academic requirements for the

MASTERS DEGREE IN TECHNOLOGY

Durban University of Technology, Chemistry Department,

Durban, South Africa.

2013

PREFACE

The work described in this thesis was performed by the author under the supervision of Professor N. Deenadayalu at Durban University of Technology, Durban, South Africa, from 2011-2012. The study presents original work by the author and has not been submitted in any form to another university. Where use is made of the work of others, it has been clearly stated in the text.

Signed: Date:

Sangeeta Singh

Signed: Date:

Prof. N. Deenadayalu (Supervisor)

ACKNOWLEDGEMENTS

I would like to express my sincere gratitude to the:

- Durban University of Technology for an M.Tech. Scholarship and for giving me the opportunity to undertake my research at the institution. The National Research Foundation (SA), for financial support for the purchase of the DSA 5000 M instrument.
- Almighty God, who always gives me strength.

I deem it a great pleasure to express my deep sense of gratitude and indebtedness to my venerable supervisor **Prof. N. Deenadayalu,** Professor, and **Dr. Indra Bahadur,** Post Doctoral Fellow, Department of Chemistry, Durban University of Technology, Durban, South Africa, for introducing me to the *World of Chemical Thermodynamics,* inspiring guidance, valuable suggestions, and constant encouragement throughout the period of this research work. I am also thankful of Ms. **Indira Khiramen** of housing department for providing me good accommodation during my M.Tech studies.

My sincere thanks to the Head of Department of Chemistry, Durban University of Technology, Durban, South Africa, for providing the facilities to carry out the present work.

ABSTRACT

The thermodynamic properties of binary liquid mixtures using an ionic liquid (IL) with alcohols were determined at different temperatures. The ionic liquid used was 1-butyl-3-methylimidazolium methylsulphate $[BMIM]^+[MeSO_4]^-$. Densities, speed of sound, and refractive indices for the binary mixtures ($[BMIM]^+[MeSO_4]^-$ + methanol, or 1-propanol, or 2-propanol, or 1-butanol) were experimentally measured over the whole range of composition at T = (298.15, 303.15, 308.15, and 313.15) K. From the experimental data, excess molar volumes, V_m^E, isentropic compressibilities, κ_s, excess isentropic compressibilities, κ_S^E, deviations in refractive indices, Δn, and molar refractions, R, were calculated. The excess partial molar volumes were also calculated at T = 298.15 K.

For the binary systems, ($[BMIM]^+[MeSO_4]^-$ + methanol, or 1-propanol, or 2-propanol, or 1-butanol) V_m^E and κ_S^E are always negative and V_m^E decrease slightly when the temperature increases. The refractive index deviation at T = (298.15, 303.15, 308.15, and 313.15) K is positive over the whole composition range. The measured negative values for excess molar volume of these mixtures ($[BMIM]^+[MeSO_4]^-$ + methanol, or 1-propanol, or 2-propanol, or 1-butanol) indicate strong ion-dipole interactions and packing between alcohols and IL are present.

The Redlich-Kister smoothing polynomial equation was satisfactorily applied for the fitting of the V_m^E, κ_S^E, and Δn data to give the fitting parameters and the root-mean-square deviations. The Lorentz-Lorenz (L-L) equation was also used to correlate the volumetric property and predict the density or refractive index of the binary mixtures of ionic liquid and the organic solvents. The Lorentz-Lorenz approximation gives a higher σ when used to correlate the

excess molar volumes for the mixtures ($[BMIM]^+[MeSO_4]^-$ + methanol, or 1-propanol, or 2-propanol, or 1-butanol). The L-L equation gives good results for the prediction of density and refractive index. The results are discussed in terms of solute-solute, solute-solvent and solvent-solvent interactions.

CONTENTS **Page**

List of Tables

List of Figures

List of symbols

ρ = density ($g \cdot cm^{-3}$).

V_m = molar volume ($cm^3 \cdot mol^{-1}$).

V_m^{id} = ideal molar volume ($cm^3 \cdot mol^{-1}$).

$\Delta V_{m,f}$ = molar free volume ($cm^3 \cdot mol^{-1}$).

V_m^E = excess molar volume ($cm^3 \cdot mol^{-1}$).

$V_{m,1}$ = molar volume of the first component ($cm^3 \cdot mol^{-1}$).

$V_{m,1}^*$ = molar volume of the pure IL ($cm^3 \cdot mol^{-1}$).

$V_{m,2}^*$ = molar volume of the pure alcohols ($cm^3 \cdot mol^{-1}$).

$V_{m,1}^E$ = excess partial molar volume for the IL ($cm^3 \cdot mol^{-1}$).

$V_{m,2}^E$ = excess partial molar volume for an alcohol ($cm^3 \cdot mol^{-1}$).

T = temperature (K).

x_1 = mole fraction of the 1st component.

x_2 = mole fraction of the 2nd component.

σ = standard deviation.

α = mean molecular polarizability (cm^3).

ε_0 = permittivity of vacuum ($F \cdot m^{-1}$).

Φ_1 = volume fraction of IL.

M_1 = molar mass of ionic liquid ($g \cdot mol^{-1}$).

M_2 = molar mass of alcohol ($g \cdot mol^{-1}$).

A_i = polynomial coefficient.

N = polynomial degree.

n = number of experimental points.

N_A = Avogadro's number (mol^{-1}).

k = number of coefficients used in the Redlich-Kister correlation.

u = speed of sound ($m \cdot s^{-1}$).

κ_s = isentropic compressibility (Pa^{-1}).

κ_S^E = excess isentropic compressibility (Pa^{-1}).

Δn = refractive index deviation.

n^{id} = ideal refractive index.

R = molar refraction.

R^{id} = ideal molar refraction.

n = refractive index of mixture.

n_1 = refractive index of 1st component.

n_2 = refractive index of 2nd component.

CHAPTER 1

INTRODUCTION

Whatever you are doing, Put your whole mind on it. If you are shooting, your mind should be only on the target. Then you will never miss. If you are learning your lessons, think only of the lesson.

Swami Vivekananda

Founder of Ramakrishna Mission.

1.1 DEFINITION OF IONIC LIQUIDS

An ionic liquid (IL) is a salt in the liquid state. In some contexts, the term has been restricted to salts whose melting point is below 373.15 K (Vercher *et al*. 2007; González *et al.* 2007). ILs are largely made of ions and short-lived ion pairs (Andreatta *et al.* 2009; González *et al.* 2006) and referred to as ionic melts, ionic fluids, fused salts, liquid salts, or ionic glasses. ILs consists of a cation and anion and are held together by columbic forces.

1.2 HISTORY OF IONIC LIQUIDS

The date of discovery of the "first" ionic liquid is disputed, along with the identity of its discoverer. Ethanolammonium nitrate (m.p. 325.15–328.15 K) was reported in 1888 by S. Gabriel and J. Weiner (Gabriel and Weiner 1888). One of the earliest room temperature ionic liquids was ethylammonium nitrate (m.p. 285.15 K), synthesized in 1914 by Paul Walden (Walden 1914). In the 1970s and 1980s ionic liquids based on alkyl-substituted imidazolium and pyridinium cations, with halide or trihalogenoaluminate anions, were initially developed for use as electrolytes in battery applications (Chum *et al.* 1975; Wilkes *et al.* 1982). The usefulness of the imidazolium halogenoaluminate salts is that their viscosity, melting point, and acidity could be adjusted by changing the alkyl substituents and the imidazolium/pyridinium and halide/halogenoaluminate ratios (Gale and Osteryoung 1979). Two major drawbacks for some applications were moisture sensitivity and acidity/basicity. In 1992, Wilkes and Zawarotko obtained ionic liquids with weakly coordinating anions such as hexafluorophosphate and tetrafluoroborate allowing a much wider range of applications (Wilkes and Zaworotko 1992).

1.3 IMPORTANCE OF IONIC LIQUIDS

The ionic liquids (ILs) completely composed of ions have many unique physicochemical properties, such as a broad liquid range, negligible vapour pressure, and high thermal stability. They have been widely used as green solvents replacing traditional organic solvents in separation science (Shao *et al* 2012). ILs have attracted considerable attention because of their unique physical and chemical properties, including non volatility, thermal stability, and reusability. Particularly, ILs has controlled miscibility, which results in many possible combinations of cations and anions and allows a large variety of interactions and applications (Yao *et al* 2012). Over the last decade ionic liquids have achieved much attention and are not any longer just a class of esoteric compounds, but are proving to be valuable and

useful in a multitude of different applications (Weyershausenand and Lehmann 2005). Room temperature ionic liquids (RTILs) are a relatively new class of compound usually defined as having a melting point at or below room temperature, although the exact maximum limit of melting point in the definition of both ionic liquids and RTILs is sometimes extended upward (Fletcher *et al.* 2010). Another important feather on the cap of ILs is the ability of their molecular structure to be tailored according to application requirements. This has spurred the rise of task-specific ionic liquids, or the so-called functionalized ionic liquids (Feng *et al.* 2010). RTILs are viewed as a novel class of green, benign solvents, which promise widespread application in industry, possibly replacing currently used organic solvents (Najdanovic-Visak *et al.* 2002). ILs are considered as an attractive alternative to replace classic organic solvents, leading to a more sustainable and environmentally friendly chemical industry, especially with respect to air emissions. Their specific properties, especially their negligible vapour pressure under normal conditions and their ability to solubilize a wide variety of compounds, have originated an enormous interest by the scientific community and industry; gradually, more and more researchers, use their knowledge and resources to explore new applications for these compounds such as their use as lubricants, in bioreactor technology, as electrolytes for Li-ion batteries, in synthesis of nano objects, in separation technology or in catalysis (González *et al* 2012; Alvarez *et al* 2011). These ionic liquids have been recently used as solvents in catalysis, chemical processing, liquid-liquid separations, vapour-liquid equilibria, batteries, and fuel cells investigations (Zafarani-Moattara and Shekaari 2005; Domańska *et al*. 2009). The ILs and IL-containing mixtures are involved in the development of chemical products and synthetic procedures, which are environmentally friendly and have reduced health risks with the search for more efficient methods to do chemistry (Abdulagatov *et al.* 2008). The ILs have been considered as solvents for reactions, as absorption media for gas separations, as the separating agent in extractive distillation, as heat transfer fluids, for processing biomass, and as the working fluid in a variety of electrochemical applications (batteries, capacitors, solar cells, *etc.*). Due to their unique physical and chemical properties, some of them have been used as a lubricant and in biocatalysis with great advantages (Zhong *et al.* 2007).

1. 4 INDUSTRIAL USES OF IONIC LIQUIDS

ILs have many applications, such as solvents and electrically conducting fluids (electrolytes). Salts that are liquid at near-ambient temperature are important for electric battery applications, and have been used as sealants due to their very low vapour pressure (Zhong *et al.* 2007). Any salt that melts without decomposing or vaporizing usually yields an IL. The ionic bond is usually stronger than the Van der Waals forces between the molecules of ordinary liquids. For that reason, common salts tend to melt at higher temperatures than other solid molecules. Some salts are liquid at or below room temperature. Examples include 1-ethyl-3-methylimidazolium dicyanamide, $(C_2H_5)(CH_3)C_3H_3N^+_2 \cdot N(CN)^{-2}$, that melts at 252.15 K (MacFarlane *et al.* 2001) and 1-butyl-3,5-dimethylpyridinium bromide which becomes a glass below 249.15 K (Crosthwaite *et al*. 2005). The properties of IL are summarized in table 1.1 (Johnson 2007). However, there are two main problems with ILs (i) their resistance to photodegradation and low biodegradability, turning them into persistent pollutants that break through classic treatment systems into natural waters; (ii) their expensive production costs. These facts have led to the search for a new class of ionic liquids (Alvarez *et al* 2011).

Table 1.1 Properties of Ionic Liquids.

Property	Property value
Freezing point	< 373.15 K
Liquidus range	298.15 - 473.15 K
Thermal stability	High
Viscosity	< 100 Cp
Dielectric constant	$\leq$ 30 ($F \cdot m^{-1}$)
Polarity	47 - 49
Specific conductivity	< 10 $mS \cdot cm^{-1}$
Molar conductivity	< 10 $Scm^2 \cdot mol^{-1}$
Electrochemical window	2V- 4.5V
Solvent and / or catalyst	Excellent for many organic reactions
Vapour pressure	Usually negligible

ILs find a variety of industrial applications. A few industrial uses are described below:

1.4.1 Biphasic Acid Scavenging Utilizing Ionic Liquids (BASIL)

The first major industrial IL application was the BASIL (*B*iphasic *A*cid *S*cavenging utilizing *I*onic *L*iquids) process by BASF, in which 1-alkylimidazole scavenged the acid from an existing process. This then results in the formation of an IL which can easily be removed from the reaction mixture. This increased the time yield of the reaction by a factor of 80,000 (Plechkova and Seddon 2008).

1.4.2 Cellulose processing

Cellulose is the earth's most widespread natural organic chemical and, thus, highly important as a renewable resource. But even out of nature's annual 40 billion tons output, only approx. 5% is used as feedstock for further processing. More intensive exploitation of cellulose, as a renewable feedstock, is aided by the development of suitable solvents for mechanical and chemical processing. ILs have been shown to be highly effective at solvating cellulose to technically useful concentrations (Swatloski *et al.* 2002).

1.4.3 Pharmaceuticals

Recognising that approximately 50% of commercial pharmaceuticals are organic salts, ionic liquids formed from a number of pharmaceuticals have been investigated. Combining a pharmaceutically active cation with a pharmaceutically active anion leads to a dual active ionic liquid in which the actions of two drugs are combined (Stoimenovski *et al.* 2010).

1.4.4 Gas handling

ILs have several properties that make them useful in gas storage and handling applications, including low vapour pressure, stability at high temperatures, and solvation for a wide variety of

compounds and gases. They also have weakly coordinating anions and cations which are able to stabilize polar transition states. Many ionic liquids can be reused with minimal loss of activity.

The company Air Products uses ILs instead of pressurized cylinders as a transport medium for reactive gases such as trifluoroborane, phosphine and arsine. The gases are dissolved in the liquids at or below atmospheric pressure and are easily withdrawn from the containers by applying a vacuum.

Gas manufacturer Linde exploits the low solubility of hydrogen in ILs to compress the gas up to 450 bar in filling stations by using an ionic liquid piston compressor, IL 1-butyl-3-methylimidazolium chloride has been used for separating hydrogen from ammonia borane (Karkamkar *et al.* 2007).

1.4.5 Nuclear fuel processing

The IL 1-butyl-3-methylimidazolium chloride has been investigated as a non-aqueous electrolyte media for the recovery of uranium and other metals from spent nuclear fuel and other sources (Giridhar *et al.* 2007; Rao *et al.* 2008). Protonated betaine bis(trifluoromethanesulfonyl)imide has been investigated as a solvent for uranium oxides (Rao *et al.* 2008). Ionic liquids, N-butyl-N-methylpyrrolidinium bis(trifluoromethylsulfonyl)imide and N-methyl-N-propylpiperidinium bis(trifluoromethylsulfonyl)imide, have been investigated for the electrodeposition of Europium and Uranium metals respectively (Rao *et al.* 2009; Rao *et al*. 2011).

1.4.6 Solar thermal energy

ILs have the potential to be used for heat transfer and for heat storage in solar thermal energy systems. Concentrating solar thermal facilities such as parabolic troughs and solar power towers focus the sun's energy onto a receiver which can generate temperatures of around 873.15 K (1,112 °F). This heat can then generate electricity in a steam cycle. Although nitrate salts have been the medium of choice since the early 1980s, they freeze at 493.15 K (428 °F) and thus require heating to prevent solidification.

Ionic liquids such as $[BMIM]^+[BF_4]^-$ have a more favourable liquid-phase temperature range (198.15 to 732.15 K) and could therefore be an excellent liquid thermal storage media and heat transfer fluid (Wu *et al.* 2001).

1.4.7 Food and bioproducts

The IL, 1-butyl-3-methylimidazolium chloride completely dissolves freeze dried banana pulp and with an additional 15% DMSO, (dimethyl sulfoxide) lends itself to Carbon-13 NMR analysis. In this way the entire banana complex of starch, sucrose, glucose, and fructose can be monitored as a function of banana ripening (Fort *et al.* 2006).

ILs can extract specific compounds from plants for pharmaceutical, nutritional and cosmetic applications, such as the antimalarial drug artemisinin from the plant *Artemisia annua* (Lapkin *et al.* 2006).

1.4.8. Batteries

Researchers have identified ILs that can replace water as the electrolyte in metal-air batteries. ILs are suitable because they evaporate at much lower rates than water thereby, increasing battery life by drying slower. Further, ILs have an electrochemical window of up to six volts (Armad *et al.* 2009) (versus 1.23 for water) supporting more energy-dense metals.

A metal-air battery draws oxygen through a porous ambient "air" electrode (-cathode) and produces water, hydrogen peroxide, or hydroxide anions depending on the nature oxygen reduction catalyst and electrolyte. These compounds store the electrons released by the oxidation at the anode.

1.5 THERMODYNAMIC PROPERTIES DETERMINED IN THIS WORK

In this work, the IL used was: 1-butyl-3-methylimidazolium methylsulfate, $[BMIM]^+[MeSO_4]^-$. The alcohols used in this work namely: methanol, or 1-propanol, or 2-propanol, or 1-butanol are versatile compounds that are used as solvents in chemical and technological processes, and are inexpensive, are easily available at high purity. The chosen solvents, methanol, or 1-propanol, or 2-propanol, or 1-butanol are completely miscible in $[BMIM]^+[MeSO_4]^-$ and because of their small size fit into the interstices of the IL upon mixing. The solubility decreases with an increase of the alkyl chain length of the alcohols and the packing effect becomes less efficient therefore the study is limited to small chain alcohols. The IL chosen is based on the $MeSO_4$ anion because it is the most common halogen free IL and does not undergo hydrolysis. ILs are an important class of solvents because of their properties, such as very low vapour pressure at normal temperature and pressure conditions, low melting point, ability to dissolve organic, inorganic, and polymeric materials, good thermal stability, and their wide liquid range. These novel solvents can also be used as replacement solvents for traditional volatile organic solvents (VOCs). They are easy to recycle and, in general, non-flammable. Alcohols were chosen for this study because they have hydrogen bonding and their interaction with ILs will help in understanding the intermolecular interactions. Also, their thermodynamic properties are used for the development of specific chemical processes.

Excess molar volume, V_m^E, excess isentropic compressibility, κ_S^E, refractive index deviation Δn, and molar refraction, R, values of ($[BMIM]^+[MeSO_4]^-$ + methanol, or 1-propanol, or 2-propanol, or 1-butanol) have been calculated from the density, speed of sound, and refractive index data at $T =$ (298.15, 303.15, 308.15, and 313.15) K over the whole range of concentrations.

The Redlich-Kister smoothing equation was applied successfully for the correlation of V_m^E, κ_S^E, and Δn. The Lorentz-Lorenz equation was also used to correlate the volumetric property and predict the refractive index or density of the binary mixtures of the ionic liquid and alcohols.

The structure of the IL used in this work is presented in Figure 1.1

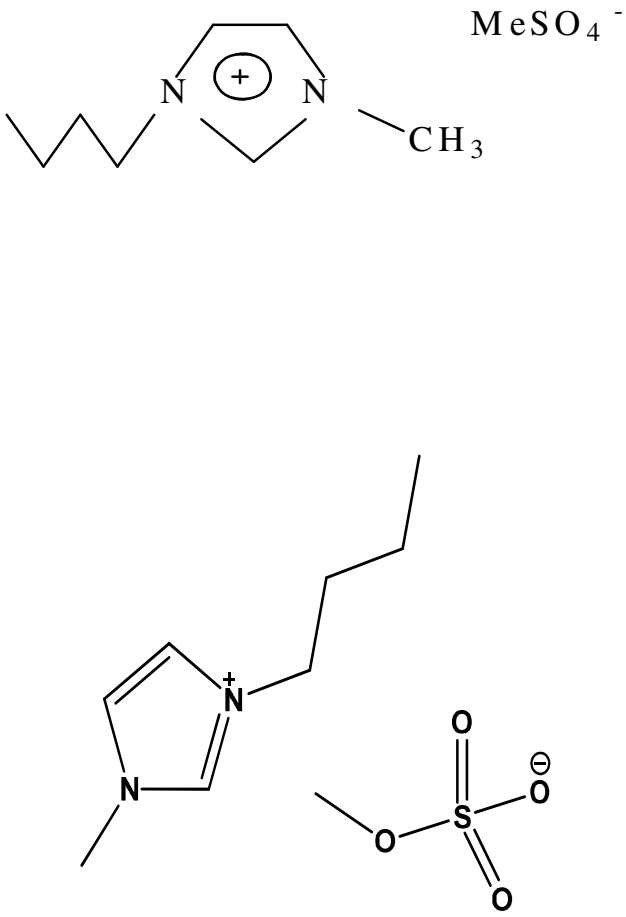

Figure 1.1 Chemical structure of 1-butyl-3-methylimidazolium methylsulphate ($[BMIM]^+[MeSO_4]^-$).

1.6 SCOPE OF THE PRESENT WORK

In this work the thermodynamic properties were determined for the binary systems ($[BMIM]^+[MeSO_4]^-$ + methanol, or 1-propanol, or 2-propanol, or 1-butanol) at T = (298.15, 303.15, 308.15, and 313.15) K. Studies on thermodynamic, transport properties, and spectroscopic studies of binary liquid mixtures provide information on the nature of interactions in the constituent binaries (Hasan *et al.* 2010). To design any process involving ionic liquids on an industrial scale, it is necessary to know a range of physical properties including density, speed of sound, refractive index among others. Physical properties are necessary for hydraulic calculations, fluid transport through pipes and pore surfaces, mass and energy transfers, etc., and are very useful for the characterization of mixtures of unknown compositions. The main process in which the ionic liquids are used are separation processes, including liquid-liquid extraction and separation by distillation (González *et al.* 2008).

The volumetric properties (density, excess molar volumes, apparent molar volumes, and partial molar volumes) provide useful information on the structural and intermolecular interactions between the solvent and solute molecules with different sizes, shapes, and chemical nature (Abdulagatov *et al.* 2008). Measurements of the speed, u, in liquids is a powerful source of information (*e.g.* to detect small changes in gas composition or the effects of small concentrations changes) on the composition and chemical nature of the mixtures. The excess molar volume V_m^E, data can be used to predict (vapour + liquid) equilibria using appropriate EOS models (Sibiya and Deenadayalu 2008).

The objective of studying thermophysical properties of binary mixtures of ILs is to contribute to a data bank of thermodynamic properties of IL mixtures and to investigate the relationship between the structure of the IL and the derived thermodynamic properties, in order to establish principles for the molecular design of suitable ILs for chemical separation processes (Azevedo *et al.* 2004).

CHAPTER 2

LITERATURE REVIEW

The need for studying thermophysical properties of composite materials (or pure substances) is often due to the deviation from ideality on mixing, or a specific application for the required property (Blandamer 1973; Franks and Reid 1973; Millero 1971; Millero 1980; Hoiland 1986).

The composition dependence of the excess molar volume is used to understand the nature of the molecular interactions in these mixtures.

A few authors have published the V_m^E, κ_S^E, and Δn data for the IL $[BMIM]^+[MeSO_4]^-$ with alcohols. There is no systematic study of all three properties for the binary mixtures ($[BMIM]^+[MeSO_4]^-$ + an alcohol) and at many temperatures. The literature systems for an (IL + an alcohol) together with the V_m^E, κ_S^E, and Δn data are given in the tables 2.1, 2.2, and 2.3, respectively.

In summary, the data presented in table 2.1 is only for T = 298.15 K for an (IL + an alcohol) where the cation or the anion and the alcohol is common to that used in this work and indicates that V_m^E is negative, except for the octyl sulphate anion. For a higher carbon number alcohol V_m^E is positive.

The range of the negative V_m^E data for the common cation or anion with an alcohol used in this work is -1.24 $cm^3 \cdot mol^{-1}$ to -0.761 $cm^3 \cdot mol^{-1}$.

When analysing the cation or anion with the alcohols used in this work it was found that the $[MMIM]^+$ cation and the $[MeSO_4]^-$ anion gave the lowest V_m^E values.

Table 2.1 Qualitative V_m^E data for ILs and alcohols with a common cation or anion or a common alcohol obtained from the literature.

Author	Systems	V_m^E
Heintz *et al.* (2002)	($[BMPy]^+[BF_4]^-$ + methanol)	negative
Zafarani-Moattar and Shekaari (2005)	($[BMIM]^+[PF_6]^-$ + methanol or acetonitrile)	negative
Domańska *et al*. (2006)	($[MMIM]^+[MeSO_4]^-$ + methanol, ethanol, or 1-butanol or water), ($[BMIM]^+[MeSO_4]^-$ + methanol or ethanol or 1-butanol or 1-hexanol or 1-octanol or 1-decanol or water) and ($[BMIM]^+[OcSO_4]^-$ + methanol or 1-butanol or 1-hexanol or 1-octanol or 1-decanol).	positive and negative
Zafarani and Shekaari *et al.* (2006)	($[BMIM]^+[BF_4]^-$ or $[BMIM]^+[PF_6]^-$ + methanol or acetonitrile)	negative
Pereiro and Rodríguez (2007)	(ethanol + $[MMIM]^+[MeSO_4]^-$ or $[BMIM]^+[MeSO_4]^-$ or $[BMIM]^+[PF_6]^-$ or $[HMIM]^+[PF_6]^-$ or $[MOIM]^+[PF_6]^-$)	negative

Bhujrajh and Deenadayalu (2007)	($[EMIM]^+[CH_3(OCH_2CH_2)_2OSO_3]^-$ or $[BMIM]^+$ $[CH_3(OCH_2CH_2)_2OSO_3]^-$ or 1-$[MOIM]^+[CH_3(OCH_2CH_2)_2OSO_3]^-$ + methanol)	negative
Zhong *et al.* (2007)	($[BMIM]^+[PF_6]^-$ + aromatic benzyl alcohol or benzaldehyde)	negative
Zafarani and Majdan-Cegincara (2007)	($[BMIM]^+[PF_6]^-$ + tetrahydrofuran or dimethylsulfoxide or methanol or acetonitrile)	negative
González *et al.* (2008)	($[BMIM]^+[MeSO_4]^-$ + ethanol or water)	negative
Yu *et al.* (2011)	($[BMIM]^+[Ala]^-$ + methanol or benzylalcohol)	negative

Heintz *et al*. (2002) presented experimental data of densities for the system (4-methyl-*N*-butylpyridinium tetrafluoroborate + methanol) at T = (298.15, 313.15 and 323.15) K. The $V^{E}_{m,min}$ is -0.850 $cm^3 \cdot mol^{-1}$ for mole fraction x_1 = 0.389. The negative values of excess molar volumes indicate that relatively few methanol molecules fit into the free volume between the relatively large ions of $[BMPy]^+[BF_4]^-$ upon mixing.

Zafarani-Moattar and Shekaari (2005) reported the density (ρ) data for 1-butyl-3-methylimidazolium hexafluorophosphate ($[BMIM]^+[PF_6]^-$) + methanol (MeOH) and ($[BMIM]^+[PF_6]^-$) + acetonitrile (MeCN) binary mixtures over the entire range of their compositions at T = (298.15 to 318.15) K.

The $V^{E}_{m,min}$ values for (MeCN + $[BMIM]^+[PF_6]^-$) system at T = 298.15 K at x_1 = 0.2966 is -1.296 $cm^3 \cdot mol^{-1}$, and for (MeOH + $[BMIM]^+[PF_6]^-$) system at T = 298.15 K at x_1 = 0.2156 is -0.761 $cm^3 \cdot mol^{-1}$. The V^{E}_{m} values for MeCN mixtures are more negative than for the MeOH mixtures. The larger negative V^{E}_{m} values for the (MeCN + $[BMIM]^+[PF_6]^-$) than the (MeOH + $[BMIM]^+[PF_6]^-$) imply that in the MeCN solutions there are stronger ion-dipole interactions and packing effects than for the MeOH solutions.

Domańska *et al.* (2006) determined the V^{E}_{m} for 1-methyl-3-methylimidazolium methylsulfate, $[MMIM]^+[MeSO_4]^-$, solutions with an alcohol (methanol, ethanol or 1-butanol) and with water; for 1-butyl-3-methylimidazolium methylsulfate, $[BMIM]^+[MeSO_4]^-$, with an alcohol (methanol, ethanol, 1-butanol, 1-hexanol, 1-octanol or 1-decanol) and with water; and for 1-butyl-3-methylimidazolium octylsulfate, $[BMIM]^+[OcSO_4]^-$, with an alcohol (methanol, 1-butanol, 1-hexanol, 1-octanol or 1-decanol) at 298.15 K.

The values of V_m^E are negative for all mixtures of ($[MMIM]^+[MeSO_4]^-$ + an alcohol) over the entire composition range. The excess molar volume data become less negative in the following order: methanol < ethanol < 1-butanol. The $V_{m,min}^E$ values are -1.24 $cm^3 \cdot mol^{-1}$ at x_1 = 0.256, -1.18 $cm^3 \cdot mol^{-1}$ at x_1 = 0.442, and -1.00 $cm^3 \cdot mol^{-1}$ at x_1 = 0.766 for methanol, ethanol, or 1-butanol respectively.

The values of V_m^E are negative for all mixtures of ($[BMIM]^+[MeSO_4]^-$ + an alcohol (methanol, ethanol or 1-butanol) and positive for mixtures of ($[BMIM]^+[MeSO_4]^-$ + an alcohol (1-hexanol, 1-octanol or 1-decanol). The $V_{m,min}^E$ values for ($[BMIM]^+[MeSO_4]^-$ + methanol, ethanol or 1-butanol) system are -1.1339 $cm^3 \cdot mol^{-1}$ at x_1 = 0.1550, -0.6625 $cm^3 \cdot mol^{-1}$ at x_1 = 0.3448, and -0.1540 $cm^3 \cdot mol^{-1}$ at x_1 = 0.5603.

The V_m^E values are positive for all mixtures of ($[BMIM]^+[OcSO_4]^-$ + an alcohol) over the entire composition range. $[MMIM]^+[MeSO_4]^-$ gives the most negative value with the methanol system.

Zafarani and Shekaari (2006) reported the excess molar volumes for binary mixtures of 1-*n*-butyl-3-methylimidazolium hexafluorophosphate ($[BMIM]^+[PF_6]^-$ or 1-*n*-butyl-3-methylinmidazolium tetrafluoroborate $(BMIM]^+[BF_4]^-$) in methanol and acetonitrile at T = (298.15 to 318.15) K.

The $V_{m,min}^E$ value is -1.40 $cm^3 \cdot mol^{-1}$ at x_1 = 0.256, for ([MeCN + $[BMIM]^+[BF_4]^-$) system at T = 298.15 K and -1.25 $cm^3 \cdot mol^{-1}$ at x_1 = 0.253, for ([MeCN + $[BMIM]^+[PF_6]^-$) system at T = 298.15 K. since $[BF_4]^-$ is smaller anion than $[PF_6]^-$ and thus has high charge density. It means that $[BMIM]^+[BF_4]^-$ interacts with MeCN stronger than $[BMIM]^+[PF_6]^-$ leading to more negative V_m^E values in ([MeCN + $[BMIM]^+[BF_4]^-$) mixture. Similar behaviour was also observed for the mixture of (MeOH + ILs).

Pereiro and Rodríguez (2007) calculated experimental densities of the binary mixtures of ethanol with $[MMIM]^+[MeSO_4]^-$ (1,3-dimethylimidazolium methylsulfate), $[BMIM]^+[MeSO_4]^-$ (1-butyl-3-methylimidazolium methylsulfate), $[BMIM]^+[PF_6]^-$ (1-butyl-3-methylimidazolium hexafluorophosphate), $[HMIM]^+[PF_6]$- (1-hexyl-3-methylimidazolium hexafluorophosphate) and $[OMIM]^+[PF_6]^-$ (1-methyl-3-octylimidazolium hexafluorophosphate) from T = (293.15 to 303.15) K.

The $V^{E}_{m,min}$ values at T = 298.15 K are x_1 = 0.4290 is -1.142 $cm^3 \cdot mol^{-1}$, x_1 = 0.2990 is -0.706 $cm^3 \cdot mol^{-1}$, x_1 = 0.4960 $cm^3 \cdot mol^{-1}$ is -0.502, x_1 = 0.2033 $cm^3 \cdot mol^{-1}$ is -0.556, and x_1 = 0.1976 $cm^3 \cdot mol^{-1}$ is -0.494, for (ethanol + $[MMIM]^+[MeSO_4]^-$ or $[BMIM]^+[MeSO_4]^-$ or $[BMIM]^+[PF_6]^-$ or $[HMIM]^+[PF_6]^-$ or $[MOIM]^+[PF_6]^-$) system. $[MMIM]^+[MeSO_4]^-$ gives the most negative value with the ethanol system.

Bhujrajh and Deenadayalu (2007) reported the binary excess molar volumes, from density measurements, of ionic liquids 1-ethyl-3-methyl-imidazolium diethyleneglycol monomethylether sulphate $[EMIM]^+[CH_3(OCH_2CH_2)_2OSO_3]^-$ or 1-butyl-3-methyl-imidazolium diethyleneglycol monomethylethersulphate $[BMIM]^+[CH_3(OCH_2CH_2)_2OSO_3]^-$ or 1-methyl-3-octyl-imidazolium diethyleneglycol monomethylethersulphate $[MOIM]^+[CH_3(OCH_2CH_2)_2OSO_3]^-$ + methanol and $[EMIM]^+[CH_3(OCH_2CH_2)_2OSO_3]^-$ + water at T = 298.15, 303.15 and 313.15 K. The V^{E}_{m} values were found to be negative for all systems studied.

The $V^{E}_{m,min}$ values at T = 298.15 K for the $[EMIM]^+[CH_3(OCH_2CH_2)_2OSO_3]^-$ or $[BMIM]^+[CH_3(OCH_2CH_2)_2OSO_3]^-$ or $[MOIM]^+[CH_3(OCH_2CH_2)_2OSO_3]^-$ + methanol is -0.933 $cm^3 \cdot mol^{-1}$ at x_1 = 0.747, -0.786 $cm^3 \cdot mol^{-1}$ at x_1 = 0.775 and -0.721 $cm^3 \cdot mol^{-1}$ at x_1 = 0.803, respectively.

The densities of the pure ILs as well those of their mixtures decreased with an increase in temperature and an increase in the size of the cation, *i.e.*, density of $[EMIM]^+$ > $[BMIM]^+$ > $[MOIM]^+$. For each of the three (ionic liquids + methanol) systems the most negative V^{E}_{m} values were obtained for

the ($[EMIM]^+[CH_3(OCH_2CH_2)_2OSO_3]$- + methanol) system and the least negative V_m^E values were obtained for the ($[MOIM]^+[CH_3(OCH_2CH_2)_2OSO_3]^-$ + methanol) system.

Zhong *et al.* (2007) reported the density of two binary mixtures formed by 1-butyl-3-methylimidazolium hexafluorophosphate $[BMIM]^+[PF_6]^-$ with aromatic compound (benzyl alcohol or benzaldehyde) at the temperature from 298.15 K to 313.15 K.

The V_m^E values for benzaldehyde mixtures are more negative than those for the benzyl alcohol mixtures, the $V_{m,min}^E$ values for ($[BMIM]^+[PF_6]^-$ + benzyl alcohol) and ($[BMIM]^+[PF_6]^-$ + benzaldehyde) at T = 298.15 K at x_1 = 0.3001 is -0.8941 $cm^3 \cdot mol^{-1}$, and x_1 = 0.2996 is -1.2954 $cm^3 \cdot mol^{-1}$. It implies that in the benzaldehyde solutions there are stronger ion-dipole interactions and packing effects than in the benzyl alcohol solutions.

Zafarani and Cegincara (2007) determined the experimental density for solutions of $[BMIM]^+[PF_6]^-$ + tetrahydrofuran (THF) or dimethylsulfoxide (DMSO) at T = 298.15 K. From the experimental density V_m^E were calculated. V_m^E is more negative for ($[BMIM]^+[PF_6]^-$ + THF) system than ($[BMIM]^+[PF_6]^-$ + DMSO) system. The most negative value for ($[BMIM]^+[PF_6]^-$ + THF) system indicates that a more efficient packing and/ or attractive interaction occurred when the IL and organic molecular liquids were mixed.

González *et al.* (2008) determined the experimental densities of its binary systems 1-butyl-3-methylimidazolium methylsulphate with ethanol and water at several temperatures T = (298.15, 313.15, and 328.15) K.

The excess molar volume is negative over the entire composition range for (ethanol + $[BMIM]^+[MeSO_4]^-$) presenting a minimum in V^E_m at a mole fraction of 0.65 of -0.833 $cm^3 \cdot mol^{-1}$, -0.948 $cm^3 \cdot mol^{-1}$, and -1.076 $cm^3 \cdot mol^{-1}$, respectively, for the three studied temperatures. The sign of the excess molar volume of the system (water + $[BMIM]^+[MeSO_4]^-$) is negative over the composition range for the first two temperatures. At T = 328.15 K, this system present one maximum at x_1 = 0.95 is 0.005 $cm^3 \cdot mol^{-1}$.

Yu *et al.* (2011) determined densities for IL 1-butyl-3-methylimidazolium alanine $[BMIM]^+[Ala]^-$ with methanol or benzyl alcohol, at T = (298.15, 303.15, 308.15 and 313.15) K. The $V^E_{m,min}$ values for ($[BMIM]^+[Ala]^-$ + methanol, or benzylalcohol) at T = 298.15 K at x_1 = 0.2015 is -1.2276 $cm^3 \cdot mol^{-1}$, and at x_1 = 0.3971 is -0.8032 $cm^3 \cdot mol^{-1}$.

From table 2.2 all the κ_S^E values for the (IL + an alcohol) systems are negative. The range of the negative data for the κ_S^E values for the (IL + an alcohol) at T = 298.15 K system is ± -143 TPa^{-1} to -55.25 TPa^{-1}.

When analysing the cation or anion with the alcohols used in this work it was found that the 1-butylpyridinium tetrafluoroborate IL gave the lowest κ_S^E values indicating that this ionic liquid + alcohol is the least compressible.

Table 2.2 κ_S^E data for (ILs + an alcohol) obtained from the literature.

Author	Systems	κ_S^E
Zafarani and Shekaari (2006)	($[BMIM]^+[BF_4]^-$ or $[BMIM]^+[PF_6]^-$ + methanol, or acetonitrile)	negative
Vercher *et al.* (2007)	($[EMIM]^+[triflate]^-$ + methanol, or ethanol, or 1-propanol, or water)	negative
García –Mardones *et al.* (2010)	($[bpy]^+[BF_4]^-$ + methanol, or ethanol)	negative
Vercher *et al.* (2011)	($[EMIM]^+[triflate]^-$ + 2-propanol, or THF)	negative
García –Mardones *et al.* (2012)	($[b_3mpy]^+[BF_4]^-$, or $[b_4mpy]^+[BF_4]^-$ + methanol, or ethanol)	negative

Zafarani and Shekaari (2006) reported the speed of sound u, isentropic compressibility κ_s, and excess isentropic compressibility κ_S^E, data for the binary mixture of 1-*n*-butyl-3-methylimidazolium tetrafluoroborate or 1-*n*-butyl-3-methylimidazolium ($[BMIM]^+[BF_4]^-$) in methanol and acetonitrile at T = (298.15 to 318.15) K.

The $\kappa_{S,min}^E$ values at T = 298.15 K is negative for (an IL + methanol) systems.

Vercher *et al*. (2007) measured the speed of sound of mixtures of 1-ethyl-3-methylimidazolium trifluoromethanesulfonate ($[EMIM]^+[triflate]^-$) with methanol, or ethanol, or 1-propanol, and water at (T = 278.15 to 338.15) K.

The $\kappa_{S,min}^E$ values at T = 298.15 K at x_1 = 0.1502 is -129.43 TPa^{-1}, x_1 = 0.1999 is -94.93 TPa^{-1}, x_1 = 0.3002 is -55.25 TPa^{-1}, x_1 = 0.1004 is -63.40 TPa^{-1}, for ($[EMIM]^+[triflate]^-$ + methanol, or ethanol, or 1-propanol and water), respectively. κ_S^E increases when temperature decreases or the aliphatic chain length increases.

García-Mardones *et al.* (2010) determined speeds of sound for the binary mixtures (1-butylpyridinium tetrafluoroborate + methanol, or ethanol) over the temperature range 293.15 K to 323.15 K. From experimental values excess isentropic compressibility has been calculated. The mixtures give negative values for the excess properties. Values of the excess properties are larger in absolute value for the mixture containing methanol than for the system with ethanol.

The $\kappa_{S,min}^E$ values at T = 298.15 K was estimated from the data and found to be ± -143 TPa^{-1}, x_1 = ± 0.18 for methanol and ± -115 TPa^{-1} at x_1 = ± 0.24 for ethanol.

Vercher *et al*. (2011) measured speeds of sound of 1-ethyl-3-methylimidazolium trifluoromethanesulfonate mixtures with 2-propanol and tetrahydrofuran (THF), as well as of the pure components, over the whole range of compositions at T = (278.15 to 328.15) K. From these experimental data, the excess speed of sound and excess isentropic compressibility has been calculated.

The $\kappa_{S,min}^{E}$ values at T = 298.15 K at x_1 = 0.2994 is -89.52 TPa^{-1} for ($[EMIM]^+[triflate]^-$ + 2-propanol).

García –Mardones *et al*. (2012) calculated speeds of sound for the binary mixtures containing an ionic liquid (1-butyl-3-methylpyridinium tetrafluoroborate or 1-butyl-4-methylpyridinium tetrafluoroborate) and an alkanol (methanol or ethanol) over the temperature range (293.15 to 323.15) K. Excess isentropic compressibilities have been measured from speed of sound data.

The $\kappa_{S,min}^{E}$ values at T = 298.15 K was estimated from the data and found to be ± -138 TPa^{-1}, x_1 = ± 0.15 for methanol and ± -98 TPa^{-1} at x_1 = ±0.38 for ethanol. All the mixtures show negative values for the κ_S^E. The $\kappa_{S,min}^{E}$ at T = 298.15 K for ($[b_3mpy]^+$ $[BF_4]^-$ + methanol, or ethanol) at x_1 = 0.1980 is -200.12 TPa^{-1}, x_1 = 0.2201 is -140.04 TPa^{-1} for ($[b_4mpy]^+$ $[BF_4]^-$ + methanol, or ethanol) at x_1 = 0.1650 is -170.21 TPa^{-1} , x_1 = 0.2112 is -138.15 TPa^{-1}.

Table 2.3 Δn data for (an ILs + an alcohol) obtained from the literature.

Author	Systems	Δn
Pereiro and Rodriguez (2007)	(Ethanol + $[MMIM]^+[MeSO_4]^-$ or $[BMIM]^+[MeSO_4]^-$ or $[BMIM]^+[PF_6]^-$ or $[HMIM]^+[PF_6]^-$ or $[MOIM]^+[PF_6]^-$)	positive
Pereiro and Rodriguez (2007)	($[BMIM]^+[PF_6]^-$ or $[MMIM]^+[CH_3SO_4]^-$ + 2-butanone or ethylacetate or 2-propanol, $[HMIM]^+[PF_6]^-$ +2-propanol, and $[OMIM]^+[PF_6]^-$ + ethylacetate)	positive
González *et al.* (2008)	($[BMIM]^+[MeSO_4]^-$ + ethanol or water)	positive
Iglesias-Otero *et al.* (2008)	($[BMIM]^+[BF_4]^-$ or $[BMIM]^+[MeSO_4]^-$ + ethanol + or nitromethane + or 1,3-dichloropropane + or ethylene glycol + or DEGEE)	positive
González *et al.* (2009)	($[EpyESO_4]$ + ethanol or 1-propanol)	positive
Yu *et al.* (2011)	($[BMIM]^+[Ala]^-$ + methanol or benzylalcohol)	positive

Pereiro and Rodriguez (2007) determined experimental densities, speeds of sound and refractive indices of the binary mixtures of ethanol with $[MMIM]^+[MeSO_4]^-$ (1,3-dimethylimidazoliummethyl sulfate), $[BMIM]^+[MeSO_4]^-$ (1-butyl-3-methylimidazolium methyl sulfate), $[BMIM]^+[PF_6]^-$ (1-butyl-3-methyl imidazolium hexafluorophosphate), $[HMIM]^+[PF_6]^-$ (1-hexyl-3-methylimidazolium hexafluorophosphate) and $[OMIM]^+[PF_6]^-$ (1-methyl-3-octylimidazoliumhexafluorophosphate) from T = (293.15 to 303.15) K.

Changes of refractive index Δn is positive over the whole composition range. The $\Delta n_{,max}$ at T = 298.15 K at x_1 = 0.3317 is 0.0363, x_1 = 0.2990 is 0.0396, x_1 = 0.4960 is 0.0162, x_1 = 0.3120 is 0.0221, x_1 = 0.2897 is 0.0252 for (ethanol + $[MMIM]^+[MeSO_4]^-$, or $[BMIM]^+[MeSO_4]^-$, or $[BMIM]^+[PF_6]^-$, or $[HMIM]^+[PF_6]^-$, or $[OMIM]^+[PF_6]^-$) system. Δn increases as the temperature increases.

Pereiro and Rodriguez (2007) determined refractive indices of the binary mixtures of $[BMIM]^+[PF_6]^-$ (1-butyl-3-methylimidazolium hexafluorophosphate), $[HMIM]^+[PF_6]^-$ (1-hexyl-3-methylimidazolium hexafluorophosphate), $[OMIM]^+[PF_6]^-$ (1-methyl-3-octylimidazolium hexafluorophosphate), and $[MMIM]^+[CH_3SO_4]^-$ (1,3-dimethylimidazolium methyl sulfate) with 2-butanone, ethylacetate, and 2-propanol from (293.15 to 303.15) K.

Changes of refractive index on mixing were calculated for the above systems. Changes of refractive index on mixing for the binary mixtures are positive over the entire composition range. The $\Delta n_{,max}$ at T = 298.15 K at x_1 = 0.2992 is 0.0135, x_1 = 0.2939 is 0.0140, x_1 = 0.7136 is 0.0063 for ($[BMIM]^+[PF_6]^-$ + 2-butanone, or ethylacetate, or 2-propanol), x_1 = 0.4893 is 0.0122 for ($[HMIM]^+[PF_6]^-$ + 2-propanol), x_1 = 0.2941 is 0.0186 for ($[OMIM]^+[PF_6]^-$ + ethylacetate), x_1 = 0.7074 is 0.0177,

x_1 = 0.8549 is 0.0092, x_1 = 0.4055 is 0.0238 for ([MMIM]$^+$[MeSO$_4$]$^-$ + 2-butanone, or ethylacetate, or 2-propanol) system.

González *et al.* (2008) reported refractive indices and their derived property of its binary systems 1-butyl-3-methylimidazolium methylsulphate with ethanol and with water at several temperatures T = (298.15, 313.15, 328.15) K.

Refractive indices were measured from T = 298.15 K over the whole composition range for the binary system. The results were used to calculate deviations in the refractive index. Δn is positive at T = 298.15 K. over the whole composition range for the binary system. 0.0386 is the maximum deviation in refractive index at mole fraction x_1 = 0.7142.

Iglesias-Otero *et al.* (2008) measured the refractive index for a set of systems ([BMIM]$^+$[BF$_4$]$^-$ or [BMIM]$^+$[MeSO$_4$]$^-$ + ethanol, or nitromethane, or 1,3-dichloropropane, or ethylene glycol, or DEGEE) at atmospheric pressure at 298.15 K throughout the composition range. The data were used to calculate excess volumes and refractive index deviations. Δn is positive in the whole range of compositions and temperatures.

González *et al.* (2009) reported refractive index for (EpyESO$_4$ + ethanol, or 1-propanol) at temperatures T = (298.15) K over the whole composition range. The results were used to calculate deviations in the refractive index.

Deviations in the refractive index are positive at 298.15 K. The $\Delta n_{,\max}$ at x_1 = 0.6033 is 0.0448 for (ethanol + EpyESO$_4$) and x_1 = 0.6013 is 0.0295 for (1-propanol + EpyESO$_4$) system.

Yu *et al.* (2011) determined refractive indices for two ionic liquid (IL) mixtures formed by 1-butyl-3-methylimidazolium alanine acid salt ($[BMIM]^+[Ala]^-$) with methanol or benzylalcohol, respectively, over the mole fraction range from (0.1 to 0.9) and at temperatures from (298.15 to 313.15) K at intervals of 5 K.

At 298.15 K the $\Delta n_{,max}$ at $x_1 = 0.2837$ is 7.8488 for ($[BMIM]^+[Ala]^-$) + methanol) system and at $x_1 = 0.3971$ is 0.0765 for ($[BMIM]^+[Ala]^-$) + benzylalcohol) system. Δn is positive in the whole range of compositions and temperatures.

CHAPTER 3

EXPERIMENTAL METHODS AND THEORETICAL FRAMEWORK

A. EXPERIMENTAL METHODS

3.1 EXCESS MOLAR VOLUMES

3.1.1 Theory

The excess molar volume $V_{\mathrm{m}}^{\mathrm{E}}$ is defined as (Walas 1985; Letcher 1975):

$$V_{\mathrm{m}}^{\mathrm{E}} = V_{\mathrm{mixture}} - \sum x_{\mathrm{i}} V_{\mathrm{i}}^{0} \tag{3.1}$$

where x_i is the mole fraction of component i, V_{mixture} and $V_{\mathrm{i}}^{\mathrm{o}}$ are the molar volumes of the mixture component i, respectively. For a binary mixture,

$$V_{\mathrm{m}}^{\mathrm{E}} = V_{\mathrm{mixture}} - \left(x_1 V_1^0 + x_2 V_2^0\right) \tag{3.2}$$

The change in volume on mixing two liquids, 1 and 2 can be attributed to a number of processes: (a) the breakdown of 1-1 and 2-2 intermolecular interaction which have a positive effect on the volume, (b) the formation of 1-2 intermolecular interaction which results in a decrease of the volume of the mixture, (c) packing effect caused by the difference in the size and shape of the component species and which may have positive or negative effect on the particular species involved and (d) formation of new chemical species (Redhi 2003).

There is no volume change upon mixing two liquids to form a thermodynamically ideal solution at constant temperature and pressure, but a volume change may occur when two real liquids are mixed (Battino 1971).

Volume change on mixing of binary liquid mixtures, V_m^E, at constant pressure and temperature is of interest to chemists and chemical engineers, and is an indicator of the non-idealities present in real mixtures. It is also important to thermochemists because it serves as a sensitive indicator for the applicability of liquid theories to liquid mixtures (Redhi 2003).

The volume, (V), of a mixture is a function of temperature, (T), pressure, (P), and number of moles, (n), i.e.:

$$V = V(T, P, n_1, n_2, n_3 ... n_f) \tag{3.3}$$

At constant temperature and pressure this is:

$$V = V(n_1, n_2, n_3 ... n_f) \tag{3.4}$$

The ideal volume of the mixture $V_{m,ideal}$ at atmospheric pressure may be written as:

$$V_{m,ideal} = \sum x_1 V_{m,i}^0 \tag{3.5}$$

where $V_{m,i}^0$ is the molar volume of the pure species i.

Once the liquids have been mixed together the volume of the mixture $V_{m,mix}$ is not normally the sum of the volumes of the pure liquids but is given by:

$$V_{m,mix} = (V_{m,real}) \neq x_1 V_{m,1} + x_2 V_{m,2} + ... x_i V_{m,i} = \sum x_i V_{m,i}^0 \tag{3.6}$$

The excess molar volume of mixing, V_m^E, is given by:

$$V_m^E = V_{m,mix} - V_{m,pure} = V_{m,real} - V_{m,ideal} = \sum x_I (V_{m,i} - V_{m,i}^0) \tag{3.7}$$

where V_m^E is the excess molar volume at constant temperature and pressure (Smith *et al.*1989).

$V_{m,i}$ is the partial molar volume of the i^{th} component and $V_{m,i}^0$ is the molar volume of the pure species i.

3.1.2 Experimental methods for measurement of excess molar volumes

The excess molar volume, V_m^E, at a constant concentration of x_1 of component1and x_2 of component 2 is defined as:

$$V_m^E = V_{m,mix} - \left(x_1 V_1^0 + x_2 V_2^0\right) \tag{3.8}$$

where V_1^0 and V_2^0 are the volume of pure first and second component respectively.

The excess molar volume, V_m^E, upon mixing two liquids may be measured either directly or indirectly. The direct measurements involve mixing the liquids and determining the volume change (dilatometric method) and the indirect measurements involve measuring the density of the pure liquid and the density of the mixture by (pycnometer or densitometer) and calculating, V_m^E, using equations (3.7 and 3.8) (Battino 1971; Letcher 1975; Handa and Benson 1979; Beath *et al.* 1969; Pflug and Benson 1968; Stokes and Marsh 1972; Marsh 1980, 1984; Kumaran and McGlashan 1977; Govender 1996; Nevines 1997; Redhi 2003). The details for the instrument used in this work are given in chapter 4. A summary of the various techniques (direct and indirect methods) are given here.

3.1.2.1 Direct method

The direct method measures the volume change that occurs when the liquids are mixed. Direct methods of measurement of, V_m^E, include batch dilatometer and continuous dilution dilatometer.

Batch dilatometer is characterized by the determination of a single data point per loading of the apparatus and continuous dilatometer is characterized by the determination of many data points per loading of the apparatus (Handa and Benson 1979; Nevines 1997; Redhi 2003).

(i) Batch dilatometer

An example of a batch dilatometer is shown in Figure 3.1.

The dilatometer is filled with known masses of pure liquids, which are separated by mercury. The height of mercury in the calibrated graduated column is noted. The liquids are mixed by rotating the dilatometer and the volume change on mixing is indicated by the change in the height of the mercury in the calibrated capillary. The, V_m^E, is determined from the volume change and the masses of the components. It was reported that a precision of ± 0.003 $cm^3 \cdot mol^{-1}$ in the, V_m^E, could be achieved over the temperature range of (280 to 350) K using this technique. A disadvantage of this apparatus is that it is difficult to fill the dilatometer and this is usually accomplished using a narrow needle. A major source of error in this method is the determination of the composition as is it necessary to weigh the dilatometer as it contains mercury. This results in large errors in the measured mass. The error associated with taking a difference in large masses is usually quiet significant (Keyes and Hildebrand 1917; Nevines 1997; Redhi 2003).

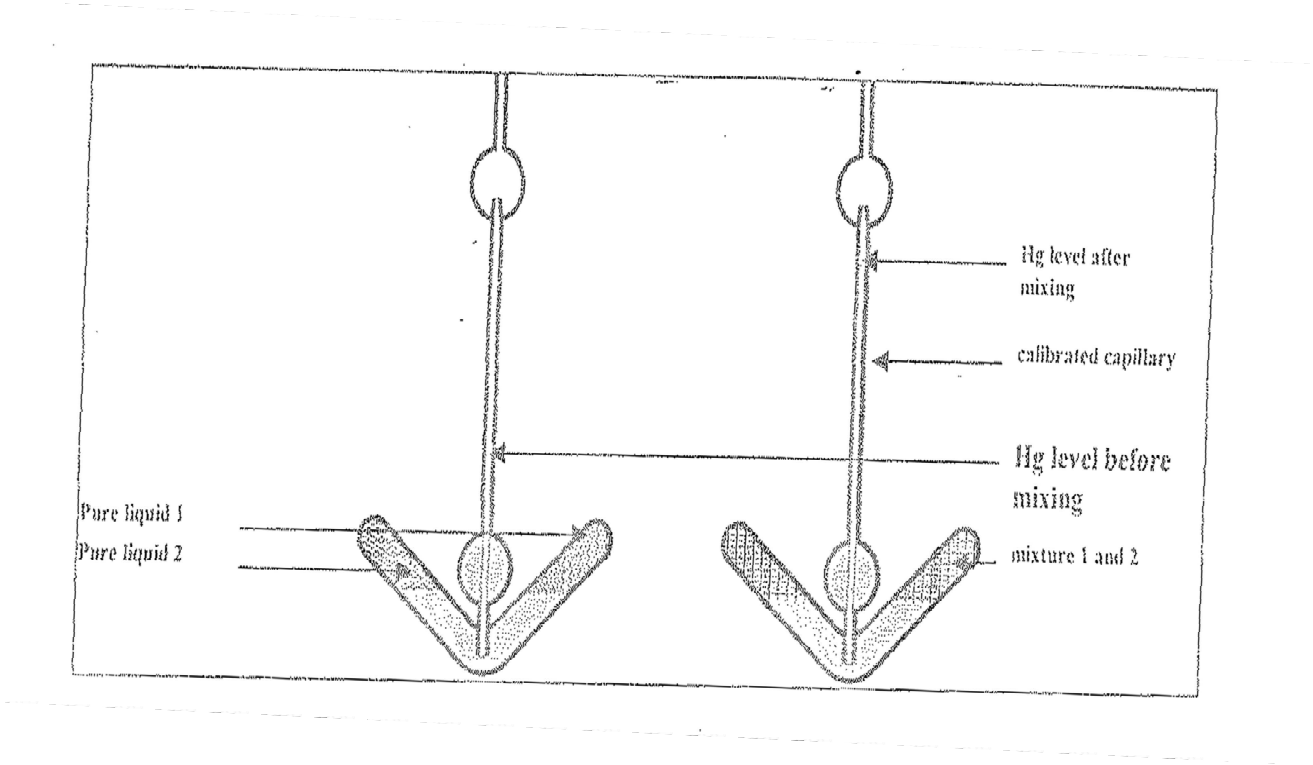

Figure 3.1 Schematic representation of a typical batch dilatometer.

(Nevines, 1997; Redhi, 2003; Sibiya, M.Tech thesis, 2008)

(ii) Continuous dilatometer

This technique has become more popular than the batch technique because it is less time consuming and more data is generated per loading. The mode of operation involves the successive addition of one liquid into the reservoir, which contains the other liquid and detecting the volume change that accompanies the addition.

The dilatometer of Kumaran and McGlashan (1977) which is based on the design of Bottomly and Scott (1974) is presented in Figure 3.2. Both are considered superior to other continuous dilatometer because mercury and the liquids do not pass through the greased gas. The instrument of Kumaran and McGlashan (1977) is considered an improvement on the one developed by Bottomly and Scott (1974) because it is easier to load. Kumaran and McGlashan (1977) reported a precision of 0.0003 $cm^3 \cdot mol^{-1}$ in V_m^E, for their apparatus.

A measurement is made by filling the burette (e) with one of the pure liquids and the bulb (d) with the other pure liquid. As the dilatometer is tilted some of the mercury is displaced into the burette through a capillary (c) and collects at the bottom of the burette. This displaced mercury forces some of the pure liquid from the burette into the bulb through the higher capillary (b). After mixing the change in volume is registered as a change in the level of the mercury in the calibrated capillary (a). The amount of pure liquid that is displaced is determined from the height of the mercury in the burette. Because mercury is used, a capillary pressure effect is possible and the compressibility of mercury has to be considered when determining the excess molar volume.

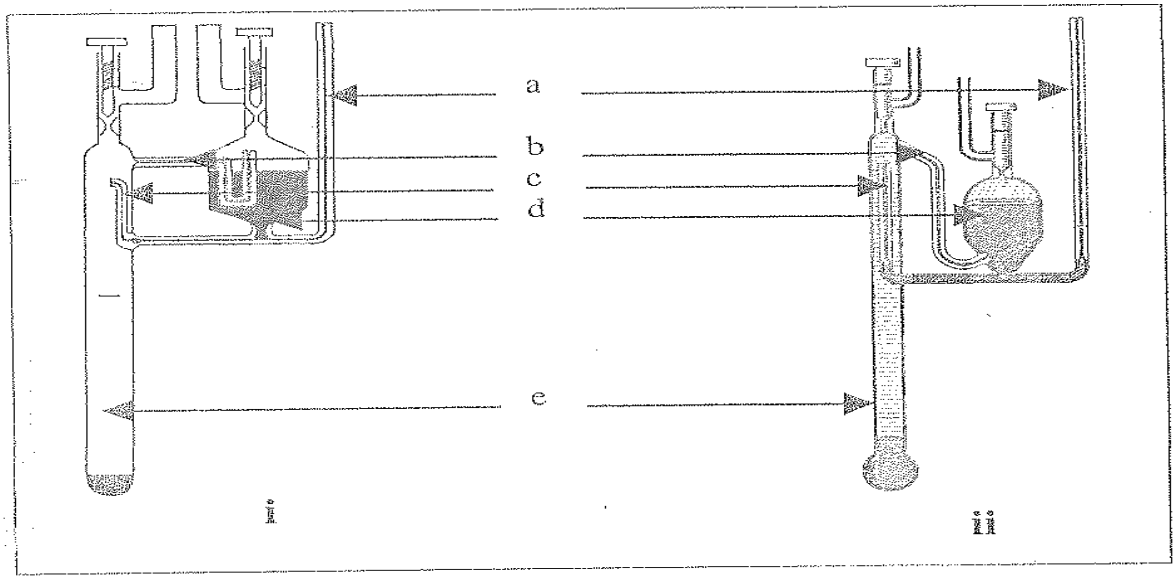

Figure 3.2 Schematic representation of a continuous dilatometer (i) design of Bottomly and Scott (1974), (ii) design of Kumaran and McGlashan (1977). a; calibrated capillary from which the volume change is determined, b; liquid capillary, c; mercury capillary, d; bulb that contains mercury, e; burette liquid 2.

(Bottomly and Scott, 1974; Kumaran and McGlashan, 1977; Sibiya, M.Tech thesis, 2008)

3.1.2.2 Indirect method

As the development of the dilatometer was accompanied by a greater accuracy than was possible from density measurement techniques, the latter method became less popular for determination of V_m^E, However the development of highly accurate vibrating tube densitometers has made it possible to determine, V_m^E, with acceptable accuracy from density measurements. This method is also very simple.

The excess molar volume for a binary V_m^E, are determined from density measurements using the following equations, respectively:

$$V_m^E = \frac{x_1 M_1 + x_2 M_2}{\rho} - \frac{x_1 M_1}{\rho_1} - \frac{x_2 M_2}{\rho_2} \tag{3.9}$$

where x_1 , and x_2 are the mole fractions, M_1 , and M_2 are molar masses, ρ_1, and ρ_2 , ρ are the densities where 1and 2 refers to the component 1, and 2 respectively and ρ is the density of the mixture (Govender 1996; Nevines 1997; Redhi 2003).

(i) Pycnometry

Pycnometry involves the determination of the mass for a fixed volume. A vessel with a known volume is filled with a liquid mixture of known composition. It is then weighed and this mass, together with the composition and volume previously calibrated with a recommended standard liquid is used to determine V_m^E. A pycnometer capable of a precision of 5×10^{-6} g·cm^{-3} for density measurement translates into a precision of 0.001 cm^3·mol^{-1} for V_m^E, has been reported by (Wood and Brusie 1943). The pycnometer based on the design of (Wood and Brusie 1943) is shown in Figure 3.3.

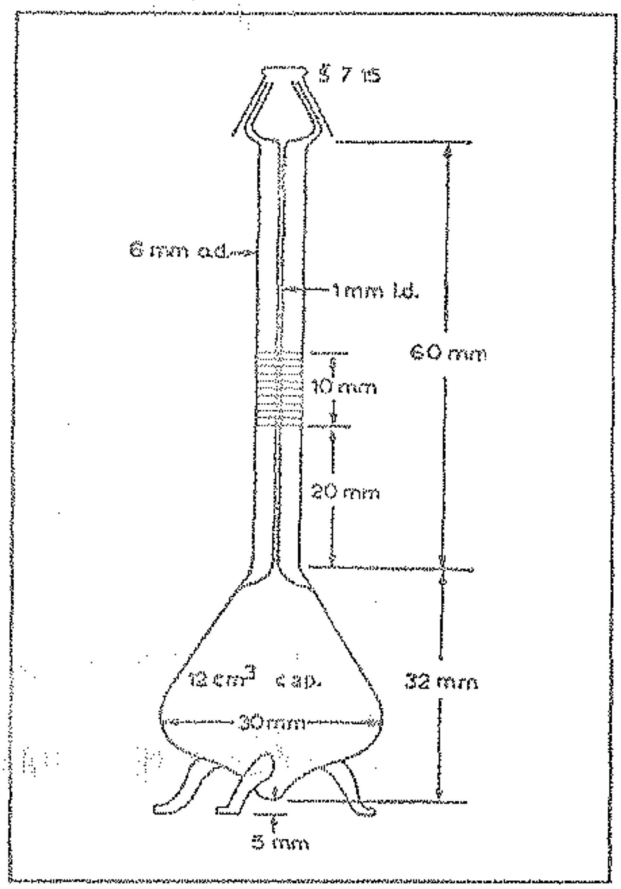

Figure 3.3 Schematic representation of a pycnometer based on the design of Wood & Brusie (1943).

(Wood and Brusie, 1943; Sibiya, M.Tech thesis, 2008)

(ii) Magnetic float densimeter

The mode of operation of a magnetic float densimeter is based on the determination of the height of a magnetic float in a liquid mixture. The height of this magnetic float in the presence of a known magnetic field is a function of the buoyancy of the liquid. The buoyancy of the liquid is related to the density of the liquid. An instrument with a precision 3×10^{-6} g·cm^{-3} has been reported and this translates to a precision of 0.0008 cm^{3}·mol^{-1} (Franks and Smith 1967). The magnetic float densitometer based on the design of (Franks and Smith 1967) is shown in Figure 3.4.

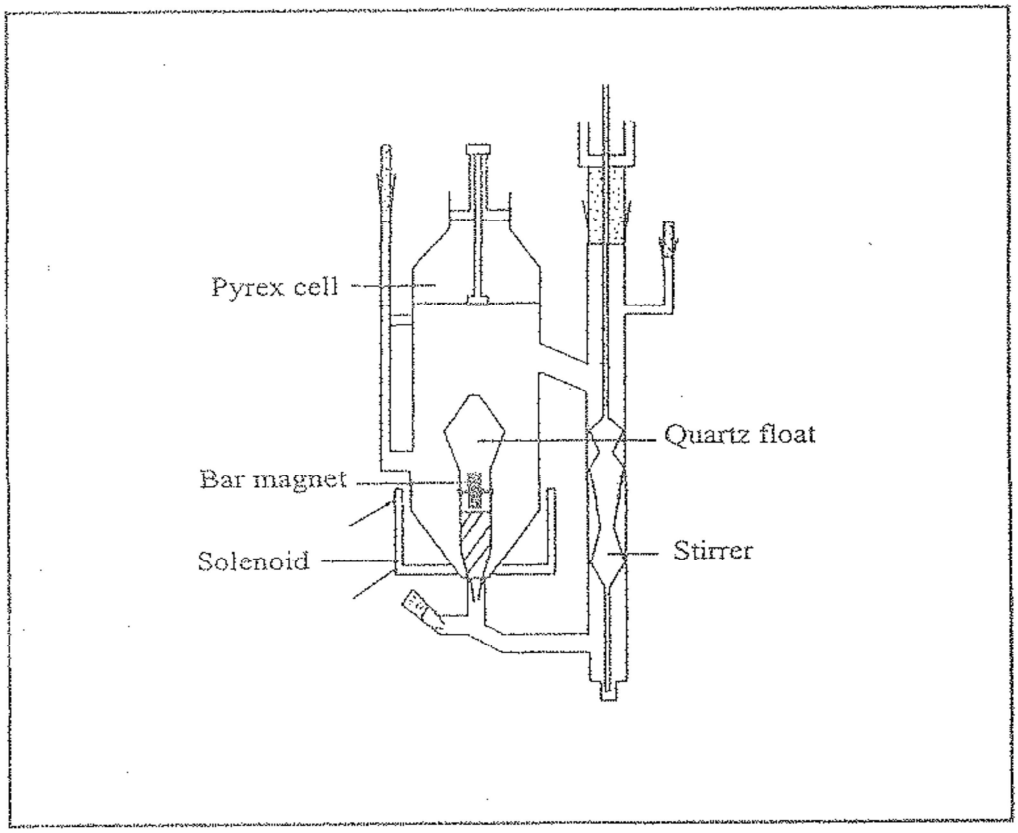

Figure 3.4 Schematic representation of a magnetic float densimeter (1967).

(Franks and H.T. Smith, 1967; Sibiya, M.Tech thesis, 2008)

(iii) Mechanical oscillating densitometer

Mechanical oscillating (vibrating tube) densimeters linked to digital output displays are widely used in the chemical industry and in research laboratories to measure densities of pure liquids and liquid mixtures. The frequency of the vibrating tube containing a liquid that is subjected to a constant electric stimulation is related to the density of the liquid. According to Handa and Benson (1979), the frequency of vibration of an undamped oscillator (e.g. tube containing a liquid) connected by a spring with a constant elasticity, c, is related to the mass of the oscillator and the liquid, M, by the following equation:

$$2\pi v = \left(\frac{c}{M}\right)^{\frac{1}{2}} \tag{3.10}$$

where M is the mass of the contents in the tube and M_0 is the mass of the empty oscillator. Since the oscillator is a hollow tube if a liquid with a density, ρ, fills the hollow tube occupying a volume V, then:

$$M = M_0 + \rho V \tag{3.11}$$

Substitution of equation (3.10) into equation (3.11) and solving for ρ:

$$\rho = -\frac{M_0}{V} + \left(\frac{c}{4\pi^2}\right)\left(\frac{1}{V^2}\right) \tag{3.12}$$

where $\frac{-M_0}{V}$ and $\frac{}{4\pi^2 V}$ are constants. Therefore the following equation is valid:

$$\rho = A + B\left(\frac{1}{v}\right)^2 \tag{3.13}$$

The constants A and B are characteristics of the oscillator, τ is the period and density is given by the symbol, ρ, hence:

$$\rho = A + B\tau^2 \tag{3.14}$$

where A and B are determined by calibration. This involves determining the period for two pure substances of known density.

Since densities are measured relative to a reference material:

$$\rho - \rho_o = B\left(\tau^2 - \tau_o^2\right) \tag{3.15}$$

Commercially available vibrating tube densimeters with a precision of 0.001 % are available. This implies a precision of 0.003 $cm^3 \cdot mol^{-1}$ in the measurement of V_m^E (Nevines 1997).

In this work an Anton Paar DSA 5000 M instrument was used to measure the density and speed of sound.

3.2 SPEED OF SOUND AND ISENTROPIC COMPRESSIBILITY

3.2.1 Theory

Measurement of the speed of sound, *u*, in liquids is a useful source of information to detect small changes in gas composition or the effect of small concentration changes (Azevedo *et al.* 2004).

Speed of sound and density are used to calculate the isentropic compressibility by means of the Newton-Laplace equation:

$$k_s = \frac{1}{\rho u^2} \tag{3.16}$$

3.2.1.1 Instruments used for the measurement of the speed of sound

(i) Mittal Ultrasonic interferometer M-81G

This instrument is a Mittal multifrequency ultrasonic interferometer. It is not a simple device and the frequency is used to determine the ultrasonic velocity in liquids with a high degree of uncertainty. The frequency for a series of readings needs to be taken and the average reading calculated leading to higher errors.

It consists of a:

(a) high frequency generator, which is designed to excite the quartz plate fixed at the bottom of the measuring cell at its resonance frequency to generate ultrasonic waves in the experimental liquid in the measuring cell. A macro-ammeter senses the changes in the current and controls for the sensitivity regulation and initial adjustments of the micro-ammeter are provided on the high frequency generator.

(b) measuring cell, which is a specially designed double walled cell for maintaining the temperature of the liquid constant during the experiment. A fine micrometer screw is provided at the top, which can lower or raise the reflector plate in the cell through a known distance. It has a quartz plate fixed at the bottom.

A diagram showing the Ultrasonic Interferometer M-81G and interferometer is shown in Figures 3.5

Figure 3.5 Diagram of an Ultrasonic interferometer M-81G.

(Taken from Instruction Manual of Mittal Enterprises Ultrasonic Interferometer for Liquids)

The principle used in the measurement of velocity, u, is based on the accurate determination of the wavelength, λ, in the medium. Ultrasonic waves of known frequency, ν, are produced by a quartz plate cell. A movable plate kept parallel to the quartz plate reflects the waves. If the separation between these plates is exactly a whole multiple of the sound wavelength, standing waves are formed in the

medium. The acoustic resonance gives rise to an electrical reaction on the generator driving the quartz plate such that the anode current of the generator becomes a maximum.

If the distance between the reflector and crystal is increased or decreased and the variation is exactly one half wavelength, ($\lambda/2$) or multiple of it, the anode current again becomes a maximum. From the knowledge of wavelength, (λ), the velocity or speed of sound, (u), can be obtained by the relation:

Speed of sound = Wavelength × frequency

$$u = \lambda \times \nu \tag{3.17}$$

In this work a DSA 5000 M is used for the determination of speed of sound and isentropic compressibilities. The description of the instrument is given in chapter 4 and in section 4.1.5.

3.3 REFRACTIVE INDICES AND MOLAR REFRACTION

3.3.1 Theory

The refractive index, n, is a constant for a pure solvent. It can be defined as:

$$n = \frac{\text{speed of light in material 1}}{\text{speed of light in material 2}} \tag{3.18}$$

This is usually written $n_{1,2}$ and is the refractive index in material 2 relative to material 1. The incident light is in material 1 and the refracted light is in material 2.

If the incident light is in a vacuum this value is called the absolute refractive index of material 2. By definition the refractive index in a vacuum is 1. In practice, air makes little difference to the refraction of light with an absolute refractive index of 1.0008, so the value of the absolute refractive index can be used assuming the incident light is in air.

The refractive index is also defined as the ratio of the speed of a wave either light or sound in a reference medium to a second medium.

It is most commonly used in the context of the speed of the wave of light with a vacuum as a reference medium, although historically other reference media (e.g. air at a standardized pressure and temperature) have been used. In the case of light the refractive index is given by:

$$n = \sqrt{\varepsilon_r \mu_r} \tag{3.19}$$

where ε_r is the material's relative permittivity, and μ_r is its relative permeability. For most naturally occurring materials, μ_r is very close to 1 (Urzhumov and Yaroslav 2007). Therefore n is approximately $\sqrt{\varepsilon_r}$. Contrary to a widespread misconception, the real part of a complex n may be less

than one, depending upon the material and wavelength. This has practical technical applications, such as effective mirrors for X-rays based on total external reflection.

Another common definition of the refractive index is the ratio of the sine of the angle of incidence (medium 1) θ_1 and the angle of refraction of (medium 2) θ_2 and is given by (Iglesias-Otero *et al.* 2008):

$$n = \frac{\sin\theta_1}{\sin\theta_2} \tag{3.20}$$

The angles are measured to the normal of the surface. This definition is based on Snell's law (Iglesias-Otero *et al.* 2008) and is equivalent to the definition above if the light enters from the reference medium (a vacuum).

3.3.1.1 Instruments used for the determination of refractive index

(i) ATAGO RX 5000 Refractometer

The RX-5000 digital refractometer gives quick and accurate measurements. The RX-5000 measures sample for refractive index with an accuracy and resolutions of ± 0.00004 and 0.00001/0.01 in four seconds the instrument ranges from 132700-1.5800*n*. All data, including date, time, current temperature, measurement result, measurement temperature, etc., are electronically displayed. It is used for testing and developing medicines, or chemical products, or processed foods, by checking the refractive index and concentration of materials as an auxillary means of analysis.

The instrument includes a printer output, RS-232C output, AC adapter (AD-11), power cable, keyboard mask, 3 plastic spoons, and 2 meters of tubing for connecting to separate circulating constant temperature bath, 10 tube tie bands, test report and instruction manual with Overall Dimensions is 37 × 20 × 12cm. Figure 3.6 shows the diagram of an ATAGO RX 5000 Refractometer.

(ii) Abbemat Digital Refractometer

Abbemat digital refractometers allow fast but less accurate refractive index measurements. They are factory calibrated with official standards from the Physikalisch-Technische Bundesanstalt (PTB, National Metrology Institute of Germany). Refractive index results from an Abbemat 300/350 are accurate to ± 0.0001 nD and for an Abbemat 500/550 ± 0.00002.

Abbemat 350/550 refractometers are set up conveniently with touchscreen. The instrument has a coloured LCD screen and membrane keys which are resistant to spillage and dirt. Instrument generates automatic warning if the sample is not large enough. There is a quick wipe system which cleans the prism after each measurement. Abbemat 350/550 measures turbid, coloured or opaque samples and all samples from liquids to pastes and polymers to solids. There is no influence from humidity, temperature or vibrations. A wide range of scales are stored in the Abbemat for converting refractive index into concentrations. Figure 3.7 shows the diagram of an Abbemat Digital Refractometer.

(iii) In this work for the measurement of refractive index the instrument Anton Paar refractive index analyzer RXA 156 was used. The description of the instrument is given in chapter 4 under section 4.2.

Figure 3.6 Diagram of an ATAGO RX 5000 Refractometer.

Figure 3.7 Diagram of an Abbemat Digital Refractometer 350/550.

B. THEORETICAL FRAMEWORK

3.4 LORENTZ-LORENZ EQUATION

In its original form the Lorentz-Lorenz equation derived for a binary mixture is due to Lorentz only (H. A. Lorentz "The theory of electrons and its application to the phenomena of light and radiant heat", 2nd ed. Dover publications, New York, 1953 (the first ed. was from Teabner, Leipzig, 1909). The reference as Lorentz-Lorenz equation is for the one component system which was derived independently by H. A. Lorentz and L. Lorentz (L. Lorentz, "Ueber die refraktionsconstante" Wied. Ann. 11 (1880) 70-103).

The Lorentz-Lorenz relationship between the refractive index at zero frequency and mean molecular polarizability, α, of a nonpolar, nonmagnetic material results in the following definition (Brocos *et al.* 2003) of molar refraction R,

$$R = V_{\mathrm{m}} \frac{\left(n^2 - 1\right)}{\left(n^2 + 2\right)} \tag{3.21}$$

where V_{m} is the molar volume. The molar refraction is also given by:

$$R = \frac{N_{\mathrm{A}} \alpha}{3\varepsilon_{\mathrm{o}}} \tag{3.22}$$

where N_{A} is the Avogadro constant and ε_{o} is the permittivity of free space.

Simple calculations show that, for a hard-core spherical model, $\alpha = 4\pi\varepsilon_0 a^3$, a being the sphere radius. Substitution for α into equation (3.22) yields $R = N_{\mathrm{A}} 4\pi a^3/3$; therefore, R represents the hard-core molar volume. Although these equations only hold at the zero frequency limit, they are also applicable at optical frequencies in non-highly conductive, non-magnetic materials (Brocos *et al.* 2003) and is an accurate expression for real liquids (Brocos *et al.* 2003; Iglesias *et al.* 2008). The molar refraction and molar volume can be used to obtain the molar free volume, $V_{\mathrm{m,f}}$, which represents the volume not occupied by molecules or ions, as $V_{\mathrm{m,f}} = V_{\mathrm{m}} - R$. This free volume expression is used in many liquid-state models, for instance, in those based on the van der Waals equation-of-state. Therefore, a joint analysis of

density and refractive index can provide highly useful information about the volumetric behaviour of a system.

The magnitude of the refractive index for mixtures presents some difficulties, since the refractive index values for an ideal solution are not as easily defined as those of typical Solution Thermodynamics quantities such as the volume, heat capacity, or enthalpy. This is a result of the refractive index not being an equilibrium property, since it is determined at frequencies of ±1015 Hz, which is very far from the zero frequency limits.

Very simple and reasonable assumptions can be used to establish a meaningful definition of "ideal" refractive index to obtain results consistent with thermodynamic data, and also useful for interpreting microscopic phenomena related to the mixing process (Marchetti *et al.*1999). The ideal molar refraction is obtained by using the expression:

$$R^{id} = x_1 R_1 + x_2 R_2 \tag{3.23}$$

where x_1 is the mole fraction of IL, x_2 is the mole fraction of alcohols, R^{id} is the "ideal molar refraction" R_1 is the molar refraction of IL and R_2 is the molar refraction of alcohols. The deviation in refractive index, ΔR, is equivalent to an excess function for an equilibrium quantity, and is given by $\Delta R = R - R^{id}$. If R is assumed to be equivalent to a hard-core volume, then ΔR should be small relative to the excess volume since changes in volume upon mixing are mainly a result from rearrangement at relative positions of the particles forming the mixture (Brocos *et al.* 2003) (*i.e.* changes in free volume).

Therefore, the hard-core volume of the particles changes very little from the pure liquids to a mixture, hence the molar refraction of the mixture is very similar to R^{id}. The application of equation (3.23) to real mixtures yields very small ΔR values relative to excess volumes (Brocos *et al.* 2002 and 2003); by contrast, other definitions, such as, that which calculates R^{id} by weighing pure component molar refractions with mole fractions, can provide ΔR values that are even higher than excess volumes (Fermeglia and Torriano 1999).

A rigorous definition of the "ideal" refractive index, n^{id}, can be obtained from the "ideal" volume and ''ideal" molar refraction, using equation (3.21), by assuming both quantities obey the volume additivity rule in terms of mole fractions. Based on these assumptions and equation (3.23), n^{id} is given by:

$$n^{id} = \left(\frac{n_1^2 n_2^2 + 2\phi_1 n_1^2 + 2\phi_2 n_2^2}{2 + \phi_1 n_2^2 + \phi_2 n_1^2} \right)^{1/2} \tag{3.24}$$

where $\phi_1 = \dfrac{x_1 V_{m,1}}{x_1 \dfrac{M_1}{\rho_1} + x_2 \dfrac{M_2}{\rho_2}}$ is the volume fraction of the IL and $V_{m,1}$ is the molar volume of the IL, M_1 is the molar mass of IL, M_2 is the molar mass of alcohols, ρ_1 is the density of IL and ρ_2 is the density of alcohols. Under the assumption that the difference between the refractive indices of the two components is small, equation (3.24) can be substantially simplified (Missen1969) to:

$$n^{id} = \phi_1 n_1 + \phi_2 n_2 \tag{3.25}$$

The deviation of the refractive index is defined as $\Delta n = n - n^{id}$, n^{id} being given by equations (3.24) or (3.25). The latter definition of n^{id} has been frequently used and provided good, consistent results (Brocos *et al.* 2003; Marchetti *et al.* 1999; Mosteiro *et al.* 2001). This is not the case with other definitions of n^{id} such as that based on mole fraction, $n^{id} = x_1 n_1 + x_2 n_2$, which is also frequently used but has no physical ground and usually gives meaningless results (Ritzoulis and Fidantsi 2000; Nath and Mishra 1998; Jiménez *et al.* 2000).

Because the approximation that molar refraction behaves ideally equation (3.23) is highly accurate for most of the binary systems studied to date (Brocos *et al.* 2003) and it can be used to make accurate predictions. Thus, the density and refractive index of pure compounds, and the refractive index of their mixture can be used in conjunction with equation (3.23) to estimate the density of the mixture. The refractive index of the mixture can be estimated by using the inverse procedure if the density and

refractive index of the pure components, and the density of the mixture, are known (Fermeglia and Torriano, 1999).

3.4.1 Prediction of density by the Lorentz-Lorentz (L-L) approximation

If the experimental molar refraction is assumed to behave as an ideal mixture, the following predictive expression for ρ can be obtained from equations (3.21) and (3.23) within the frame-work of the Lorentz–Lorenz approximation.

$$\rho = \frac{\left(\frac{n^2-1}{n^2+2}\right)\left(x_1 M_1 + x_2 M_2\right)}{\left(\frac{n_1^2-1}{n_1^2+2}\right)x_1 \frac{M_1}{\rho_1} + x_2\left(\frac{n_2^2-1}{n_2^2+2}\right)\frac{M_2}{\rho_2}} \tag{3.26}$$

Equation (3.26) was used to predict the density of the binary mixture, ρ, hence, if ρ_i and n_i for the pure components, and n for the mixture, are known, the density of the mixture can be estimated.

3.4.2 Correlation of excess molar volume by the Lorentz-Lorenz approximation

Correlation of the excess molar volume can be obtained using the refractive index obtained for the binary mixtures by the Lorentz-Lorenz approximation.

Within the framework of the Lorentz-Lorenz approximation, V_m^E can be correlated via the change in reduced free volume, namely:

$$\Delta\left(\frac{V_{m,f}}{R}\right) = \frac{V_{m,f}}{R} - \left(\frac{V_{m,f}}{R}\right)^{id}$$

(3.27) Application of the Lorentz-Lorenz equation allows this expression to be reduced to:

$$\Delta\left(\frac{V_{m,f}}{R}\right) = \frac{3}{n^2-1} - \frac{3}{\left(n^{id}\right)^2-1} \tag{3.28}$$

The assumption $R = R^{id}$, is most often a highly accurate approximation. The following expression can then be obtained from equation (3.28).

$$\Delta\left(\frac{V_{m,f}}{R}\right) = \frac{V_m^E}{R} \tag{3.29}$$

where $V_m^f - V_{m,f}^{id} = V_{m,f} = V_m^E$

Therefore,

$$V_m^E = (-\Delta n)\frac{3R(n^{id} + n)}{(n^2-1)((n^{id})^2-1)} = (-\Delta n) f(R, n^{id}, n) \tag{3.30}$$

3.4.3 Prediction of refractive index by Lorentz-Lorenz approximation

From equation (3.31) can be obtained and allows one to obtain the inverse prediction *i.e.*, to predict *n* from the pure solvent density and refractive index data and from the experimental density of the mixture. The Lorentz-Lorenz equation for the prediction of *n* is given below:

$$n = \left(\frac{2\left[\left(\frac{n_1^2-1}{n_1^2+2}\right)x_1\rho\frac{M_1}{\rho_1} + x_2\left(\frac{n_2^2-1}{n_2^2+2}\right)\rho\frac{M_2}{\rho_2}\right] + \left[x_1 M_1 + x_2 M_2\right]}{\left[x_1 M_1 + x_2 M_2\right] - \left[\left(\frac{n_1^2-1}{n_1^2+2}\right)x_1\rho\frac{M_1}{\rho_1} + x_2\left(\frac{n_2^2-1}{n_2^2+2}\right)\rho\frac{M_2}{\rho_2}\right]} \right)^{1/2} \tag{3.31}$$

On simplifying equation (3.26) equation (3.31) is obtained. The derivation is given below:

$$\rho = \frac{\left(\frac{n^2-1}{n^2+2}\right)(x_1 M_1 + x_2 M_2)}{\left(\frac{n_1^2-1}{n_1^2+2}\right)x_1\frac{M_1}{\rho_1} + x_2\left(\frac{n_2^2-1}{n_2^2+2}\right)\frac{M_2}{\rho_2}} \tag{3.26}$$

$$1 = \frac{\left(\frac{n^2-1}{n^2+2}\right)\left(x_1 M_1 + x_2 M_2\right)}{\left(\frac{n_1^2-1}{n_1^2+2}\right)x_1\rho\frac{M_1}{\rho_1} + x_2\rho\left(\frac{n_2^2-1}{n_2^2+2}\right)\frac{M_2}{\rho_2}} \tag{3.32}$$

Assume:

$$a = x_1M_1 + x_2M_2 \text{ and} \tag{3.33}$$

$$b = \left(\frac{n_1^2-1}{n_1^2+2}\right)x_1\rho\frac{M_1}{\rho_1} + x_2\rho\left(\frac{n_2^2-1}{n_2^2+2}\right)\frac{M_2}{\rho_2} \tag{3.34}$$

Equation (3.32) becomes

$$1 = \frac{\left(\frac{n^2-1}{n^2+2}\right)a}{b} \tag{3.35}$$

$$\frac{b}{a} = \frac{n^2-1}{n^2+2} \tag{3.36}$$

$$b\,(n^2+2) = a\,(n^2-1) \tag{3.37}$$

$$n^2 = \frac{2b+a}{a-b} \tag{3.38}$$

$$n = \sqrt{\frac{2b+a}{a-b}} \tag{3.39}$$

after substituting the values of *a* and *b* from equations (3.33) and (3.34) in equation (3.39) the Lorentz-Lorenz predictive equation (3.31) for *n* is obtained.

CHAPTER 4

EXPERIMENTAL

A. EXCESS MOLAR VOLUME AND ISENTROPIC COMPRESSIBILITY

4.1 APPARATUS AND TECHNIQUE

4.1.1 Density and sound velocity meter (DSA 5000 M)

In this work ρ and u were determined using the Anton Paar oscillating U-tube DSA 5000 M. This device simultaneously determines two independent physical properties using one sample. The two-in-one instrument is equipped with a density cell and a sound velocity cell thus combining the Anton Paar oscillating U-tube method with a highly accurate instrument for the measurement of sound velocity. Both cells are temperature-controlled by a built-in Peltier thermostat. The temperature is controlled to

± 0.02 K.

4.1.2 Definition of density

The density ρ of a sample is defined as the mass, (m) divided by the volume, (V):

$$\rho = \frac{m}{V} \tag{4.1}$$

Density values are highly temperature dependent.

4.1.3 Oscillating U-tube method

The sample is introduced into a U-shaped borosilicate glass tube that is excited to vibrate at its characteristic frequency electronically. The characteristic frequency changes depending on the density of the sample. Through a precise determination of the characteristic frequency and a mathematical conversion, the density of the sample can be measured. Figures 4.1 and 4.2 shows the photographs of the DSA 5000 M and the DSA 5000 M together with the RXA 156 and Xsample 452.

The density, ρ, is calculated from the quotient of the period of oscillation of the U-tube and the reference oscillator:

$$\rho = KA \times Q^2 \times f_1 - KB \times f_2 \qquad (4.2)$$

KA, KB Apparatus constant

Q Quotient of the period of oscillation of the U-tube divided by the period of oscillation of the reference oscillator

f_1, f_2 Correction terms for temperature, viscosity and non-linearity

The value of the density is displayed on the LCD screen. The DSA 5000 M is coupled with a computer which is loaded with software that stores all the measured density values.

Figure 4.1 Photograph of the Density and Sound Velocity Meter (DSA 5000 M).

(Taken from Instruction Manual of Anton Paar DSA 5000 M)

Figure 4.2 Photograph of the DSA 5000 M along with RXA 156 and Xsample 452.

(Taken from Instruction Manual of Anton Paar DSA 5000 M)

4.1.4 Sound velocity analyser

The sample is introduced into the sound velocity measuring cell that is bordered by an ultrasonic transmitter on the one side, and a receiver on the other side. The transmitter sends sound waves of a known period through the sample. The velocity of sound, u, can be calculated by using the period of the sound waves and the distance between the transmitter and receiver.

$$u = \frac{l \times (1 + 1.6 \times 10^{-5} \times \Delta T)}{\frac{\mathrm{P_s}}{512} - \mathrm{A} \times \mathrm{f_3}} \tag{4.3}$$

where l is the original path length of the sound waves, ΔT is the temperature deviation to 278.15 K, P_S is the oscillation period of the received sound waves, A is apparatus constant for sound velocity, and f_3 is the correction term for temperature.

Due to the high temperature dependency of the density and velocity of sound, the measuring cells are thermostated precisely, using the Peltier elements.

4.1.5 Features of DSA 5000 M

4.1.5.1 Accuracy

DSA 5000 M instrument is equipped with the world's most advanced digital density and sound velocity measurement technology where:

- the period of oscillation of the U-tube is measured by optical pickups.
- two integrated Pt 100 platinum thermometers together with the Peltier elements provide an extremely precise thermostatting of the sample.
- there is a ThermoBalance which is an additional reference oscillator that provides long-term stability and enables precise measurements over the whole temperature range of the instrument with only one adjustment at 293.15 K.
- viscosity-related errors are automatically corrected over the full viscosity range by measuring the damping effect of the viscous sample followed by a mathematical correction for the density value.
- special adjustments with standards of high viscosity and high density lead to an enhanced precision when samples with high viscosity and high density are used.

4.1.5.2 Error detection

A major source of measuring errors when using a density and sound velocity meter are gas bubbles in the measuring cells. To reduce the formation of gas bubbles Anton Paar introduced two new features:

- Filling Check: The instrument automatically detects gas bubbles in the density measuring cell by an advanced analysis of its oscillation pattern and generates a warning message.
- U-View: Using a real-time camera with zoom function the U-tube can be visually inspected for gas bubbles in the density measuring cell.

The Specifications for the DSA 5000 M is given in table 4.1

Table 4.1 Specifications of the DSA 5000 M.

Measuring range density	0 to 3 g/cm^3
Measuring range sound velocity	1000 to 2000 m/s
Measuring range temperature	273.15 to 343.15 K (32 to 158 ^{o}F)
Pressure range	0 to 3 bar (0 to 44 psi)
Repeatability density	0.000001 g/cm^3
Repeatability sound velocity	0.1 m/s
Repeatability temperatures	273.151 K (0.002 ^{o}F)
Measuring time per sample	1 to 4 minutes
Sample volume	approx. 3 ml
Ambient air pressure sensor	yes
Reference oscillator	yes
Automatic bubble detection	yes
Visual check of the density measuring cell	camera

B. REFRACTIVE INDEX

4.2 EXPERIMENTAL APPARATUS

In this work Δn was determined using the Anton Paar refractive index analyzer RXA 156. The DSA 5000 M was coupled with the RXA 156.

4.2.1 An overview of Anton Paar refractive index analyzer RXA 156

The RXA 156 and RXA 170 modules are equipped with a micro flow cell and an integrated Peltier thermostat ensuring accurate and automatic temperature control. Fast and non-destructive measurements, requiring only small sample volume, yield to refractive index (RI) and RI-derived results. Both RXA types can be used as a module in measuring systems.

4.2.2 Features of Anton Paar refractive index analyzer RXA 156

- It can be combined with a DMA 4100/4500/5000 M, DSA 5000 M or Soft Drink Analyzer M.
- RXA 156/170 instruments can be used separately.
- For pasty or expensive samples, manual filling of the refractometer is possible.
- Simple adjustment of the DSA 5000 M and RXA 156/170 using air and water in one procedure.
- Automatic filling and cleaning of the DSA 5000 M and RXA 156/170 sample changer.

One measuring cycle, three sample parameters

- Save time by simultaneously determining the density, sound velocity, and refractive index.
- Fast and reliable results.

Reliable measuring methods

- Established U-tube method for measuring density.
- Highly accurate measurement of the angle of total reflection for determining the refractive index.

Table 4.2 lists the specifications of the refractometer RXA 156.

Table 4.2 Specifications of the refractometer RXA 156.

Refractive index	
Measuring range	1.32 – 1.56 nD
Resolution	0.000001
Accuracy	0.00002
Temperature	
Measuring temperature	283.15 - 343.15 K
Resolution	273.16 K
Accuracy	273.18 K
Stability	273.152 K
Speed of temperature change from ambient temperature to 293.15 K	20 s

4.3 CHEMICALS

The alcohols used in this work were purchased from Sigma Aldrich with a mass % purity >99.5 % for 1- propanol and 2-propanol >99.9 % methanol and for 1-butanol >99.0 %. The IL was supplied by Aldrich with a purity >97.0 %. The IL and alcohols were used without any further purification and stored in a desiccator with molecular sieves to reduce absorption of moisture. The water content in the IL was determined using a Metrohm Karl Fischer coloumeter and found to be 0.0024 mole fraction. The purity of the solvents was assessed by comparison of the experimental density, speed of sound and refractive index value with literature values. The purity of alcohols were analysed by g.l.c. and found to have a single peak which shows that alcohols used in this work are 99.0 % pure and are not contaminated with any other organic solvents.

A summary of the chemicals, used in this work their suppliers are given in table 4.3.

Tables 4.4, 4.5 and 4.6 gives the experimental and literature values for densities, speeds of sound and refractive indices of the pure compounds, respectively. The maximum deviation between the literature and experimental ρ, u and n is $\pm$ 0.0007 g·cm^{-3}, $\pm$ 4 m·s^{-1} and $\pm$ 0.001 respectively.

Table 4.3 Chemicals, suppliers and mass % purity.

Chemicals	Suppliers	Mass % Purity
Methanol	Sigma Aldrich	99.9
1-Propanol	Sigma Aldrich	99.5
2-Propanol	Sigma Aldrich	99.5
1-Butanol	Sigma Aldrich	99.0
$[BMIM]^+[MeSO_4]^-$	Sigma	97.0

Table 4.4 Literature and experimental densities, ρ, of pure components at T = (298.15, 303.15, 308.15, and 313.15) K.

Chemicals	ρ / (g · cm^{-3})					
	Literature	Experimental				
	T/K 298.15	T/K 298.15	T/K 303.15	T/K 308.15	T/K 313.15	Deviation
Methanol	0.786710[a]	0.787405	0.782688	0.777941	0.773168	0.0007
1-Propanol	0.799527[b]	0.800008	0.795970	0.791892	0.787772	0.0005
2-Propanol	0.780824[b]	0.781123	0.776845	0.772487	0.768053	0.0003
1-Butanol	0.805778[b]	0.805930	0.802088	0.798214	0.794301	0.0002
$[BMIM]^+[MeSO_4]^-$	1.21222[c]	1.212060	1.208702	1.205348	1.202010	0.0002
Ultra-pure water	0.99705[d]	0.99704	0.99564	0.99403	0.99221	0.00001

[a] (Alvarez *et al.* 2011).

[b] (Zafarani-Moattara *et al.* 2006).

[c] (Pereiro *et al.* 2007).

[d] (Calvar *et al.* 2007).

Table 4.5 Literature and experimental speed of sound, *u*, of pure components at *T* = (298.15, 303.15, 308.15, and 313.15) K.

Chemicals	***u* / (m · s^{-1})**					
	Literature	**Experimental**				
	T/K 298.15	*T*/K 298.15	*T*/K 303.15	*T*/K 308.15	*T*/K 313.15	Deviation
Methanol	1102.98[a]	1104.30	1088.26	1072.04	1055.91	1.32
1-Propanol	1205.76[b]	1205.93	1189.26	1172.37	1155.53	0.17
2-Propanol	1138.87[b]	1138.71	1121.43	1103.94	1086.62	0.16
1-Butanol	1239.39[c]	1239.28	1222.88	1206.26	1189.68	0.11
$[BMIM]^+[MeSO_4]^-$	1658.4[d]	1654.61	1642.21	1629.95	1617.92	3.79
Ultra-pure water	1497.0[e]	1497.00	1509.44	1520.12	1529.18	0.00

[a] (Alvarez *et al.* 2011).

[b] (Zafarani-Moattara *et al.* 2006).

[c] (Zorębski and Geppert-Rybczyńska 2010).

[d] (Pereiro *et al.* 2007).

[e](Calvar *et al.* 2007).

Table 4.6 Literature and experimental refractive index, *n*, of pure components at *T* = (298.15, 303.15, 308.15, and 313.15) K.

Chemicals	*n*					
	Literature	Experimental				
	T/K 298.15	*T*/K 298.15	*T*/K 303.15	*T*/K 308.15	*T*/K 313.15	Deviation
Methanol	1.32645[a]	1.327198	1.325520	1.323624	1.321707	0.0007
1-Propanol	1.38317[b]	1.383336	1.381308	1.379257	1.377217	0.0002
2-Propanol	1.37521[c]	1.375271	1.373142	1.370929	1.368704	0.00006
1-Butanol	1.3975[d]	1.397467	1.395487	1.393417	1.391377	0.00003
$[BMIM]^+[MeSO_4]^-$	1.47942[e]	1.478238	1.477044	1.475766	1.474429	0.0012
Ultra-pure water	1.33251[f]	1.33250	1.331932	1.331295	1.330586	0.00001

[a] (Marino *et al.* 2001).

[b] (Tu Chein-Hsiun *et al.* 2001).

[c] (Rodriguez *et al.* 2001).

[d] (Arce *et al.* 2001).

[e] (Pereiro *et al.* 2007).

[f](Calvar *et al.* 2007).

4.4 PREPARATION OF MIXTURES

The binary mixtures were prepared by transferring the pure liquids via a syringe into stoppered bottles to prevent evaporation. An OHAUS (Pine Brook, NJ, USA) mass balance was used to determine the exact mass of each component of the mixture. The mass balance has a precision of 0.0001 g. The mixtures were shaken in order to ensure complete homogeneity of the two compounds, since the ionic liquid is slightly viscous. All samples were prepared immediately prior to performing the density, speed of sound or refractive index measurements to avoid variations in composition due to evaporation of solvent.

C. EXPERIMENTAL PROCEDURE FOR INSTRUMENT

4.5 DENSITIES AND SPEED OF SOUND

The density and speed of sound of pure liquids and mixtures were measured using a digital vibrating-tube densimeter and speed of sound analyzer (Anton Paar DSA 5000 M) with an accuracy and repeatability of ± 0.001 K for temperature, (± $5 \cdot 10^{-6}$ and ± 10^{-6}) g·cm^{-3} for density, and (± 0.01 and ± 0.1) m·s^{-1} for speed of sound. The two-in-one instrument is equipped with a density cell and a sound velocity cell. Both cells are temperature-controlled by a built-in Peltier thermostat. The density and speed of sound experimental uncertainties were less than ± $3 \cdot 10^{-5}$ g·cm^{-3} and ± 0.5 m·s^{-1}.

Prior to each experimental run, the cell was first cleaned with ethanol (liquid 1) and then dried with acetone (liquid 2) using a fully automatic Xsample 452 Module. Xsample 452 performs a cleaning routine after each measurement. Rinsing ethanol (liquid 1) dissolves sample residues in the measuring cell of the DSA 5000 M. Rinsing acetone (liquid 2) is highly volatile and soluble in rinsing liquid 1. Acetone removes cleaning liquid 1 and is easily evaporated by a stream of dry air in order to accelerate drying of the cell. Acetone is a good solvent for removing ethanol. After rinsing and cleaning the instrument was calibrated by Ultra-pure water and ambient air. The goal of a calibration is to validate the accuracy of the

density measurement. The accuracy of the sound velocity measurement can be validated by comparing it with the literature values of the sound velocity for ultra-pure water standard (Anton Paar GmbH). Each binary mixture is placed in a vial 12 mL and sealed with a cap. Each vial is placed onto the Xsample 452 with a 48-position magazine. The DSA 5000 M automatically detects the connected Xsample 452. The sample changer automatically fills the binary solutions from each sample vial into the measuring cell of the DSA 5000 M. The binary mixtures are filled easily and safely without evaporation losses or the formation of bubbles. The instrument automatically detects gas bubbles in the measuring cell by an advanced analysis of its oscillations pattern and generates a warning message. The instrument software also allows visual inspection for one of the gas bubble on an external PC using a real time camera with zoom function. After each measurement, the measuring cell is automatically rinsed and cleaned with up to two rinsing liquids and subsequently dried. Density and speed of sound results are shown together on the LED display, and the computer software.

4.6 REFRACTIVE INDICES

Measurement of the refractive index of pure liquids and mixtures were obtained using a digital automatic refractometer (Anton Paar RXA 156) with accuracy and repeatability of ± 0.03 K for temperature and ± $2 \cdot 10^{-5}$ for refractive index. The RXA 156 measuring module is operated in combination with the density and sound velocity analyzer DSA 5000 M. The measuring results of the RXA 156 are transmitted to the DSA 5000 M instrument where refractive indices are displayed, saved and can be exported or printed. The LED screen displays the result of all three properties namely, density, speed of sound and refractive index. The instrument was calibrated by measuring the refractive index of Ultra-pure water before each series of measurements according to the procedure in the instruction manual. The calibration was checked with pure liquids with known refractive indices. The refractive index experimental uncertainties were less than ± $2 \cdot 10^{-5}$.

4.7 VALIDATION OF EXPERIMENTAL TECHNIQUE

The experimental technique was assessed by determining the excess molar volume, deviation in isentropic compressibility and change in refractive index on mixing for the test system (diethyl carbonate + ethanol) at the temperature 298.15 K and comparing it with literature values (Rodriguez *et al.* 2001). The difference between experimental and literature excess molar volume, deviation in isentropic compressibility and change of refractive index on mixing for the test system were within the experimental error. The root mean square deviation, RMSD, between experimental and literature excess molar volume, deviation in isentropic compressibility and change of refractive index on mixing for the test system at T = 298.15 K are 0.002 $cm^3 \cdot mol^{-1}$, 0.7 × 10^{12} Pa^{-1} and 0.00009 respectively. Equation (4.4) is used to calculate the root-mean-square deviations. Where $Z_{exp,}$ $Z_{cal,}$ and n, are the values of the experimental and calculated property and the number of experimental data points, respectively.

$$\mathrm{RMSD} = \left(\frac{\sum_{i}^{n} \left(Z_{\mathrm{exp}} - Z_{\mathrm{cal}} \right)^2}{n\text{-}1} \right)^{1/2} \tag{4.4}$$

The graphs of the literature and experimental data for $V_{\mathrm{m}}^{\mathrm{E}}$, $\Delta\kappa_s$, and Δn are given in figures 4.3, 4.4 and 4.5, respectively.

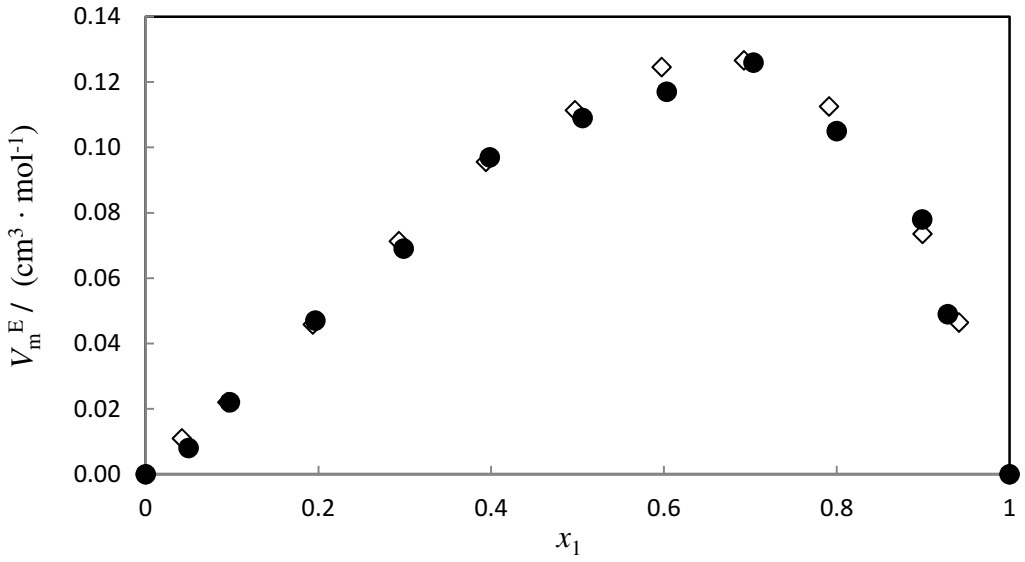

Figure 4.3 Comparison of the V_m^E from this work with the literature data for the mixtures {$C_5H_{10}O_3$ (x_1) + C_2H_6O (x_2)} at T = 298.15 K, ●, literature data (Rodriguez *et al*. 2001); ◊, this work.

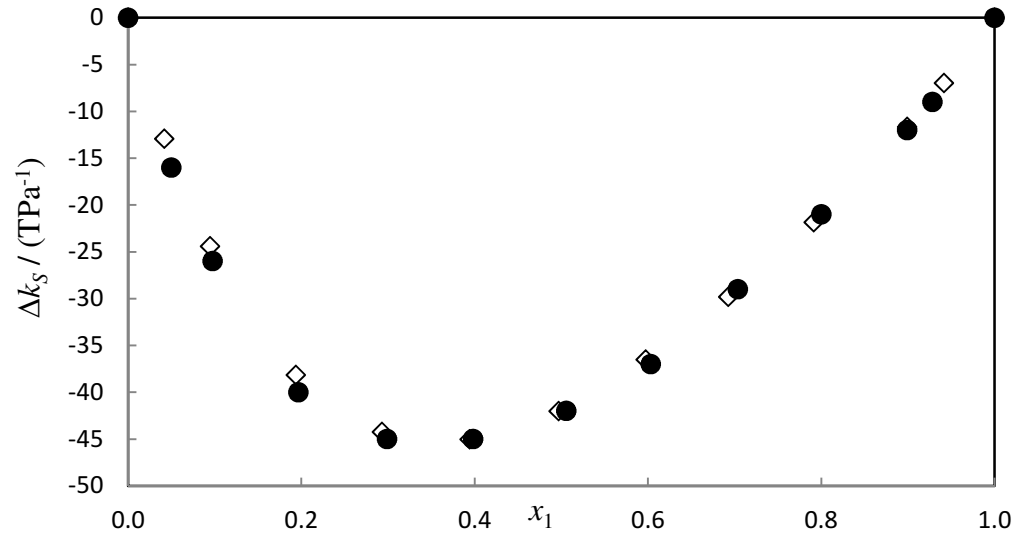

Figure 4.4 Comparison of the $\Delta\kappa_s$ from this work with the literature data for the mixtures {$C_5H_{10}O_3$ (x_1) + C_2H_6O (x_2)} at T = 298.15 K, ●, literature data (Rodriguez *et al*. 2001); ◊, this work.

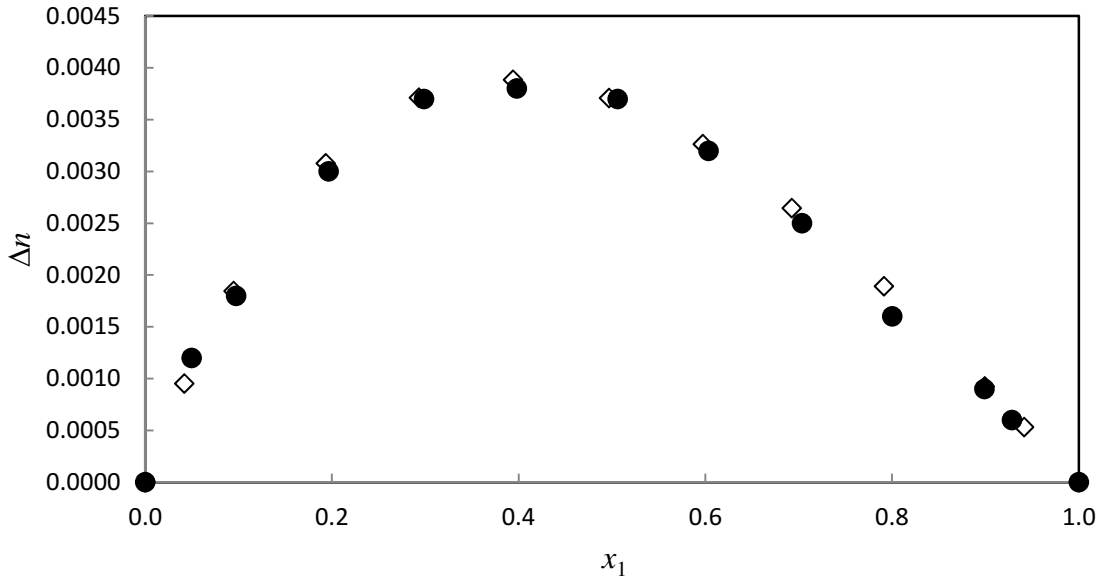

Figure 4.5 Comparison of the Δn from this work with the literature data for the mixtures {$C_5H_{10}O_3$ (x_1) + C_2H_6O (x_2)} at T = 298.15 K, ●, literature data (Rodriguez *et al*. 2001); ◊, this work.

4.8 SYSTEMS STUDIED IN THIS WORK

The densities, speed of sound, and refractive indices for the binary systems ($[BMIM]^+[MeSO_4]^-$ + methanol, or 1-propanol, or 2-propanol, or 1-butanol) were experimentally measured over the whole range of composition at T = (298.15, 303.15, 308.15, and 313.15) K. From the experimental data, excess molar volumes, excess isentropic compressibilities, deviation in refractive indices and molar refractions were calculated. The Redlich-Kister smoothing polynomial equation was satisfactorily applied for the correlation of V_m^E, κ_S^E, and Δn to give the fitting parameters and the root-mean-square deviations. The Lorentz-Lorenz equation was also used to correlate the volumetric property and for the refractive index prediction or of the density of binary mixtures of the ionic liquid and organic solvents.

CHAPTER 5

RESULTS

5.1 EXCESS MOLAR VOLUME, V_m^E, CHANGE IN REFRACTIVE INDEX ON MIXING, Δn, EXCESS ISENTROPIC COMPRESSIBILITY, κ_S^E, AND MOLAR REFRACTION, R

The density, speed of sound, excess molar volume, isentropic compressibility and excess isentropic compressibility, of the binary mixtures ($[BMIM]^+[MeSO_4]^-$ + methanol, or 1-propanol, or 2-propanol, or 1- butanol) in the range at T = (298.15, 303.15, 308.15 and 313.15) K are presented in tables 5.1-5.4. The values of the pure component isobaric thermal expansivity, α_P, and heat capacity, C_P, at several temperatures is given in table 5.5.

$$V_m^E = V_m - V_m^{id} = \frac{x_1 M_1 + x_2 M_2}{\rho} - \frac{x_1 M_1}{\rho_1} - \frac{x_2 M_2}{\rho_2} \quad (5.1)$$

In this equation, x_1 and x_2 are the mole fractions, V_m is the molar volume and V_m^{id} is the ideal molar volume, M_1 and M_2 are the molar masses, ρ_1 and ρ_2 are the densities of the pure components, where 1 and 2 refer to the IL and the alcohol, respectively, and ρ is the density of the mixture.

Equation (5.2) was used to calculate the excess isentropic compressibilities, κ_S^E

$$\kappa_S^E = \kappa_S - \kappa_S^{id} \quad (5.2)$$

The isentropic compressibility (Vercher *et al.* 2010) was calculated using the expression:

$$\kappa_S^{id} = \phi_1 \kappa_{S,1}^o + \phi_2 \kappa_{S,2}^o + T\left[\frac{\phi_1 V_1^o \left(\alpha_{P,1}^o\right)^2}{C_{P,1}^o} + \frac{\phi_2 V_2^o \left(\alpha_{P,2}^o\right)^2}{C_{P,2}^o} - \frac{V_m^{id}\left(\alpha_P^{id}\right)^2}{C_{P,m}^{id}}\right] \tag{5.3}$$

where κ_S^E, $\kappa_{S,1}^o$, $\alpha_{P,1}^o$, and $C_{P,1}^o$ are the excess isentropic compressibility, isentropic compressibility, the isobaric thermal expansivity, and the isobaric molar heat capacity, respectively, of pure component *i* of the mixture. α_P^{id} and $C_{P,m}^{id}$ for the ideal mixture is defined as:

$$\alpha_P^{id} = \phi_1 \alpha_{P,1}^o + \phi_2 \alpha_{P,2}^o \tag{5.4}$$

$$C_{P,m}^{id} = x_1 C_{P,1}^o + x_2 C_{P,2}^o \tag{5.5}$$

The isobaric thermal expansivity α_P of pure components, defined as:

$$\alpha_P = \frac{1}{V_m}\left(\frac{\partial V_m}{\partial T}\right)_P = -\frac{1}{\rho}\left(\frac{\partial \rho}{\partial T}\right)_P \tag{5.6}$$

The pure component isobaric thermal expansivity, α_p, and heat capacity, C_p, needed for the calculation of κ_S^E are given in table 5.5.

The excess partial molar volumes along with partial molar volumes were calculated at T = 298.15 K and are given in tables 5.6-5.9. The values of the measured molar volumes were used to calculate the excess partial molar volumes at each mole fraction using the relationship $V_{m,1}^E = \left(V_{m,1} - V_{m,1}^*\right)$ and $V_{m,2}^E = \left(V_{m,2} - V_{m,2}^*\right)$ where $V_{m,1}^*$ and $V_{m,2}^*$ represent the molar volumes of the pure components at each mole fraction. The partial molar volumes $V_{m,1}$ and $V_{m,2}$ were evaluated (Pal and Singh 1996) over the whole composition range by using equations (5.7) and (5.8):

$$V_{m,1} = V_{m,1}^* + V_m^E + x_1\left(\delta V_m^E / \delta x_1\right) \tag{5.7}$$

$$V_{m,2} = V^{*}_{m,2} + V^{E}_{m} + x_2\left(\delta V^{E}_{m} / \delta x_2\right) \tag{5.8}$$

The derivatives in equations (5.7) and (5.8) were obtained by differentiation of equation (5.13).

Refractive index deviations are calculated by volume fraction using the expressions:

$$\Delta n = n - n^{id} \tag{5.9}$$

$$n^{id} = \phi_1 n_1 + \phi_2 n_2 \tag{5.10}$$

n^{id} is calculated by using volume fraction rather than using the molar volume which is:

$$n^{id} = x_1 n_1 + x_2 n_2 \tag{5.11}$$

The molar refraction, R, can be defined from refractive index and molar volume as:

$$R = \left(\frac{n^2 - 1}{n^2 + 2}\right) V_m \tag{5.12}$$

In these equations, x_1 and x_2 represents the mole fraction of component 1 or 2, n_1 and n_2 are the refractive index of pure components of 1 or 2, and V_m is the molar volume.

The refractive index, change in refractive index, and molar refraction are given in tables 5.10-5.13.

Table 5.1 Density (ρ), excess molar volume (V^E), speed of sound (u), isentropic compressibility (κ_s), and excess isentropic compressibility (κ_S^E), for the binary mixture {[BMIM]$^+$[MeSO$_4$]$^-$ (x_1) + Methanol (x_2)} at T = (298.15 to 313.15) K.

x_1	ρ / (g · cm^{-3})	V_m^E / (cm^3 · mol^{-1})	u / (m · s^{-1})	κ_s / 10^{10} Pa^{-1}	κ_S^E / 10^{10} Pa^{-1}
		T = 298.15 K			
0.0000	0.78741	0.000	1104.3	10.4	0.0
0.0422	0.87119	-0.337	1191.8	8.1	-74.3
0.0940	0.94240	-0.510	1273.9	6.5	-112.1
0.1857	1.02784	-0.877	1384.7	5.1	-123.1
0.2858	1.08479	-1.043	1464.0	4.3	-109.2
0.3729	1.11830	-1.093	1512.2	3.9	-92.2
0.4772	1.14638	-1.014	1553.5	3.6	-72.0
0.5769	1.16612	-0.897	1583.1	3.4	-54.3
0.6775	1.18129	-0.732	1606.1	3.3	-38.6
0.7947	1.19494	-0.498	1627.0	3.2	-22.7
0.8923	1.20415	-0.306	1641.7	3.1	-11.2
0.9526	1.20898	-0.170	1649.4	3.0	-4.7
1.0000	1.21206	0.000	1654.6	3.0	0.0
		T = 303.15 K			
0.0000	0.78269	0.000	1088.3	10.8	0.00
0.0422	0.86677	-0.354	1176.5	8.3	-75.2

Table 5.1 continued

0.0940	0.93821	-0.537	1259.6	6.7	-113.7
0.1857	1.02391	-0.912	1371.1	5.2	-125.0
0.2858	1.08104	-1.079	1450.9	4.4	-111.1
0.3729	1.11465	-1.128	1499.4	4.0	-93.9
0.4772	1.14282	-1.045	1540.9	3.7	-73.4
0.5769	1.16261	-0.923	1570.7	3.5	-55.4
0.6775	1.17783	-0.752	1593.8	3.3	-39.4
0.7947	1.19150	-0.508	1614.7	3.2	-23.2
0.8923	1.20073	-0.309	1629.5	3.1	-11.4
0.9526	1.20560	-0.172	1637.2	3.1	-4.8
1.0000	1.20870	0.000	1642.2	3.1	0.0
		T = 308.15 K			
0.0000	0.77794	0.000	1072.0	11.2	0.0
0.0422	0.86233	-0.373	1161.3	8.6	-74.6
0.0940	0.93401	-0.566	1245.1	6.9	-112.8
0.1857	1.01999	-0.949	1357.5	5.3	-124.2
0.2858	1.07729	-1.118	1437.7	4.5	-110.5
0.3729	1.11100	-1.166	1486.4	4.1	-93.5
0.4772	1.13926	-1.079	1528.3	3.8	-73.0
0.5769	1.15912	-0.952	1558.2	3.6	-55.2
0.6775	1.17438	-0.774	1581.4	3.4	-39.2
0.7947	1.18807	-0.519	1602.4	3.3	-23.1
0.8923	1.19733	-0.313	1617.2	3.2	-11.4
0.9526	1.20223	-0.174	1624.9	3.2	-4.8

Table 5.1 continued

1.0000	1.20535	0.000	1630.0	3.1	0.0
		T = 313.15			
0.0000	0.77317	0.000	1055.9	11.6	0.0
0.0422	0.85789	-0.393	1146.2	8.9	-74.7
0.0940	0.92982	-0.596	1230.8	7.1	-113.1
0.1857	1.01606	-0.989	1343.9	5.4	-124.9
0.2858	1.07354	-1.159	1424.6	4.6	-111.3
0.3729	1.10737	-1.205	1473.6	4.2	-94.2
0.4772	1.13572	-1.114	1515.7	3.8	-73.6
0.5769	1.15564	-0.982	1545.9	3.6	-55.7
0.6775	1.17094	-0.797	1569.2	3.5	-39.6
0.7947	1.18465	-0.531	1590.3	3.3	-23.3
0.8923	1.19393	-0.316	1605.1	3.3	-11.5
0.9526	1.19887	-0.177	1612.9	3.2	-4.9
1.0000	1.20201	0.000	1617.9	3.2	0.0

Table 5.2 Density (ρ), excess molar volume (V_m^E), Speed of sound (u), isentropic compressibility (κ_s), and excess isentropic compressibility (κ_S^E), for the binary mixture {[BMIM]$^+$[MeSO$_4$]$^-$ (x_1) + 1-Propanol (x_2)} at T = (298.15 to 313.15) K.

x_1	ρ / (g · cm^{-3})	V_m^E / (cm^3 · mol^{-1})	u / (m · s^{-1})	κ_s / 10^{10}Pa^{-1}	κ_S^E / 10^{10}Pa^{-1}
		T = 298.15 K			
0.0000	0.80001	0.000	1205.9	8.6	0.0
0.0482	0.85243	-0.200	1242.8	7.6	-35.2
0.0965	0.89646	-0.287	1276.0	6.9	-57.2
0.1937	0.96758	-0.383	1338.1	5.8	-77.4
0.2929	1.02311	-0.410	1394.2	5.0	-79.9
0.3903	1.06653	-0.449	1443.9	4.5	-73.8
0.4958	1.10430	-0.444	1491.7	4.1	-62.7
0.5900	1.13204	-0.422	1529.8	3.8	-51.1
0.6907	1.15690	-0.366	1566.3	3.5	-38.1
0.7981	1.17934	-0.305	1601.1	3.3	-24.3
0.8932	1.19648	-0.255	1629.0	3.1	-12.6
0.9510	1.20524	-0.126	1643.1	3.1	-5.5
1.0000	1.21206	0.000	1654.6	3.0	0.0
		T = 303.15 K			
0.0000	0.79597	0.000	1189.3	8.9	0.0
0.0482	0.84850	-0.214	1227.1	7.8	-33.4
0.0965	0.89260	-0.308	1276.0	6.9	-54.6
0.1937	0.96382	-0.410	1323.8	5.9	-74.0

Table 5.2 continued

0.2929	1.01943	-0.440	1380.5	5.1	-76.5
0.3903	1.06293	-0.479	1430.6	4.2	-70.8
0.4958	1.10077	-0.472	1478.8	3.8	-60.3
0.5900	1.12856	-0.446	1517.2	3.6	-49.2
0.6907	1.15344	-0.385	1553.9	3.4	-36.7
0.7981	1.17592	-0.317	1588.9	3.2	-23.5
0.8932	1.19293	-0.237	1616.9	3.1	-12.2
0.9510	1.20187	-0.128	1630.9	3.1	-5.3
1.0000	1.20870	0.000	1642.2	8.9	0.0
		T = 308.15 K			
0.0000	0.79189	0.000	1172.4	9.2	0.0
0.0482	0.84455	-0.230	1211.1	8.1	-32.8
0.0965	0.88872	-0.331	1245.5	7.3	-53.5
0.1937	0.96004	-0.440	1309.3	6.1	-72.8
0.2929	1.01575	-0.472	1366.6	5.3	-75.4
0.3903	1.05934	-0.513	1417.3	4.7	-69.9
0.4958	1.09725	-0.504	1465.8	4.2	-59.5
0.5900	1.12508	-0.474	1504.5	3.9	-48.6
0.6907	1.15000	-0.407	1541.4	3.7	-36.3
0.7981	1.17252	-0.333	1576.6	3.4	-23.2
0.8932	1.18933	-0.210	1604.7	3.3	-12.1
0.9510	1.19850	-0.133	1618.7	3.2	-5.4
1.0000	1.20535	0.000	1630.0	3.1	0.0

Table 5.2 continued

		T = 313.15 K			
0.0000	0.78777	0.000	1155.5	9.5	0.0
0.0482	0.84056	-0.247	1195.2	8.3	-31.1
0.0965	0.88482	-0.356	1230.2	7.5	-50.8
0.1937	0.95626	-0.472	1294.9	6.2	-69.4
0.2929	1.01208	-0.508	1352.8	5.4	-72.1
0.3903	1.05575	-0.549	1404.0	4.8	-66.9
0.4958	1.09374	-0.538	1453.0	4.3	-57.1
0.5900	1.12162	-0.505	1492.0	4.0	-46.7
0.6907	1.14658	-0.431	1529.1	3.7	-34.9
0.7981	1.16913	-0.349	1564.4	3.5	-22.4
0.8932	1.18578	-0.189	1592.5	3.3	-11.6
0.9510	1.19515	-0.137	1606.6	3.2	-5.2
1.0000	1.20201	0.000	1617.9	3.2	0.0

Table 5.3 Density (ρ), excess molar volume (V_m^E), Speed of sound (u), isentropic compressibility (κ_s), and excess isentropic compressibility (κ_S^E), for the binary mixture {[BMIM]$^+$[MeSO$_4$]$^-$ (x_1) + 2-Propanol (x_2)} at T = (298.15 to 313.15) K.

x_1	ρ / (g · cm^{-3})	V_m^E / (cm^3 · mol^{-1})	u / (m · s^{-1})	κ_s / 10^{10}Pa^{-1}	κ_S^E / 10^{10}Pa^{-1}
		T = 298.15 K			
0.0000	0.78112	0.000	1138.7	9.9	0.0
0.0482	0.83517	-0.247	1181.3	8.6	-50.9
0.0965	0.88067	-0.361	1219.7	7.6	-83.7
0.1938	0.95534	-0.560	1292.5	6.3	-115.2
0.2928	1.01351	-0.628	1358.2	5.3	-120.6
0.3902	1.05905	-0.667	1415.0	4.7	-112.5
0.4960	1.09929	-0.717	1470.4	4.2	-96.4
0.5903	1.12861	-0.692	1514.7	3.9	-79.0
0.6902	1.15450	-0.600	1556.6	3.6	-59.4
0.7978	1.17797	-0.471	1596.4	3.3	-38.2
0.9531	1.20560	-0.216	1642.9	3.1	-8.6
1.0000	1.21206	0.000	1654.6	3.0	0.0
		T = 303.15 K			
0.0000	0.77685	0.000	1121.4	10.2	0.0
0.0482	0.83110	-0.272	1165.3	8.9	-51.1
0.0965	0.87670	-0.396	1204.4	7.9	-84.0
0.1938	0.95152	-0.605	1278.2	6.4	-115.8
0.2928	1.00981	-0.677	1344.3	5.5	-121.3

Table 5.3 continued

0.3902	1.05542	-0.713	1401.7	4.8	-113.3
0.4960	1.09574	-0.760	1457.6	4.3	-97.1
0.5903	1.12513	-0.732	1502.1	3.9	-79.6
0.6902	1.15105	-0.630	1544.2	3.6	-59.9
0.7978	1.17452	-0.487	1584.2	3.4	-38.5
0.9531	1.20222	-0.219	1630.7	3.1	-8.7
1.0000	1.20870	0.000	1642.2	3.1	0.0
		T = 308.15 K			
0.0000	0.77249	0.000	1103.9	10.6	0.0
0.0482	0.82696	-0.298	1148.9	9.2	-45.6
0.0965	0.87270	-0.435	1188.9	8.1	-75.3
0.1938	0.94768	-0.655	1263.7	6.6	-104.4
0.2928	1.00609	-0.731	1330.4	5.6	-109.9
0.3902	1.05178	-0.764	1388.3	4.9	-103.0
0.4960	1.09220	-0.809	1444.6	4.4	-88.7
0.5903	1.12171	-0.783	1489.5	4.0	-72.9
0.6902	1.14761	-0.665	1531.7	3.7	-55.0
0.7978	1.17115	-0.516	1571.9	3.5	-35.4
0.9531	1.19885	-0.224	1618.5	3.2	-8.0
1.0000	1.20535	0.000	1630.0	3.1	0.0
		T = 313.15 K			
0.0000	0.76805	0.000	1086.6	11.0	0.0
0.0482	0.82277	-0.327	1132.5	9.5	-43.7
0.0965	0.86865	-0.477	1173.3	8.4	-72.2

Table 5.3 continued

0.1938	0.94383	-0.711	1249.1	6.8	-100.5
0.2928	1.00239	-0.793	1316.5	5.8	-106.0
0.3902	1.04813	-0.818	1375.0	5.0	-99.6
0.4960	1.08868	-0.864	1431.8	4.5	-85.8
0.5903	1.11831	-0.841	1476.9	4.1	-70.7
0.6902	1.14423	-0.709	1519.4	3.8	-53.4
0.7978	1.16777	-0.544	1559.7	3.5	-34.4
0.9531	1.19549	-0.230	1606.4	3.2	-7.8
1.0000	1.20201	0.000	1617.9	3.2	0.0

Table 5.4 Density (ρ), excess molar volume (V_m^E), Speed of sound (u), isentropic compressibility (κ_s), and excess isentropic compressibility (κ_S^E), for the binary mixture {[BMIM]$^+$[MeSO$_4$]$^-$ (x_1) + 1-Butanol (x_2)} at T = (298.15 to 313.15) K.

x_1	ρ / (g · cm^{-3})	V_m^E / (cm^3 · mol^{-1})	u / (m · s^{-1})	κ_s / 10^{10}Pa^{-1}	κ_S^E / 10^{10}Pa^{-1}
		T = 298.15 K			
0.0000	0.80593	0.000	1239.3	8.1	0.0
0.0425	0.84351	-0.084	1261.4	7.5	-20.0
0.0922	0.88229	-0.112	1285.1	6.9	-36.4
0.1929	0.94895	-0.143	1333.2	5.9	-54.3
0.2926	1.00276	-0.157	1379.6	5.2	-59.3
0.3915	1.04720	-0.165	1424.3	4.7	-57.1
0.4981	1.08751	-0.172	1471.0	4.2	-50.3
0.5997	1.12012	-0.162	1513.5	3.9	-41.4
0.7996	1.17203	-0.118	1589.4	3.4	-21.1
1.0000	1.21206	0.000	1654.6	3.0	0.0
		T = 303.15 K			
0.0000	0.80209	0.000	1222.9	8.3	0.0
0.0425	0.83974	-0.095	1245.6	7.7	-20.2
0.0922	0.87855	-0.129	1270.0	7.1	-36.8
0.1929	0.94527	-0.165	1318.8	6.1	-55.1
0.2926	0.99914	-0.183	1365.8	5.4	-60.2
0.3915	1.04364	-0.193	1411.0	4.8	-58.1
0.4981	1.08401	-0.198	1458.1	4.3	-51.3

Table 5.4 continued

0.5997	1.11666	-0.185	1500.9	4.0	-42.3
0.7996	1.16859	-0.125	1577.1	3.4	-21.5
1.0000	1.20870	0.000	1642.2	3.1	0.0
		T = 308.15 K			
0.0000	0.79821	0.000	1206.3	8.6	0.0
0.0425	0.83593	-0.107	1229.6	7.9	-20.4
0.0922	0.87479	-0.147	1254.6	7.3	-37.3
0.1929	0.94158	-0.190	1304.3	6.2	-55.9
0.2926	0.99553	-0.212	1351.8	5.5	-61.2
0.3915	1.04009	-0.222	1397.5	4.9	-59.2
0.4981	1.08052	-0.228	1445.1	4.4	-52.3
0.5997	1.11321	-0.211	1488.2	4.1	-43.2
0.7996	1.16514	-0.132	1564.7	3.5	-22.0
1.0000	1.20535	0.000	1630.0	3.1	0.0
		T = 313.15 K			
0.0000	0.79430	0.000	1189.7	8.9	0.0
0.0425	0.83210	-0.120	1213.7	8.2	-20.5
0.0922	0.87102	-0.168	1239.3	7.5	-37.5
0.1929	0.93788	-0.217	1289.8	6.4	-56.3
0.2926	0.99190	-0.242	1338.0	5.6	-61.9
0.3915	1.03654	-0.256	1384.2	5.0	-59.9
0.4981	1.07703	-0.260	1432.3	4.5	-53.0
0.5997	1.10978	-0.240	1475.7	4.1	-43.8

Table 5.4 continued

0.7996	1.16171	-0.140	1552.6	3.6	-22.4
1.0000	1.20201	0.000	1617.9	3.2	0.0

Table 5.5 Pure component isobaric thermal expansivity, α_p, and heat capacity, C_p, at several temperatures.

Property	Temperature/K			
	298.15	303.15	308.15	313.15
			IL	
α_p / kK^{-1}	0.578	0.579	0.581	0.582
C_p / J K^{-1} mol^{-1}	416.2[a]	418.5[a]	420.9[a]	423.3[a]
			Methanol	
α_p / kK^{-1}	1.143	1.150	1.157	1.164
C_p / J K^{-1} mol^{-1}	81.17[b]	82.35[b,*]	83.24[b]	84.31[b,*]
			1-Propanol	
α_p / kK^{-1}	1.000	1.005	1.010	1.016
C_p / J K^{-1} mol^{-1}	144.47[b]	147.80[b,*]	150.05[b]	153.58[b,*]
			2-Propanol	
α_p / kK^{-1}	1.152	1.159	1.165	1.172
C_p / J K^{-1} mol^{-1}	155.780[c]	157.54[c,*]	164.01[c]	167.87[c,*]
			1-Butanol	
α_p / kK^{-1}	0.938	0.953	0.969	0.984
C_p / J K^{-1} mol^{-1}	173.80[d]	177.10[d]	180.61[d]	184.28[d]

[a] (García-Miaja *et al.* 2008).

[b] (Vercher *et al.* 2007).

[c] (Cerdeiriña *et al.* 1999).

[d] (Zorębski and Deć 2012).

* Calculated from literature data.

Table 5.6 Excess partial molar volumes $V^{E}_{m,1}$ and $V^{E}_{m,2}$ and partial molar volumes $V_{m,1}$ and $V_{m,2}$ for the binary mixture {[BMIM]$^+$[MeSO$_4$]$^-$ (x_1) + Methanol (x_2)} at T = 298.15 K.

x_1	$V_{m,1}$ / (cm^3 · mol^{-1})	$V_{m,2}$ / (cm^3 · mol^{-1})	$V^{E}_{m,1}$ / (cm^3 · mol^{-1})	$V^{E}_{m,2}$ /(cm^3 · mol^{-1})
		T = 298.15 K		
0.0000	202.49	40.69	-7.6520	0.0000
0.0422	203.03	40.38	-6.0310	-0.0335
0.0940	203.56	40.28	-4.5778	-0.1376
0.1857	203.80	40.07	-2.9066	-0.4022
0.2858	203.79	40.04	-1.7712	-0.7478
0.3729	203.75	40.03	-1.0816	-1.0844
0.4772	203.90	40.10	-0.5154	-1.4986
0.5769	204.21	40.26	-0.2199	-1.8216
0.6775	204.71	40.69	-0.1225	-1.9774
0.7947	205.44	41.91	-0.1207	-1.9798
0.8923	206.02	44.00	-0.0788	-2.2416
0.9526	206.31	46.08	-0.0245	-2.9279

Table 5.7 Excess partial molar volumes $V^{E}_{m,1}$ and $V^{E}_{m,2}$ and partial molar volumes $V_{m,1}$ and $V_{m,2}$ for the binary mixture {[BMIM]$^+$[MeSO$_4$]$^-$ (x_1) + 1-Propanol (x_2)} at T = 298.15 K.

x_1	$V_{m,1}$ / (cm^3 · mol^{-1})	$V_{m,2}$ / (cm^3 · mol^{-1})	$V^{E}_{m,1}$ / (cm^3 · mol^{-1})	$V^{E}_{m,2}$ /(cm^3 · mol^{-1})
		T = 298.15 K		
0.0000	202.57	75.12	-2.9494	-0.0509
0.0482	204.40	74.97	-1.6872	-0.1459
0.0965	205.63	74.99	-0.7647	-0.2876
0.1937	206.68	75.17	-0.6337	-0.3260
0.2929	206.64	75.33	-0.5583	-0.3669
0.3903	206.13	75.30	-0.3868	-0.5057
0.4958	205.59	75.07	0.2484	-0.6686
0.5900	205.31	74.75	-0.1947	-0.7589
0.6907	205.32	74.49	-0.1911	-0.7720
0.7981	205.63	74.73	-0.1198	-1.2142
0.8932	206.03	76.07	-0.0396	-2.2175
0.9510	206.34	77.92	-2.9494	-0.0509

Table 5.8 Excess partial molar volumes $V^{E}_{m,1}$ and $V^{E}_{m,2}$ and partial molar volumes $V_{m,1}$ and $V_{m,2}$ for the binary mixture {[BMIM]$^+$[MeSO$_4$]$^-$ (x_1) + 2-Propanol (x_2)} at T = 298.15 K.

x_1	$V_{m,1}$ / (cm^3 · mol^{-1})	$V_{m,2}$ / (cm^3 · mol^{-1})	$V^{E}_{m,1}$ / (cm^3 · mol^{-1})	$V^{E}_{m,2}$ /(cm^3 · mol^{-1})
		T = 298.15 K		
0.0000	201.05	76.94	-6.3750	0.0000
0.0482	203.23	76.76	-3.8685	-0.0567
0.0965	204.71	76.81	-2.4632	-0.1626
0.1938	205.99	77.02	-1.4111	-0.3251
0.2928	206.05	77.27	-1.1868	-0.3940
0.3902	205.60	77.30	-0.9883	-0.4997
0.4960	205.05	77.01	-0.6685	-0.7571
0.5903	204.82	76.60	-0.4233	-1.0465
0.6902	204.93	76.24	-0.3012	-1.2569
0.7978	205.38	76.40	-0.2581	-1.3847
0.9531	206.24	79.82	-0.0460	-3.3780

Table 5.9 Excess partial molar volumes $V^{E}_{m,1}$ and $V^{E}_{m,2}$ and partial molar volumes $V_{m,1}$ and $V_{m,2}$ for the binary mixture {[BMIM]$^+$[MeSO$_4$]$^-$ (x_1) + 1-Butanol (x_2)} at T = 298.15 K.

x_1	$V_{m,1}$ / (cm^3 · mol^{-1})	$V_{m,2}$ (cm^3 · mol^{-1})	$V^{E}_{m,1}$ (cm^3 · mol^{-1})	$V^{E}_{m,2}$ (cm^3 · mol^{-1})
		T = 298.15 K		
0.0000	204.66	91.97	-2.3630	0.0000
0.0425	205.58	91.90	-1.2977	-0.0213
0.0922	206.32	91.94	-0.6160	-0.0684
0.1929	206.91	92.06	-0.2187	-0.1253
0.2926	206.83	92.14	-0.2437	-0.1159
0.3915	206.51	92.12	-0.2434	-0.1178
0.4981	206.17	91.96	-0.1573	-0.1887
0.5997	205.98	91.71	-0.0808	-0.2804
0.7996	206.11	91.54	-0.0858	-0.2472

Table 5.10 Refractive index (n), deviation in refractive index (Δn), molar refraction (R), for the binary mixture {$[BMIM]^+[MeSO_4]^-$ (x_1) + Methanol (x_2)} at T = (298.15 to 313.15) K.

x_1	n	Δn	R / ($cm^3 \cdot mol^{-1}$)
		T = 298.15 K	
0.0000	1.32720	0.00000	8.24
0.0422	1.35708	0.00227	10.45
0.0940	1.38272	0.00343	13.12
0.1857	1.41321	0.00497	17.83
0.2858	1.43348	0.00508	22.91
0.3729	1.44537	0.00472	27.31
0.4772	1.45531	0.00388	32.53
0.5769	1.46226	0.00309	37.51
0.6775	1.46761	0.00233	42.51
0.7947	1.47248	0.00156	48.34
0.8923	1.47576	0.00103	53.19
0.9526	1.47744	0.00066	56.18
1.0000	1.47824	0.00000	58.48
		T = 303.15 K	
0.0000	1.32552	0.00000	8.25
0.0422	1.35523	0.00208	10.38
0.0940	1.38094	0.00327	13.00
0.1857	1.41156	0.00487	17.62
0.2858	1.43193	0.00499	22.65

Table 5.10 continued

0.3729	1.44388	0.00463	27.03
0.4772	1.45387	0.00380	32.27
0.5769	1.46087	0.00301	37.27
0.6775	1.46624	0.00223	42.33
0.7947	1.47111	0.00142	48.22
0.8923	1.47441	0.00089	53.12
0.9526	1.47608	0.00051	56.15
1.0000	1.47704	0.00000	58.52
	T = 308.15 K		
0.0000	1.32362	0.00000	8.25
0.0422	1.35331	0.00202	10.38
0.0940	1.37913	0.00326	13.01
0.1857	1.40990	0.00490	17.63
0.2858	1.43036	0.00501	22.66
0.3729	1.44239	0.00467	27.04
0.4772	1.45242	0.00381	32.28
0.5769	1.45945	0.00301	37.29
0.6775	1.46485	0.00221	42.34
0.7947	1.46972	0.00137	48.23
0.8923	1.47303	0.00082	53.14
0.9526	1.47475	0.00047	56.18
1.0000	1.47577	0.00000	58.55

Table 5.10 continued

T = 313.15 K			
0.0000	1.32171	0.00000	8.26
0.0422	1.35141	0.00201	10.39
0.0940	1.37735	0.00332	13.01
0.1857	1.40827	0.00500	17.63
0.2858	1.42880	0.00510	22.67
0.3729	1.44090	0.00476	27.05
0.4772	1.45097	0.00387	32.29
0.5769	1.45804	0.00306	37.30
0.6775	1.46348	0.00227	42.36
0.7947	1.46836	0.00140	48.25
0.8923	1.47168	0.00084	53.16
0.9526	1.47338	0.00044	56.19
1.0000	1.47443	0.00000	58.57

Table 5.11 Refractive index (n), deviation in refractive index (Δn), molar refraction (R), for the binary mixture {$[BMIM]^+[MeSO_4]^-$ (x_1) + 1-Propanol (x_2)} at T = (298.15 to 313.15) K.

x_1	n	Δn	R / ($cm^3 \cdot mol^{-1}$)
		T = 298.15 K	
0.0000	1.38334	0.00000	17.54
0.0482	1.39591	0.00099	19.52
0.0965	1.40632	0.00144	21.51
0.1937	1.42298	0.00190	25.51
0.2929	1.43588	0.00201	29.59
0.3903	1.44583	0.00199	33.58
0.4958	1.45448	0.00187	37.90
0.5900	1.46078	0.00170	41.75
0.6907	1.46636	0.00141	45.87
0.7981	1.47134	0.00110	50.26
0.8932	1.47515	0.00088	54.14
0.9510	1.47760	0.00069	56.56
1.0000	1.47824	0.00000	58.48
		T = 303.15 K	
0.0000	1.38131	0.00000	17.54
0.0482	1.39407	0.00109	19.53
0.0965	1.40459	0.00159	21.52
0.1937	1.42138	0.00204	25.53
0.2929	1.43433	0.00210	29.61

Table 5.11 continued

0.3903	1.44433	0.00203	33.59
0.4958	1.45302	0.00186	37.92
0.5900	1.45937	0.00168	41.77
0.6907	1.46499	0.00138	45.89
0.7981	1.46997	0.00101	50.28
0.8932	1.47378	0.00074	54.16
0.9510	1.47628	0.00052	56.59
1.0000	1.47704	0.00000	58.52
	T = 308.15 K		
0.0000	1.37926	0.00000	17.55
0.0482	1.39212	0.00112	19.53
0.0965	1.40276	0.00168	21.53
0.1937	1.41966	0.00213	25.54
0.2929	1.43273	0.00219	29.62
0.3903	1.44280	0.00211	33.61
0.4958	1.45154	0.00192	37.93
0.5900	1.45793	0.00171	41.79
0.6907	1.46358	0.00138	45.91
0.7981	1.46856	0.00096	50.29
0.8932	1.47238	0.00067	54.19
0.9510	1.47491	0.00023	56.61
1.0000	1.47577	0.00000	58.55

Table 5.11 continued

		T = 313.15 K	
0.0000	1.37722	0.00000	17.56
0.0482	1.39019	0.00117	19.54
0.0965	1.40090	0.00174	21.54
0.1937	1.41794	0.00222	25.54
0.2929	1.43111	0.00230	29.63
0.3903	1.44126	0.00222	33.62
0.4958	1.45008	0.00203	37.95
0.5900	1.45649	0.00178	41.80
0.6907	1.46215	0.00143	45.93
0.7981	1.46716	0.00097	50.31
0.8932	1.47090	0.00056	54.05
0.9510	1.47354	0.00020	56.12
1.0000	1.47443	0.00000	58.57

Table 5.12 Refractive index (n), deviation in refractive index (Δn), molar refraction (R), for the binary mixture {$[BMIM]^+[MeSO_4]^-$ (x_1) + 2-Propanol (x_2)} at T = (298.15 to 313.15) K.

x_1	n	Δn	R / ($cm^3 \cdot mol^{-1}$)
		T = 298.15 K	
0.0000	1.37527		17.62
		0.00000	
0.0482	1.38886		19.61
		0.00127	
0.0965	1.40005		21.60
		0.00184	
0.1938	1.41819		25.59
		0.00255	
0.2928	1.43227		29.65
		0.00279	
0.3902	1.44304		33.63
		0.00269	
0.4960	1.45252		37.94
		0.00256	
0.5903	1.45942		41.79
		0.00233	
0.6902	1.46547		45.87
		0.00198	
0.7978	1.47086		50.26
		0.00150	
0.9531	1.47709		54.07
		0.00071	
1.0000	1.47824		56.59
		0.00000	
		T = 303.15 K	
0.0000	1.37314	0.00000	17.63
0.0482	1.38696	0.00141	19.62
0.0965	1.39831	0.00207	21.61
0.1938	1.41666	0.00284	25.61
0.2928	1.43067	0.00290	29.66
0.3902	1.44158	0.00283	33.65

Table 5.12 continued

0.4960	1.45108	0.00263	37.96
0.5903	1.45801	0.00235	41.81
0.6902	1.46409	0.00196	45.89
0.7978	1.46948	0.00142	50.28
0.9531	1.47576	0.00060	54.09
1.0000	1.47704	0.00000	56.61
	T = 308.15 K		
0.0000	1.37093	0.00000	17.64
0.0482	1.38495	0.00153	19.63
0.0965	1.39643	0.00225	21.62
0.1938	1.41492	0.00302	25.62
0.2928	1.42902	0.00305	29.67
0.3902	1.44001	0.00296	33.66
0.4960	1.44958	0.00272	37.97
0.5903	1.45655	0.00242	41.82
0.6902	1.46268	0.00200	45.91
0.7978	1.46810	0.00142	50.30
0.9531	1.47442	0.00055	54.11
1.0000	1.47577	0.00000	56.63
	T = 313.15 K		
0.0000	1.36870	0.00000	17.64
0.0482	1.38288	0.00162	19.63
0.0965	1.39450	0.00240	21.63
0.1938	1.41317	0.00322	25.62

Table 5.12 continued

0.2928	1.42740	0.00327	29.68
0.3902	1.43845	0.00313	33.67
0.4960	1.44808	0.00286	37.98
0.5903	1.45510	0.00254	41.83
0.6902	1.46125	0.00208	45.92
0.7978	1.46675	0.00151	50.32
0.9531	1.47306	0.00055	54.13
1.0000	1.47443	0.00000	56.65

Table 5.13 Refractive index (n), deviation in refractive index (Δn), molar refraction (R), for the binary mixture {$[BMIM]^+[MeSO_4]^-$ (x_1) + 1-Butanol (x_2)} at T = (298.15 to 313.15) K.

x_1	n	Δn	R / ($cm^3 \cdot mol^{-1}$)
		T = 298.15 K	
0.0000	1.39747	0.00000	22.17
0.0425	1.40525	0.00045	23.73
0.0922	1.41307	0.00060	25.54
0.1929	1.42652	0.00085	29.22
0.2926	1.43736	0.00100	32.86
0.3915	1.44629	0.00109	36.46
0.4981	1.45433	0.00111	40.34
0.5997	1.46080	0.00107	44.03
0.7996	1.47095	0.00083	51.27
1.0000	1.47824	0.00000	58.48
		T = 303.15 K	
0.0000	1.39549	0.00000	22.18
0.0425	1.40335	0.00048	23.74
0.0922	1.41133	0.00072	25.55
0.1929	1.42489	0.00096	29.24
0.2926	1.43578	0.00106	32.87
0.3915	1.44477	0.00112	36.48
0.4981	1.45286	0.00111	40.35
0.5997	1.45937	0.00104	44.04

Table 5.13 continued

0.7996	1.46959	0.00075	51.29
1.0000	1.47704	0.00000	58.52
	T = 308.15 K		
0.0000	1.39342	0.00000	22.18
0.0425	1.40141	0.00055	23.74
0.0922	1.40946	0.00081	25.56
0.1929	1.42315	0.00105	29.25
0.2926	1.43415	0.00117	32.89
0.3915	1.44321	0.00121	36.49
0.4981	1.45136	0.00118	40.37
0.5997	1.45792	0.00108	44.06
0.7996	1.46821	0.00074	51.31
1.0000	1.47577	0.00000	58.55
	T = 313.15 K		
0.0000	1.39138	0.00000	22.19
0.0425	1.39946	0.00059	23.75
0.0922	1.40762	0.00090	25.57
0.1929	1.42144	0.00117	29.26
0.2926	1.43253	0.00129	32.90
0.3915	1.44167	0.00133	36.50
0.4981	1.44987	0.00128	40.38
0.5997	1.45646	0.00115	44.07
0.7996	1.46682	0.00078	51.34
1.0000	1.47443	0.00000	58.57

Figures 5.1-5.4 are plots of excess molar volume values for the systems {$[BMIM]^+[MeSO_4]^-$ (x_1) + methanol, or 1-propanol, or 2-propanol, or 1-butanol (x_2)}, at T = (298.15, 303.15, 308.15, and 313.15) K. The excess molar volumes are negative, and decrease as the temperature increases for each binary system.

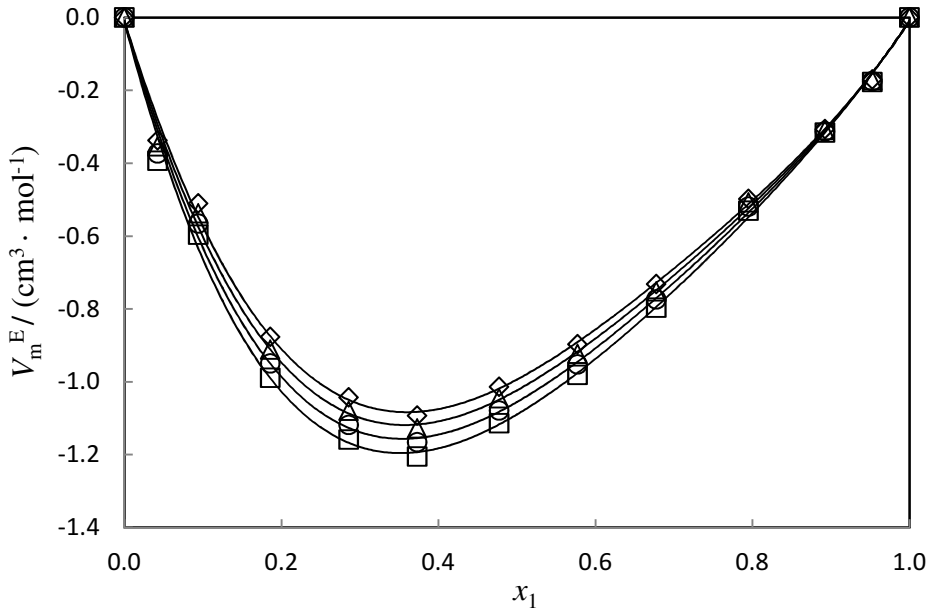

Figure 5.1 Plot of excess molar volume, V_m^E, for the binary mixture {$[BMIM]^+[MeSO_4]^-$ (x_1) + Methanol (x_2)} against mole fraction of ionic liquid; ◊ at T =298.15 K, Δ at T = 303.15 K, o at T = 308.15 K, □ at T = 313.15 K. The solid lines represent the corresponding Redlich-Kister correlation equation (5.13).

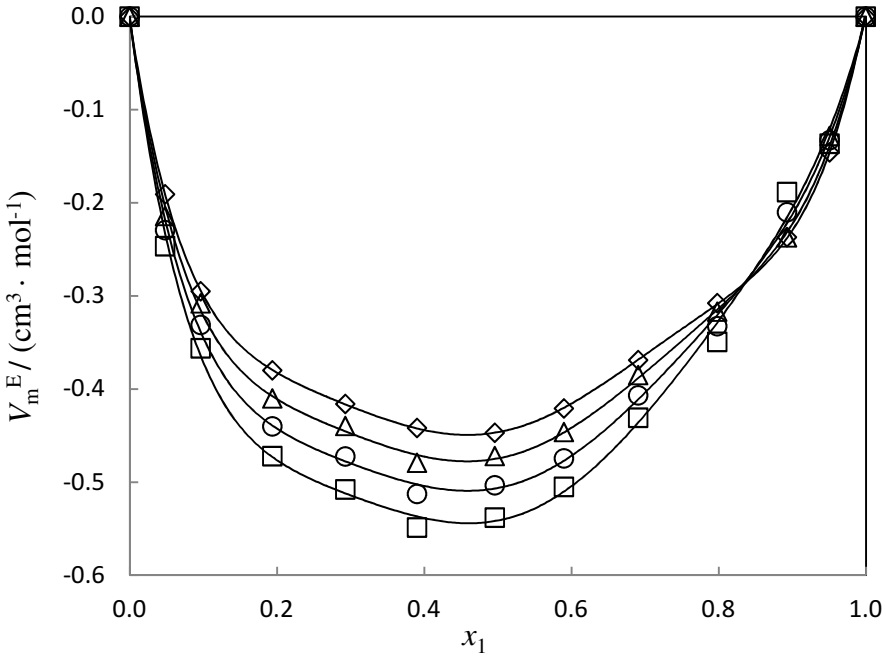

Figure 5.2 Plot of excess molar volume, V_m^E, for the binary mixture {[BMIM]$^+$[MeSO$_4$]$^-$ (x_1) + 1-Propanol (x_2)} against mole fraction of ionic liquid; ◊ at T = 298.15 K, Δ at T = 303.15 K, o at T = 308.15 K, □ at T = 313.15 K. The solid lines represent the corresponding Redlich-Kister correlation equation (5.13).

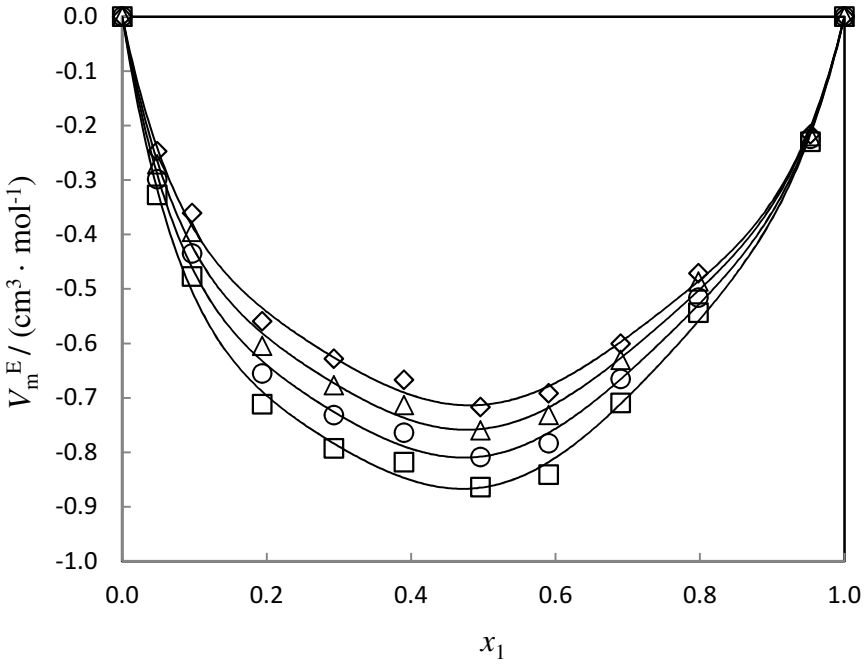

Figure 5.3 Plot of excess molar volume, V_m^E, for the binary mixture {[BMIM]$^+$[MeSO$_4$]$^-$ (x_1) + 2-Propanol (x_2)} against mole fraction of ionic liquid; ◊ at T = 298.15 K, Δ at T = 303.15 K, o at T = 308.15 K, □ at T = 313.15 K. The solid lines represent the corresponding Redlich-Kister correlation equation (5.13).

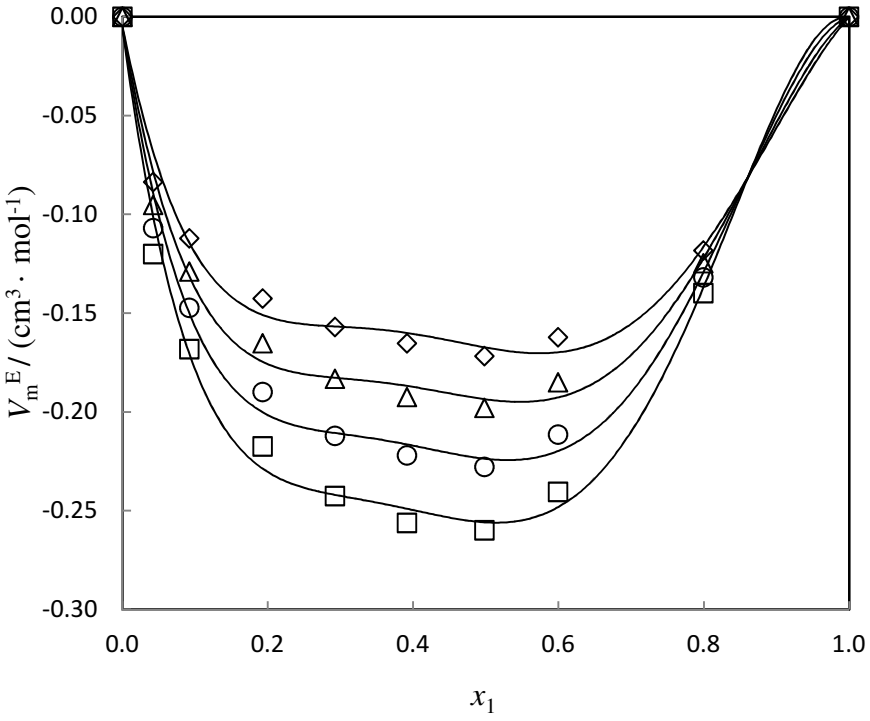

Figure 5.4 Plot of excess molar volume, V_m^E, for the binary mixture {[BMIM]$^+$[MeSO$_4$]$^-$ (x_1) + 1-Butanol (x_2)} against mole fraction of ionic liquid; ◊ at T = 298.15 K, Δ at T = 303.15 K, o at T = 308.15 K, □ at T = 313.15 K. The solid lines represent the corresponding Redlich-Kister correlation equation (5.13).

The graphs of the excess partial molar volumes calculated at T = 298.15 K are given in figures 5.5-5.8. The results calculated for $V^{E}_{m,1}$ and $V^{E}_{m,2}$ are plotted against x_1.

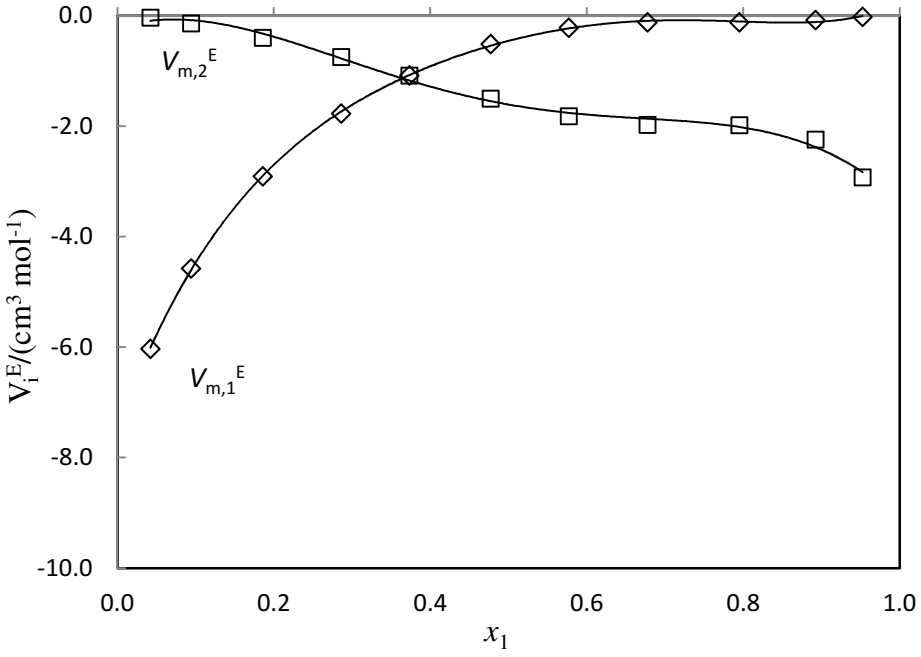

Figure 5.5 Plot of the excess partial molar volumes of [BMIM]$^+$[MeSO$_4$]$^-$ $V^{E}_{m,1}$ and Methanol $V^{E}_{m,2}$ against mole fraction of alcohol (x_2) at T = 298.15 K.

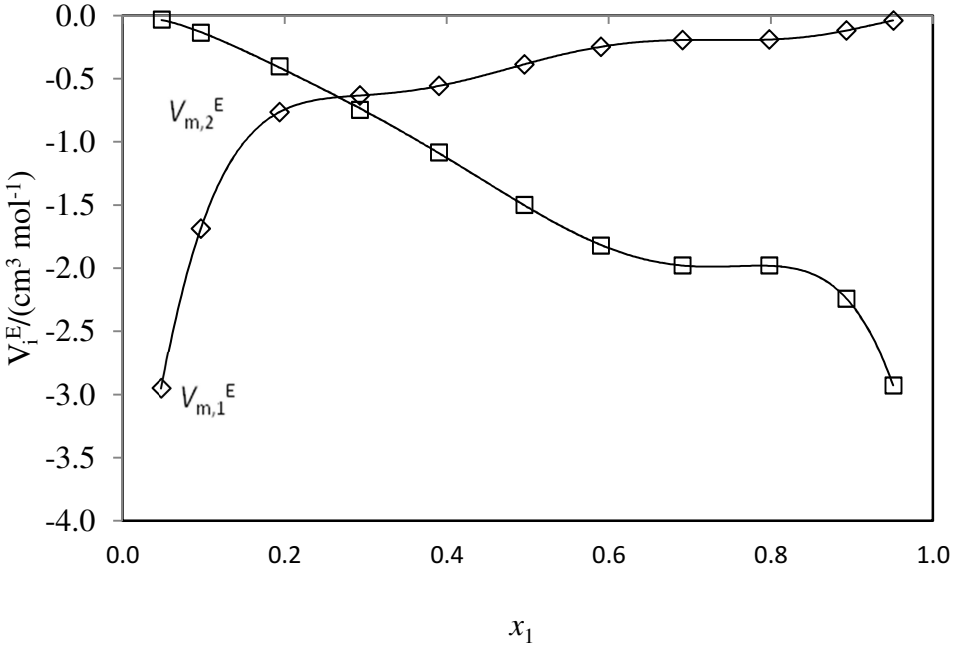

Figure 5.6 Plot of the excess partial molar volumes of [BMIM]$^+$[MeSO$_4$]$^-$ $V_{m,1}^E$ and 1-Propanol $V_{m,2}^E$ against mole fraction of alcohol (x_1) at T = 298.15K.

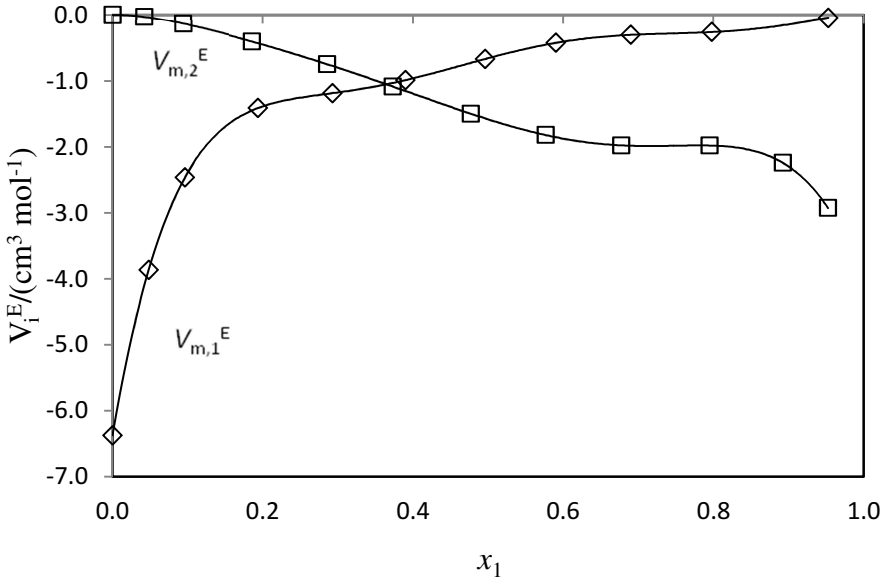

Figure 5.7 Plot of the excess partial molar volumes of [BMIM]$^+$[MeSO$_4$]$^-$ $V_{m,1}^E$ and 2-Propanol $V_{m,2}^E$ against mole fraction of alcohol (x_2) at T = 298.15K.

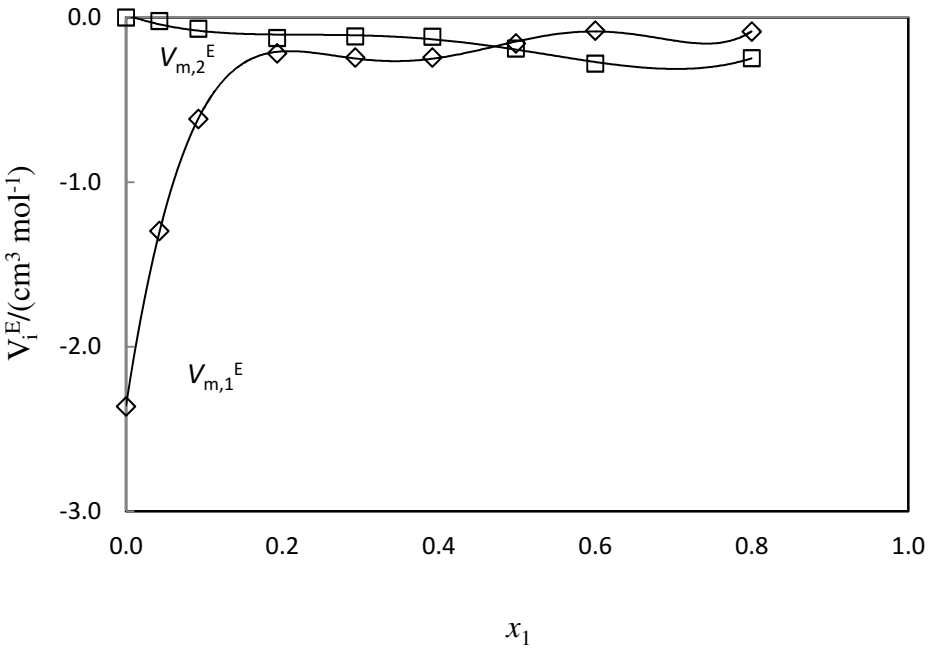

Figure 5.8 Plot of the excess partial molar volumes of $[BMIM]^+[MeSO_4]^-$ $V_{m,1}^E$ and 1-Butanol $V_{m,2}^E$ against mole fraction of alcohol (x_2) at T = 298.15 K.

The graphs of the excess isentropic compressibility are given in figures 5.9-5.12 and are very similar to that of the excess molar volume. It is also negative over the temperature range and over the entire composition.

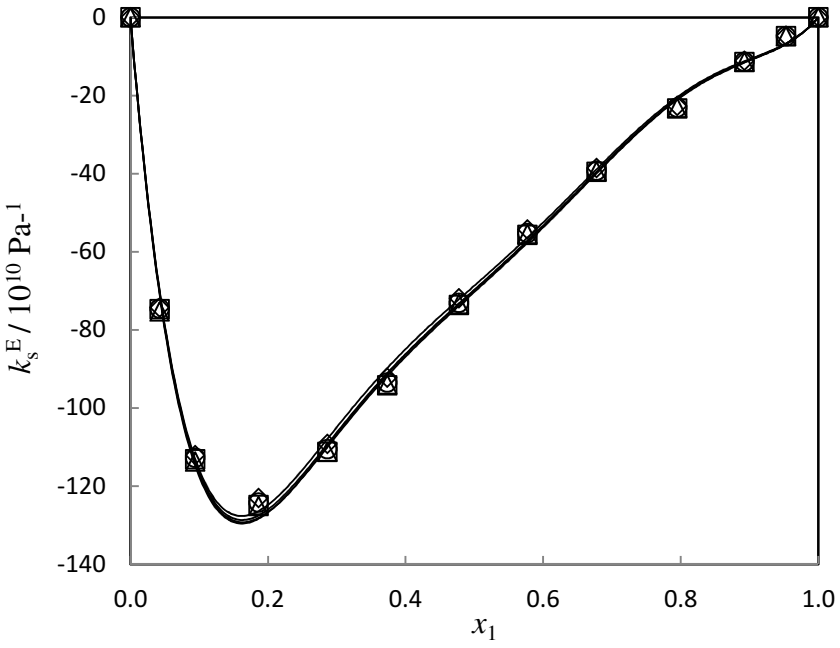

Figure 5.9 Plot of excess isentropic compressibility κ_S^E, for the binary mixture {[BMIM]$^+$[MeSO$_4$]$^-$ (x_1) + Methanol (x_2)} against mole fraction of ionic liquid; ◊ at T = 298.15 K, Δ at T = 303.15 K, o at T = 308.15 K, □ at T = 313.15 K. The solid lines represent the corresponding Redlich-Kister correlation equation (5.13).

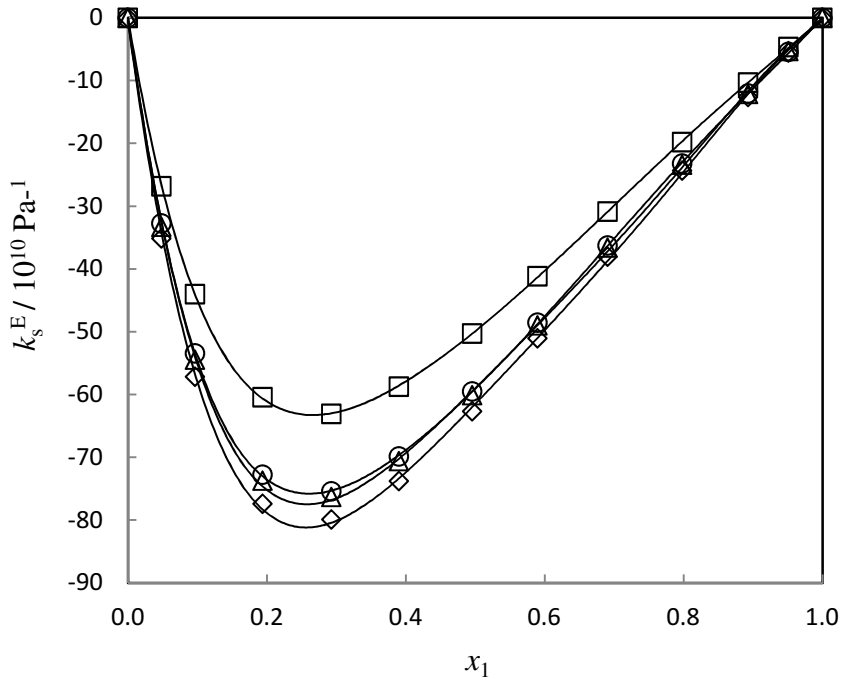

Figure 5.10 Plot of excess isentropic compressibility κ_S^E, for the binary mixture {[BMIM]$^+$[MeSO$_4$]$^-$ (x_1) + 1-Propanol (x_2)} against mole fraction of ionic liquid; ◊ at T = 298.15 K, Δ at T = 303.15 K, o at T = 308.15 K, □ at T = 313.15 K. The solid lines represent the corresponding Redlich-Kister correlation equation (5.13).

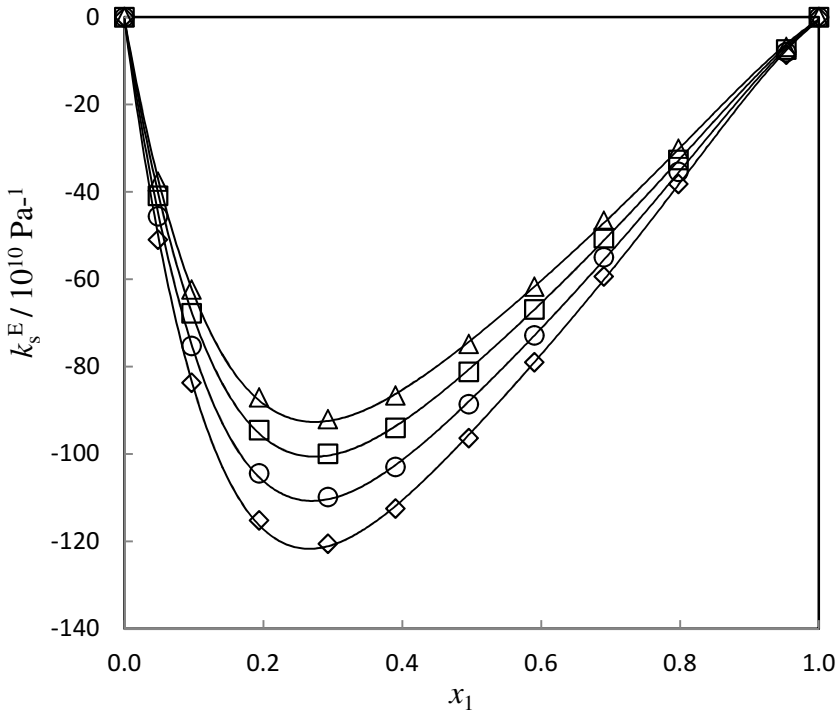

Figure 5.11 Plot of excess isentropic compressibility κ_S^E, for the binary mixture {[BMIM]$^+$[MeSO$_4$]$^-$ (x_1) + 2-Propanol (x_2)} against mole fraction of ionic liquid; ◊ at T = 298.15 K, Δ at T = 303.15 K, o at T = 308.15 K, □ at T = 313.15 K. The solid lines represent the corresponding Redlich-Kister correlation equation (5.13).

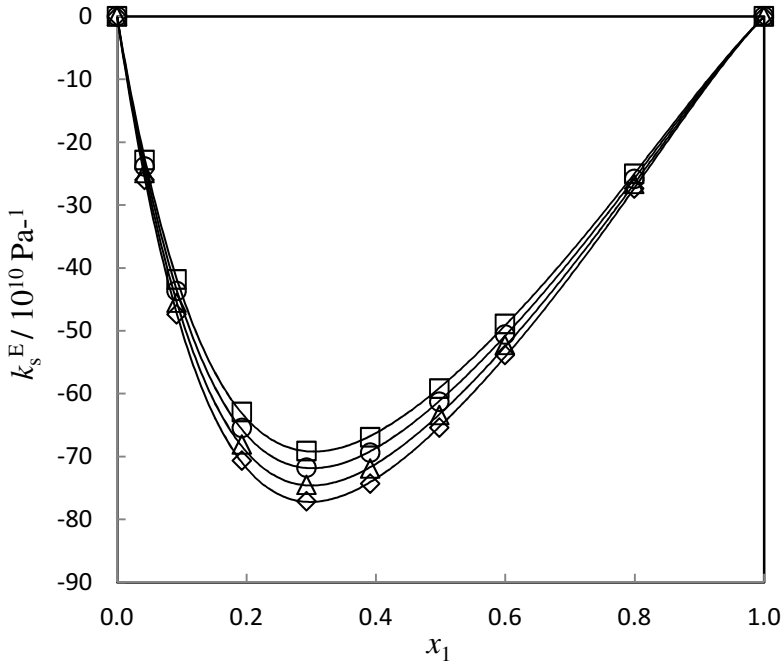

Figure 5.12 Plot of excess isentropic compressibility κ_S^E, for the binary mixture {[BMIM]$^+$[MeSO$_4$]$^-$ (x_1) + 1-Butanol (x_2)} against mole fraction of ionic liquid; ◊ at T = 298.15 K, Δ at T = 303.15 K, o at T = 308.15 K, □ at T = 313.15 K. The solid lines represent the corresponding Redlich-Kister correlation equation (5.13).

The graphs of deviation in refractive index are given in figures 5.13-5.16. The deviation in the refractive indices is always positive over the whole range of composition and temperature and it increases when temperature increases.

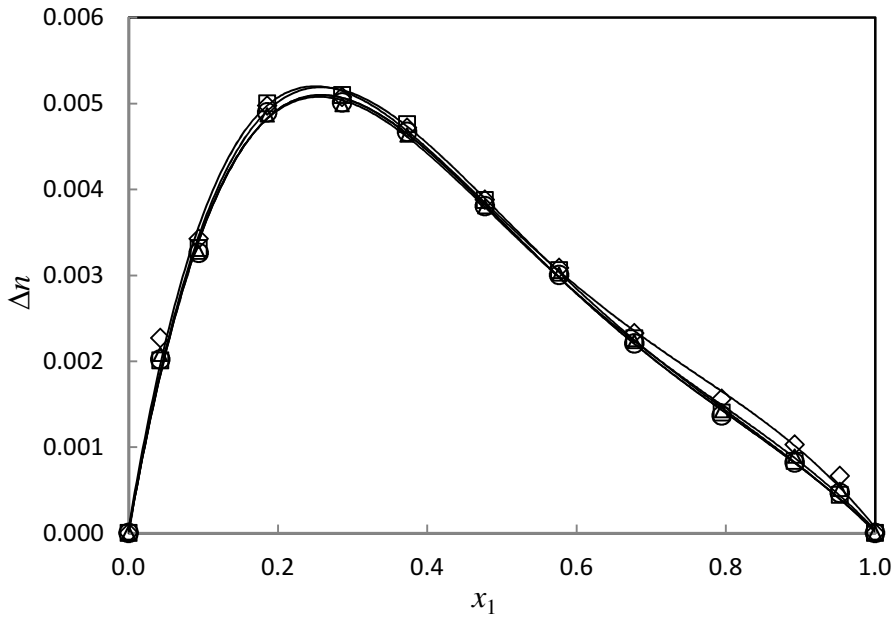

Figure 5.13 Plot of change in refractive indices on mixing Δn, for the binary mixture {[BMIM]$^+$[MeSO$_4$]$^-$ (x_1) + Methanol (x_2)} against mole fraction of ionic liquid; ◊ at T = 298.15 K, Δ at T = 303.15 K, o at T = 308.15 K, □ at T = 313.15 K. The solid lines represent the corresponding Redlich-Kister correlation equation (5.13).

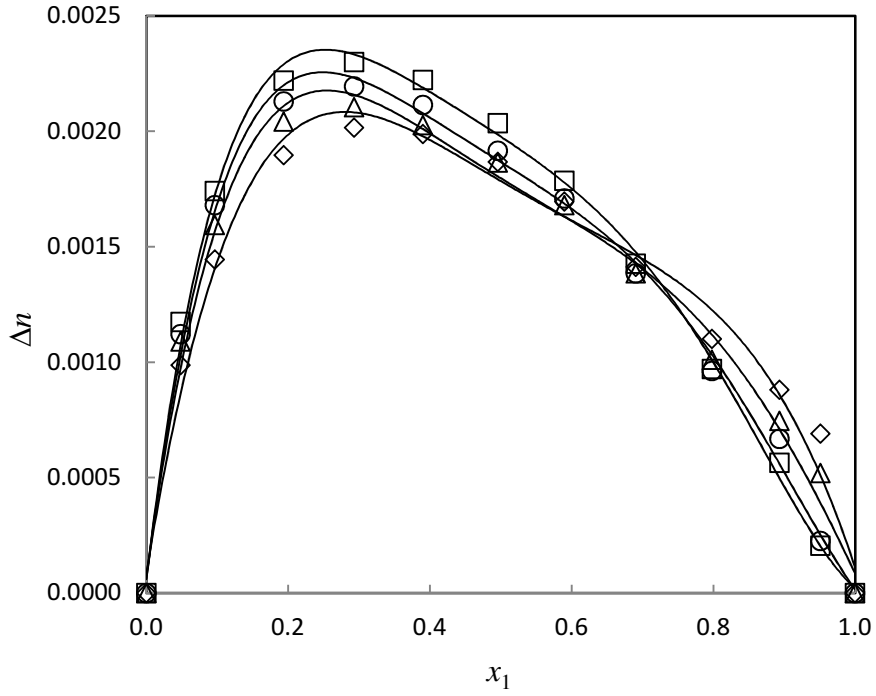

Figure 5.14 Plot of change in refractive indices on mixing Δn, for the binary mixture {[BMIM]$^+$[MeSO$_4$]$^-$ (x_1) + 1-Propanol (x_2)} against mole fraction of ionic liquid; ◊ at T = 298.15 K, Δ at T = 303.15 K, o at T = 308.15 K, □ at T = 313.15 K. The solid lines represent the corresponding Redlich-Kister correlation equation (5.13).

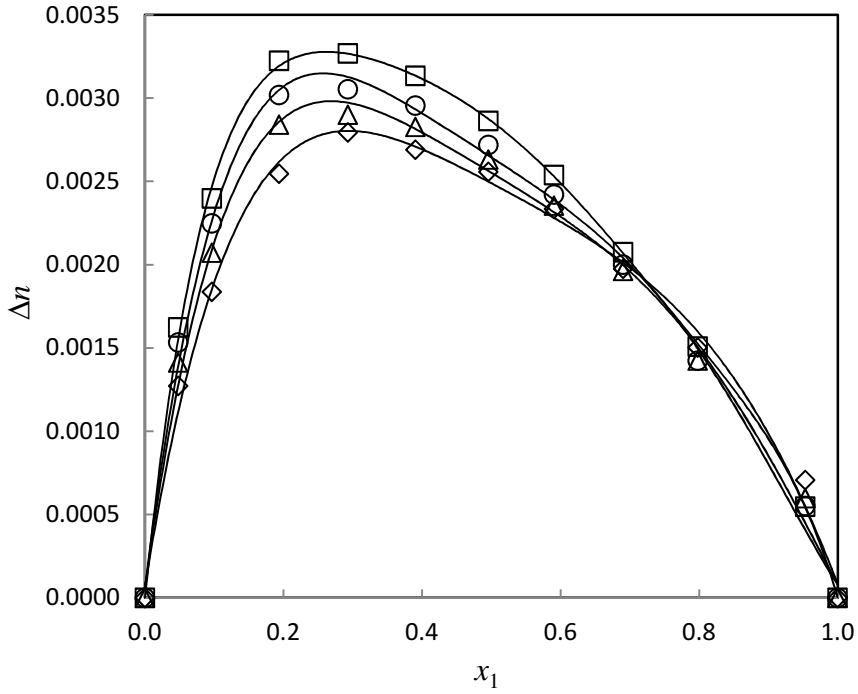

Figure 5.15 Plot of change in refractive indices on mixing Δn, for the binary mixture {[BMIM]$^+$[MeSO$_4$]$^-$ (x_1) + 2-Propanol (x_2)} against mole fraction of ionic liquid; ◊ at T = 298.15 K, Δ at T = 303.15 K, o at T = 308.15 K, □ at T = 313.15 K. The solid lines represent the corresponding Redlich-Kister correlation equation (5.13).

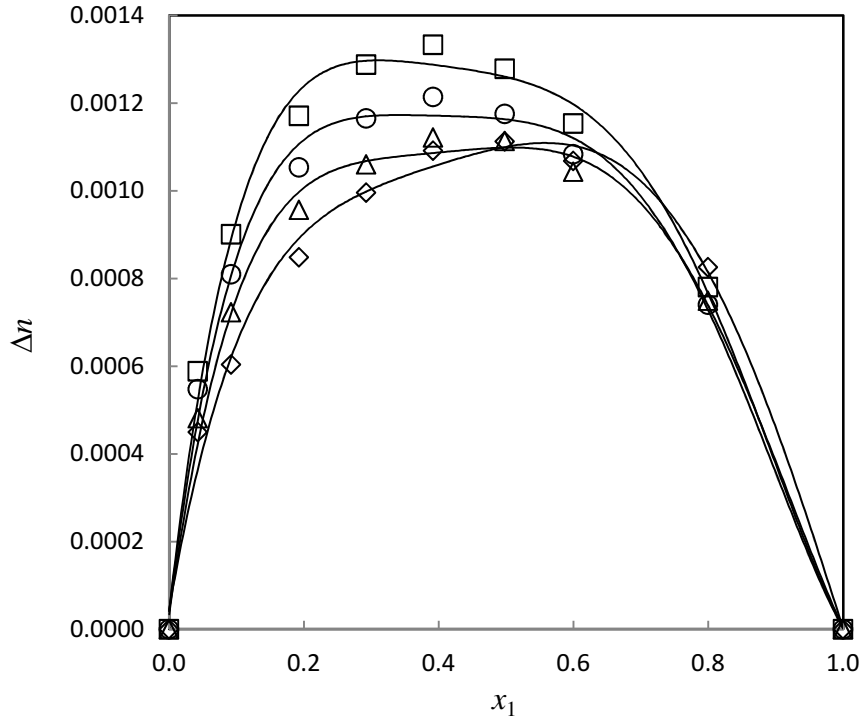

Figure 5.16 Plot of change in refractive indices on mixing Δn, for the binary mixture {[BMIM]$^+$[MeSO$_4$]$^-$ (x_1) + 1-Butanol (x_2)} against mole fraction of ionic liquid; ◊ at T = 298.15 K, Δ at T = 303.15 K, o at T = 308.15 K, □ at T = 313.15 K. The solid lines represent the corresponding Redlich-Kister correlation equation (5.13).

5.2 REDLICH-KISTER POLYNOMIAL

The calculated V_m^E, κ_S^E, and Δn data were correlated by means of the Redlich-Kister polynomial (Redlich and Kister 1948) at the temperatures (298.15, 303.15, 308.15, and 313.15) K. The Redlich-Kister equation for binary mixtures is given below:

$$Z = x_1 x_2 \sum_{i=0}^{N} A_i (2x_1 - 1)^i \tag{5.13}$$

Where Z is the excess or deviation property; x_1 is the mole fraction of the ionic liquid; x_2 is the mole fraction of the alcohols; N is the degree of polynomial expansion; and A_i is the Redlich-Kister parameters for the system. The fitting parameters are given in table 5.14 together with the root-mean-square deviations, σ.

$$\sigma = \left(\frac{\sum_{i}^{n} (Z_{exp} - Z_{cal})^2}{n-k} \right)^{1/2} \tag{5.14}$$

where Z_{exp}, Z_{cal} are the values of the experimental and calculated property, n is the number of experimental data points and k is the number of coefficients used in the Redlich-Kister correlation respectively.

Table 5.14 Redlich-Kister fitting parameters and root-mean-square deviation, σ, for binary mixtures at T = (298.15, 303.15, 308.15, and 313.15) K.

	T/K	A_0	A_1	A_2	A_3	A_4	σ
			{[BMIM]$^+$[MeSO$_4$]$^-$ (x_1) + Methanol (x_2)}				
V_m^E/(cm^3 · mol^{-1})	298.15	-4.02	-2.311	-0.431	0.504	-1.394	0.026
	303.15	-4.142	-2.397	-0.444	0.366	-1.508	0.026
	308.15	-4.277	-2.489	-0.439	0.221	-1.667	0.027
	313.15	-4.415	-2.578	-0.456	0.05	-1.786	0.028
κ_S^E /(10^{10}Pa^{-1})	298.15	-274.6	-311.3	-263.8	-654.2	-633.9	2.6
	303.15	-280.1	-317.5	-269.2	-660.1	-638.0	2.6
	308.15	-278.8	-316.0	-268.0	-652.2	-629.2	2.5
	313.15	-281.0	-318.6	-270.3	-651.4	-626.8	2.5
Δn	298.15	0.01499	0.01664	0.01104	0.00388	0.01128	0.00012
	303.15	0.01461	0.01685	0.01185	0.00340	0.00619	0.00009
	308.15	0.01464	0.01727	0.01219	0.00321	0.00440	0.00009
	313.15	0.01486	0.01752	0.01347	0.00337	0.00248	0.00009
			{[BMIM]$^+$[MeSO$_4$]$^-$ (x_1) + 1-Propanol (x_2)}				
V_m^E/(cm^3 · mol^{-1})	298.15	-1.785	-0.267	-0.044	-0.353	-2.747	0.011
	303.15	-1.899	-0.286	-0.061	-0.633	-2.643	0.008
	308.15	-2.026	-0.293	-0.079	-0.984	-2.500	0.009
	313.15	-2.165	-0.307	-0.097	-1.319	-2.389	0.015
κ_S^E /(10^{10}Pa^{-1})	298.15	-248.9	-230.4	-162.9	-146.9	-90.2	0.3
	303.15	-238.7	-219.2	-153.8	-138.4	-84.5	0.2
	308.15	-236.3	-216.7	-150.0	-132.4	-83.3	0.2
	313.15	-199.7	-179.6	-122.0	-103.6	-63.7	0.2
Δn	298.15	0.00759	0.00371	0.00001	0.00077	0.01422	0.00005
	303.15	0.00755	0.00389	0.00150	0.00387	0.01175	0.00003
	308.15	0.00770	0.00385	0.00319	0.00660	0.00729	0.00005
	313.15	0.00810	0.00402	0.00303	0.00782	0.00652	0.00004
			{[BMIM]$^+$[MeSO$_4$]$^-$ (x_1) + 2-Propanol (x_2)}				
V_m^E/(cm^3 · mol^{-1})	298.15	-2.851	-0.226	0.193	-0.223	-3.268	0.018
	303.15	-3.027	-0.303	0.200	-0.433	-3.434	0.019
	308.15	-3.229	-0.352	0.132	-0.653	-3.558	0.019
	313.15	-3.456	-0.389	0.051	-0.948	-3.646	0.022

κ_S^E /(10^{10}Pa^{-1})	298.15	-383.0	-342.2	-230.6	-193.2	-117.4	0.3
	303.15	-297.4	-256.8	-167.3	-132.2	-77.4	0.2
	308.15	-352.3	-309.1	-204.5	-166.2	-99.0	0.2
	313.15	-322.7	-279.0	-181.9	-144.1	-84.7	0.2
Δn	298.15	0.01030	0.00467	0.00269	0.00183	0.01217	0.00006
	303.15	0.01054	0.00529	0.00354	0.00493	0.01160	0.00005
	308.15	0.01091	0.00564	0.00403	0.00685	0.01166	0.00004
	313.15	0.01145	0.00624	0.00530	0.00721	0.01084	0.00004

{[BMIM]$^+$[MeSO$_4$]$^-$ (x_1) + 1-Butanol (x_2)}

V_m^E/(cm^3 · mol^{-1})	298.15	-0.692	-0.070	0.249	-0.180	-1.670	0.005
	303.15	-0.800	-0.120	0.349	-0.267	-1.838	0.006
	308.15	-0.920	-0.143	0.407	-0.476	-1.861	0.006
	313.15	-1.052	-0.201	0.533	-0.601	-2.058	0.007
κ_S^E /(10^{10}Pa^{-1})	298.15	-261.1	-205.4	-112.7	-69.3	-57.2	0.1
	303.15	-253.1	-197.4	-107.6	-65.5	-53.3	0.1
	308.15	-244.5	-189.0	-102.6	-61.8	-49.0	0.1
	313.15	-236.3	-181.0	-97.5	-58.0	-45.7	0.1
Δn	298.15	0.00452	0.00048	-0.00106	-0.00088	0.00897	0.00003
	303.15	0.00449	0.00091	-0.00044	0.00064	0.00806	0.00002
	308.15	0.00478	0.00152	-0.00118	0.00053	0.01000	0.00002
	313.15	0.00517	0.00199	-0.00111	0.00036	0.01100	0.00002

CHAPTER 6

DISCUSSION

The results obtained in this work for the binary systems ($[BMIM]^+[MeSO_4]^-$ + methanol, or 1-propanol, or 2-propanol, or 1-butanol) are compared with similar systems available in the literature. For the same systems only density was reported by Sibiya and Deenadayalu (2009) and Domanska *et al.* (2006). A comparison of the results obtained in this work with the literature data for the excess molar volumes at T = 298.15 K are given in figures 6.1-6.3 (Sibiya and Deenadayalu 2009; Domanska *et al.* 2006) and the $V^{E}_{m,min}$ is given in table 6.1. Compared to the literature the V^{E}_{m} results for the binary mixture ($[BMIM]^+[MeSO_4]^-$ + methanol) is similar to both that of Sibiya and Deenadayalu (2009) and Domanska *et al.* (2006) with a deviation of ± 0.007 $cm^3 \cdot mol^{-1}$ and ± 0.04 $cm^3 \cdot mol^{-1}$ respectively. There is a deviation of ± 0.21$cm^3 \cdot mol^{-1}$ between this work and Sibiya and Deenadayalu (2009) for the binary system ($[BMIM]^+[MeSO_4]^-$ + 1-propanol). A possible explanation is that, in this work an Anton Paar DSA 5000 M digital vibrating tube densimeter was used which gives a higher accuracy upto six decimal place in the measurement of density. Sibiya and Deenadayalu (2009) did the experimental work with an Anton Paar DMA 38 which measure density only to four decimal places. In this work IL of 97% purity was used but Sibiya and Deenadayalu (2009) used the IL with a 99.9 % purity this could be another reason for the deviation. It can be seen from table 6.1 that for the binary mixture ($[BMIM]^+[MeSO_4]^-$ + ethanol) González *et al* (2008) obtained a value of $V^{E}_{m,min}$ of -0.833 using the instrument DSA 5000 M. Sibiya and Deenadayalu (2009) obtained a value of $V^{E}_{m,min}$ of -0.647 using the Anton Paar DMA 38. There seems be a deviation of ± 0.2 $cm^3 \cdot mol^{-1}$ between the $V^{E}_{m,min}$ measurements when using the two different instruments. For the ($[BMIM]^+[MeSO_4]^-$ + 1-butanol) system the $V^{E}_{m,min}$ result from Domanska

et al (2006) as shown in figure 6.3 and table 6.1 had a deviation of ± 0.018 $cm^3 \cdot mol^{-1}$ from the result obtained in this work. Density, speed of sound and refractive index for ($[BMIM]^+[MeSO_4]^-$ + ethanol) system was not done in this work since Pereiro and Rodriguez (2007) reported these values. Others authors (Sibiya and Deenadayalu 2009; Domanska *et al.* 2006) published only density for this system ($[BMIM]^+[MeSO_4]^-$ + methanol, or 1-propanol, or 2-propanol, or 1-butanol) as well.

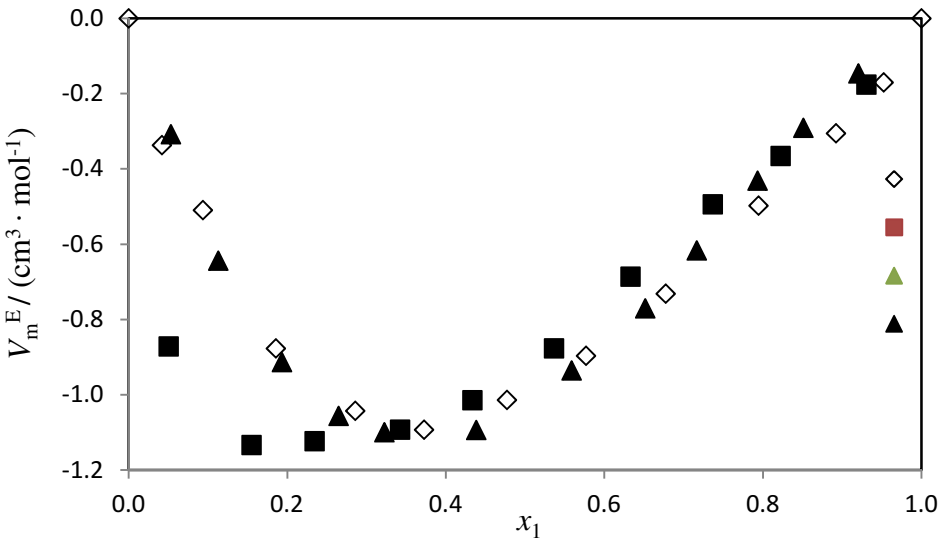

Figure 6.1 Excess molar volume, V_m^E, of the binary mixture plotted against mole fraction x_1 of IL at T = 298.15 K for {$[BMIM]^+[MeSO_4]^-$ (x_1) + Methanol (x_2)}, ◊, this work and ■, (Domanska *et al.* 2006), and▲, (Sibiya and Deenadayalu 2009), at T = 298.15 K.

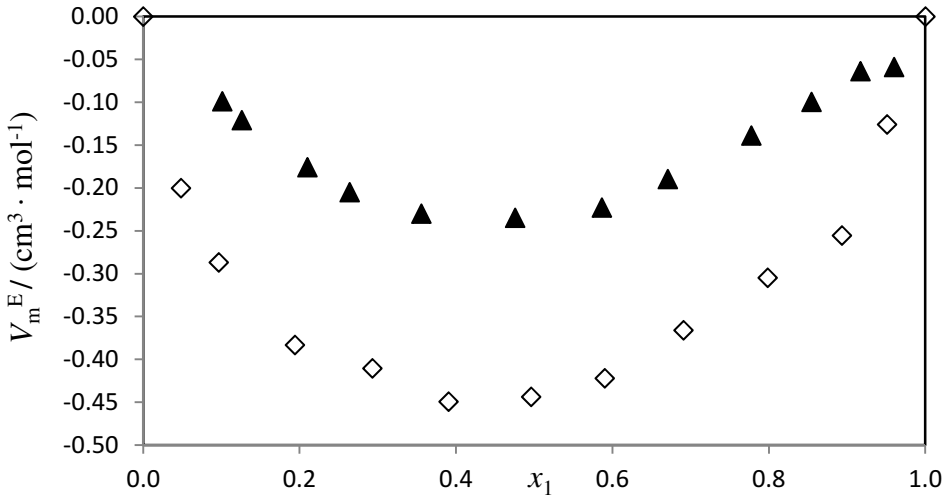

Figure 6.2 Excess molar volume, V_m^E, of the binary mixture plotted against mole fraction x_1 of IL at T = 298.15 K {[BMIM]$^+$[MeSO$_4$]$^-$ (x_1) + 1-Propanol (x_2)}, ◊, this work and ▲, (Sibiya and Deenadayalu 2009).

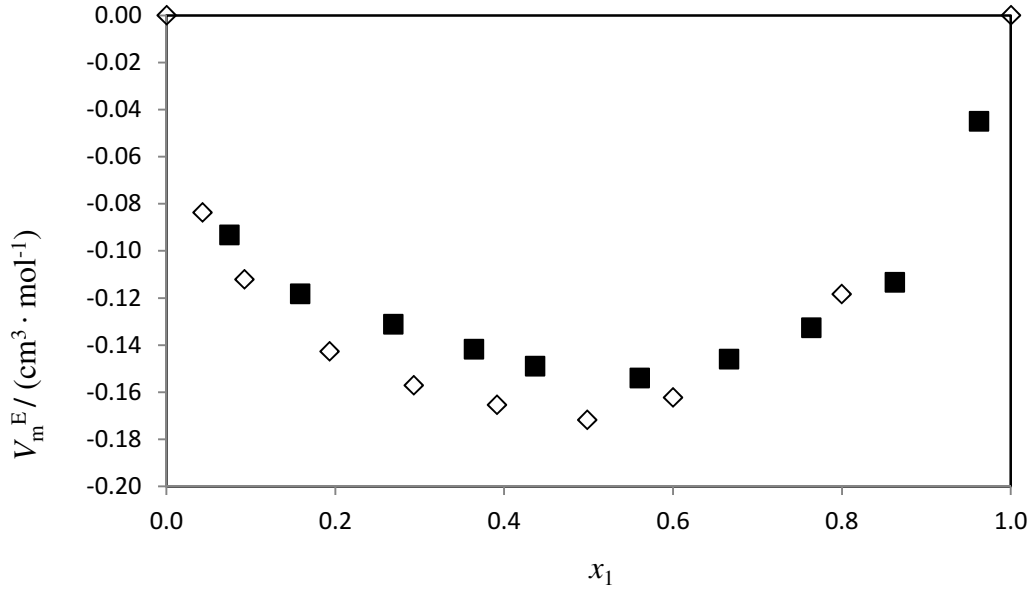

Figure 6.3 Excess molar volumeV_m^E, of the binary mixture plotted against mole fraction x_1 of IL at T = 298.15 K {[BMIM]$^+$[MeSO$_4$]$^-$ (x_1) + 1-Butanol (x_2)}, ◊, this work and ■, (Domanska *et al.* 2006).

Table 6.1 The minimum excess molar volumes, $V^{E}_{m,min}$ at T = 298.15 K for this work and literature.

System	x_1	$V^{E}_{m,min}$ / ($cm^3 \cdot mol^{-1}$)	
	Exp	Lit	Exp
		T = 298.15 K	
$[BMIM]^+[MeSO_4]^-$ + methanol	0.3729	-1.100[a]	-1.093
$[BMIM]^+[MeSO_4]^-$ + methanol		-1.1339[b]	
$[BMIM]^+[MeSO_4]^-$ + ethanol		-0.647[a]	
$[BMIM]^+[MeSO_4]^-$ + ethanol		-0.706[c]	
$[BMIM]^+[MeSO_4]^-$ + ethanol		-0.707[d]	
$[BMIM]^+[MeSO_4]^-$ + ethanol		-0.833[e]	
$[BMIM]^+[MeSO_4]^-$ + 1-propanol	0.3903	-0.235[a]	-0.449
$[BMIM]^+[MeSO_4]^-$ + 2-propanol	0.4960		-0.717
$[BMIM]^+[MeSO_4]^-$ + 1-butanol	0.4981	-0.1540[b]	-0.172

[a] Sibiya and Deenadayalu (2009).

[b] Domanska *et al.* (2006).

[c] Pereiro and Rodriguez (2007).

[d] Iglesias-Otero *et al.* (2008).

[e] González *et al.* (2008).

6.1 DENSITY

6.1.1 Effect of temperature and chain length on density

The experimental density data, ρ, of ($[BMIM]^+[MeSO_4]^-$ + methanol, or 1-propanol, or 2-propanol, or 1-butanol) binary mixtures over the entire mole fraction range and at different temperatures are listed in tables 5.2-5.5. The density of the binary mixtures decrease with an increase in temperature and the alcohol chain length.

6.1.2 Prediction of density by Lorentz-Lorenz (L-L) approximation

The molar refraction for the binary mixture is assumed to behave as an ideal mixture, the following predictive expression for ρ can be obtained from equations (3.21) and (3.23) within the frame-work of the Lorentz–Lorenz approximation.

$$\rho = \frac{\left(\frac{n^2-1}{n^2+2}\right)\left(x_1 M_1 + x_2 M_2\right)}{\left(\frac{n_1^2-1}{n_1^2+2}\right)x_1 \frac{M_1}{\rho_1} + x_2\left(\frac{n_2^2-1}{n_2^2+2}\right)\frac{M_2}{\rho_2}} \tag{3.26}$$

Equation (3.26) was used to predict the ρ since ρ_i and n_i for the pure compounds, and n for the mixture are known. Figures 6.4-6.7 are plots of the experimental and predicted density values. Root mean square deviation, RMSD, between the experimental and the predicted density for the binary mixtures at T = (298.15, 303.15, 308.15, and 313.15) K are given in table 6.2 with a maximum deviation of ± 0.0015 g · cm^{-3}. This shows that the L-L approximation is an appropriate equation to use for the prediction of density. The average absolute deviation percentage (AAD%) was calculated using the equation:

$$AAD\% = \frac{100}{N_{\mathrm{p}}} \sum_{i=1}^{N_{\mathrm{p}}} \left| 1 - \rho_{\mathrm{cal}} / \rho_{\mathrm{exp}} \right|_i \tag{6.1}$$

The AAD% is also given in table 6.2.

The maximum AAD% is 0.007.

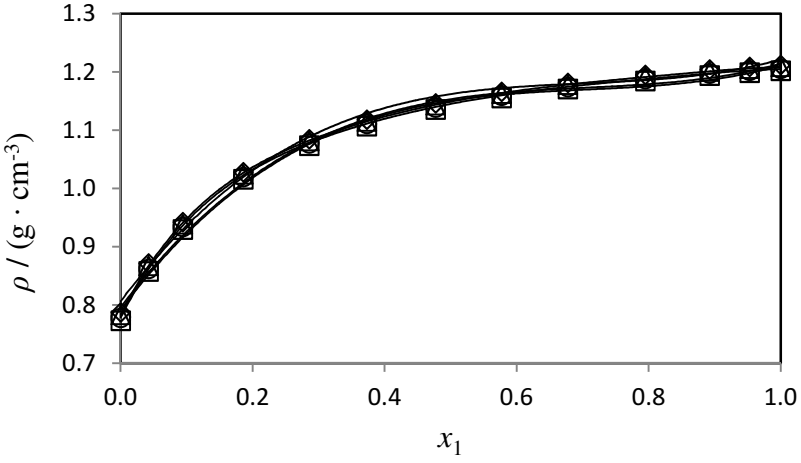

Figure 6.4 Experimental density, ρ, of the binary mixture plotted against mole fraction x_1 of IL at T = (298.15 to 313.15) K. ◊, T = 298.15 K; Δ, T = 303.15 K; ○, T = 308.15 K; and □, T = 313.15 K. For the binary mixture {[BMIM]$^+$[MeSO$_4$]$^-$ (x_1) + Methanol (x_2)}. The solid lines represent the corresponding prediction by L-L approximation.

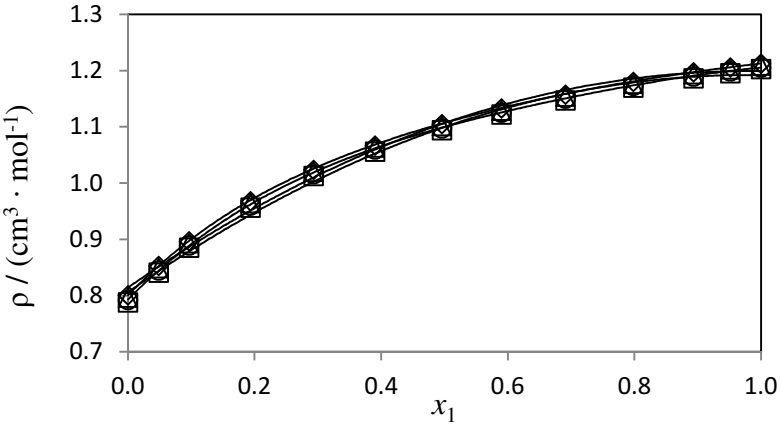

Figure 6.5 Experimental density, ρ, of the binary mixture plotted against mole fraction x_1 of IL at T = (298.15 to 313.15) K. ◊, T = 298.15 K; Δ, T = 303.15 K; ○, T = 308.15 K; and □, T = 313.15 K. For the binary mixture {[BMIM]$^+$[MeSO$_4$]$^-$ (x_1) + 1-Propanol (x_2)}. The solid lines represent the corresponding prediction by L-L approximation.

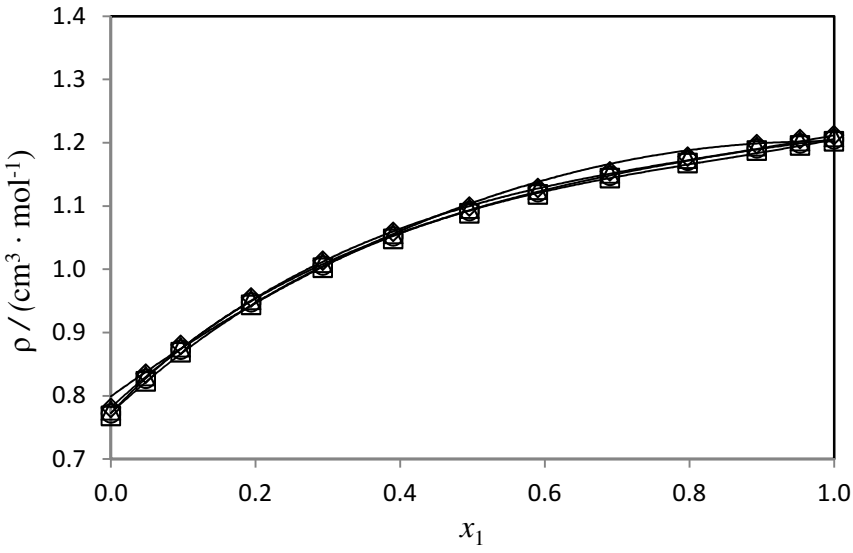

Figure 6.6 Experimental density, ρ, of the binary mixture plotted against mole fraction x_1 of IL at T = (298.15 to 313.15) K. ◊, T = 298.15 K; Δ, T = 303.15 K; ○, T = 308.15 K; and □, T = 313.15 K. For the binary mixture {[BMIM]$^+$[MeSO$_4$]$^-$ (x_1) + 2-Propanol (x_2)}. The solid lines represent the corresponding prediction by L-L approximation.

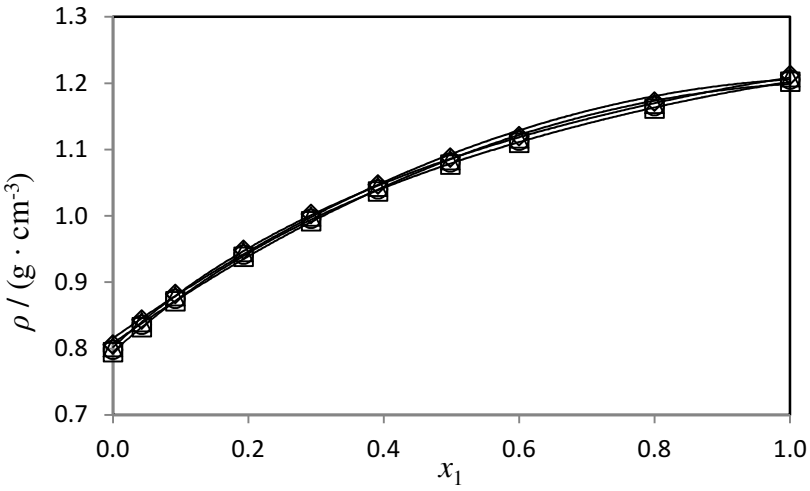

Figure 6.7 Experimental density, ρ, of the binary mixture plotted against mole fraction x_1 of IL at T = (298.15 to 313.15) K. ◊, T = 298.15 K; Δ, T = 303.15 K; ○, T = 308.15 K; and □, T = 313.15 K. For the binary mixture {[BMIM]$^+$[MeSO$_4$]$^-$ (x_1) + 1-Butanol (x_2)}. The solid lines represent the corresponding prediction by L-L approximation.

Table 6.2 Root Mean Square Deviation, RMSD, between the experimental and the predicted density for the binary mixtures at T = (298.15, 303.15, 308.15, and 313.15) K.

Property	T / K			
	298.15	303.15	308.15	313.15
		($[BMIM]^+[MeSO_4]^-$ + Methanol)		
RMSD	0.00153	0.00112	0.00092	0.00081
% AAD	0.00591	0.00456	0.00411	0.00373
		($[BMIM]^+[MeSO_4]^-$ + 1-Propanol)		
RMSD	0.00134	0.00126	0.00120	0.00117
% AAD	0.00429	0.00426	0.00423	0.00425
		($[BMIM]^+[MeSO_4]^-$ + 2-Propanol)		
RMSD	0.00123	0.00123	0.00120	0.00119
% AAD	0.00466	0.00516	0.00527	0.00536
		($[BMIM]^+[MeSO_4]^-$ + 1-Butanol)		
RMSD	0.00147	0.00140	0.00138	0.00140
% AAD	0.00662	0.00619	0.00610	0.00618

6.2 EXCESS MOLAR VOLUME

6.2.1 Effect of temperature and chain length on excess molar volume

The results for the excess molar volume for the binary systems ($[BMIM]^+[MeSO_4]^-$ + methanol, or 1-propanol, or 2-propanol, or 1-butanol) are given in tables 5.2-5.5 and are plotted in figures 5.1-5.4. The V_m^E is negative for all the systems at all temperatures and decreases when the temperature is increased. This behaviour can be explained because hydrogen bonding is certainly more *T*-dependent (becoming negligible at high temperatures) than coulombic interactions. This result agrees with the work of (González *et al.* 2007). The kinetic energy of molecules also increases when temperature increases. This leads to a decrease in interaction between the alcohol molecules and between the IL molecules with temperature. This effect is greater for the alcohols than for the ionic liquid, resulting in increased contraction in volume due to greater dipolar-ion interactions and decreasing V_m^E with temperature (Zhong *et al.* 2007).

The IL exists as a 3 D network and is bulkier than the alcohols, so it easily accommodates the smaller sized alcohols molecules into the interstices upon mixing (Zafarani-Moattar *et al* 2006; Zhong *et al.* 2007). In general V_m^E increases with increasing the alcohol chain length because of the molar volume or the size of the molecules which are in the order 1-butanol > 2-propanol > 1-propanol > methanol (Zafarani-Moattara *et al* 2006). The packing effect should be in the order methanol > 1-propanol > 2-propanol > 1-butanol. The V_m^E order for ($[BMIM]^+[MeSO_4]^-$ + methanol, or 1-propanol, or 2-propanol, or 1-butanol) systems is methanol > 2-propanol > 1-propanol >1-butanol. For the (IL + 2–propanol) system the excess molar volumes are more negative than the (IL + 1-propanol) system which implies that in the (IL + 2–propanol) system there are stronger ion-dipole interactions than in the (IL + 1-propanol) system. From the above order the ion-dipole interactions and packing effects are strongest in the (IL + methanol) system than in the (IL + 1-propanol, or 2-propanol, or 1-butanol) systems it can be caused

because the packing is stronger for primary than for secondary alcohols. This behaviour is identical to the results reported by Arce *et al.* (2006) for the systems ($[OMIM]^+[BF_4]^-$ + methanol, or ethanol, or 1-propanol, or 2- propanol) and by González *et al.* (2007) for the systems ([EMISE] + methanol, 1-propanol, and 2-propanol) at T = (298.15, 313.15, and 328.15) K. In both the cases the V_m^E for the (IL + 2-propanol) system is more negative than (IL + 1-propanol) system similar to this work.

The negative V_m^E indicate that attractive interaction and/or efficient packing occurred when the ionic liquid and the alcohols were mixed. Ion-dipole interaction between organic molecular liquid and the ionic liquid, also contribute to the negative value of the excess molar volume (Sibiya and Deenadayalu 2008).

The $V_{m,min}^E$ values at T = 298.15 K at x_1 = 0.3729 is -1.093 $cm^3 \cdot mol^{-1}$, x_1 = 0.3903 is -0.449 $cm^3 \cdot mol^{-1}$, x_1 = 0.4960 is -0.717 $cm^3 \cdot mol^{-1}$, x_1 = 0.4981 is -0.172 $cm^3 \cdot mol^{-1}$, for $[BMIM]^+[MeSO_4]^-$ + methanol, 1-propanol, or 2-propanol, or 1-butanol) respectively.

6.2.2 Excess partial molar volume

The results for the excess partial molar volumes for the binary systems $[BMIM]^+[MeSO_4]^-$ + methanol, or 1-propanol, or 2-propanol, or 1-butanol) are given in tables 5.6-5.9 and are plotted in figures 5.5-5.8. Excess partial molar volume for IL, $V_{m,1}^E$, for the (IL + methanol) binary system decreases sharply at high methanol concentrations indicative of the strong interaction by hydrogen bonding of the methanol molecules. But as the IL concentration increases the self-associated methanol structure collapses. At $x_1 = \pm 0.4$ (close to $V_{m,min}^E$) the change in $V_{m,1}^E$ is small.

The change in $V_{m,2}^E$ is significantly less than that for $V_{m,1}^E$. At low methanol concentrations there is a stronger interaction between the IL and methanol molecules possibly due to a packing effect.

For the (IL + 1-propanol) binary system $V^{E}_{m,1}$ is less negative at high 1-propanol concentrations indicative of less hydrogen bonding between the 1-propanol molecules. However when 1-propanol concentration is low there is a strong interaction with the IL. At $x_1 = \pm 0.3$ $V^{E}_{m,2}$ rapidly decreases.

For the (IL + 2-propanol) binary system the trend of $V^{E}_{m,i}$ is similar to that of (IL + methanol) binary system.

For the (IL + 1-butanol) binary system $V^{E}_{m,1}$ decreases significantly at $x_1 \leq \pm 0.4$ indicating that at low IL concentration stronger hydrogen bonding between alcohol molecules occur, but less than that for methanol molecules. $V^{E}_{m,2}$ for the (IL + 1-butanol) systems has the least change with increase in IL concentration.

6.2.3 Correlation of excess molar volume by Lorentz-Lorenz approximation

Correlation of the excess molar volume can be obtained using the refractive index obtained for the binary mixture by the Lorentz-Lorenz approximation. The experimental V^{E}_{m} and Δn data are given in tables 5.2-5.5 and 5.10-5.13. Equation (3.30) was used to correlate the experimental V^{E}_{m} data.

$$V^{E}_{m} = (-\Delta n)\frac{3R(n^{id} + n)}{(n^2 - 1)((n^{id})^2 - 1)} = (-\Delta n) f(R, n^{id}, n) \tag{3.30}$$

The function (R, n^{id}, n) is always positive; therefore the above equation provides the explicit evidence that V^{E}_{m} and Δn are of opposite signs (Iglesias *et al.* 2008). n^{id} was calculated for the system (IL + 1-propanol) using both equations (3.24-3.25). The results were same for n^{id}. Therefore only simplified equation (3.25) for n^{id} was used for the system.

In general the RMSD increased with an increase in temperature because of the increase in volatility of the alcohols. The greatest increase in RMSD occurred for (IL + methanol) system because methanol is the most volatile alcohol. The root mean square deviation, RMSD, between the experimental and correlated V_m^E, for the binary mixtures at T = (298.15, 303.15, 308.15, and 313.15) K are shown in table 6.3. The maximum RMSD is ± 0.28 $cm^3 \cdot mol^{-1}$ which was obtained for the ($[BMIM]^+[MeSO_4]^-$ + butanol) system. This method does not give a good representation of the trend of the experimental data.

Table 6.3 Root Mean Square Deviation, RMSD, between the experimental and correlated V_m^E for the binary mixtures at T = (298.15, 303.15, 308.15, and 313.15) K.

Property	T / K			
	298.15	303.15	308.15	313.15
	Root Mean Square Deviation			
	($[BMIM]^+[MeSO_4]^-$ + Methanol)			
V_m^E / ($cm^3 \cdot mol^{-1}$)	0.0858	0.1227	0.1431	0.1537
	($[BMIM]^+[MeSO_4]^-$ + 1-Propanol)			
V_m^E / ($cm^3 \cdot mol^{-1}$)	0.0407	0.0418	0.0223	0.0745
	($[BMIM]^+[MeSO_4]^-$ + 2-Propanol)			
V_m^E / ($cm^3 \cdot mol^{-1}$)	0.0168	0.0206	0.0334	0.0398
	($[BMIM]^+[MeSO_4]^-$ + 1-Butanol)			
V_m^E / ($cm^3 \cdot mol^{-1}$)	0.2765	0.2585	0.2536	0.2553

6.3 EXCESS ISENTROPIC COMPRESSIBILITY

6.3.1 Effect of temperature and chain length on speed of sound

The speed of sound, *u*, and isentropic compressibility, κ_s, data of ($[BMIM]^+[MeSO_4]^-$ + methanol, or 1-propanol, or 2-propanol, or 1-butanol) binary mixtures over the entire mole fraction range and at different temperatures are listed in tables 5.2-5.5. The speed of sound of binary mixtures decrease with an increase in temperature and increase with the alcohol chain length. The isentropic compressibility of the binary mixtures increases with an increase in temperature but decreases from methanol to 1-butanol. However the value of 2-propanol is greater than the (IL + 1-propanol, or 1-butanol) system.

For the systems ($[BMIM]^+[MeSO_4]^-$ + methanol, or 1-propanol, or 2-propanol, or 1-butanol) the values of κ_S^E are negative over the entire composition range and at all the temperatures studied. The κ_S^E for these systems follows the sequence: 1-butanol > 1-propanol > 2-propanol > methanol. There is a increase in compressibility from the ideal mixture in the order 1-butanol > 1-propanol > 2-propanol > methanol.

This behaviour of κ_S^E implies that these mixtures are less compressible than the ideal mixture. This is due to a closer approach of unlike molecules and stronger interaction between components of the mixture that leads to decrease in compressibility (Zafarani-Moattar and Shekaari 2005).

6.4 REFRACTIVE INDEX DEVIATIONS

6.4.1 Effect of temperature and chain length on refractive index

The refractive index data is given in tables 5.10-5.13. Refractive index decrease with an increase in the temperature but increases in the order methanol < 2-propanol < 1-propanol < 1-butanol.

6.4.2 Prediction of refractive index by the Lorentz-Lorenz approximation

Equation (3.26) allows one to obtain the inverse prediction *i.e.*, to calculate n from pure-solvent density and refractive index data and from the experimental density of the mixture. The Lorentz-Lorenz equation for the prediction of n is given below:

$$n = \left(\frac{2\left[\left(\frac{n_1^2-1}{n_1^2+2}\right)x_1\rho\frac{M_1}{\rho_1}+x_2\left(\frac{n_2^2-1}{n_2^2+2}\right)\rho\frac{M_2}{\rho_2}\right]+\left[x_1M_1+x_2M_2\right]}{\left[x_1M_1+x_2M_2\right]-\left[\left(\frac{n_1^2-1}{n_1^2+2}\right)x_1\rho\frac{M_1}{\rho_1}+x_2\left(\frac{n_2^2-1}{n_2^2+2}\right)\rho\frac{M_2}{\rho_2}\right]} \right)^{1/2} \tag{3.31}$$

Equation (3.31) was used to predict the refractive index. Figures 6.8-6.11 are the plots between the experimental and calculated refractive index. Table 6.4 shows the root mean square deviation, RMSD, for the binary mixtures at T = (298.15, 303.15, 308.15, and 313.15) K. The maximum RMSD is 0.0007. These results confirm the ability of the proposed method to predict accurately the refractive index data for binary systems containing RTILs. The Lorentz-Lorenz approximation gives a good prediction of refractive index of mixtures of ($[BMIM]^+[MeSO_4]^-$ + methanol, or 1-propanol, or 2-propanol, or 1-butanol) as can be seen in figures 6.8-6.11.

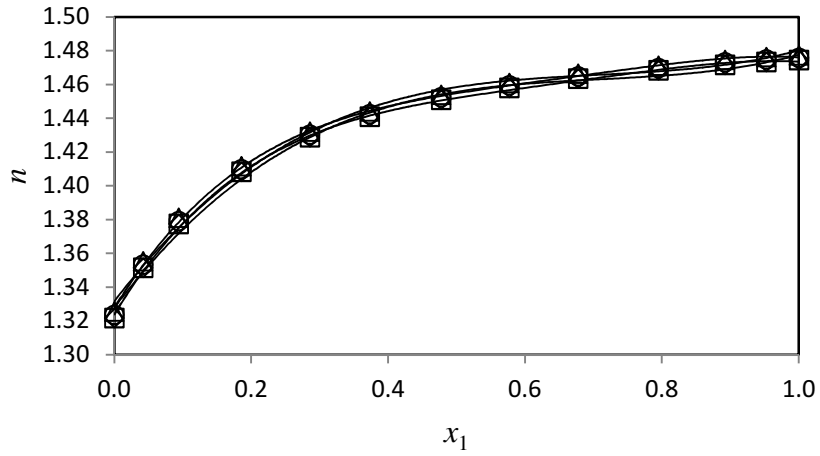

Figure 6.8 Refractive index, n, of the binary mixture plotted against mole fraction x_1 of IL at T = (298.15 to 313.15) K. ◊, T = 298.15 K; Δ, T = 303.15 K; ○, T = 308.15 K; and □, T = 313.15 K. For the binary mixture {[BMIM]$^+$[MeSO$_4$]$^-$ (x_1) + Methanol (x_2)}. The solid lines represent the corresponding prediction by L-L approximation.

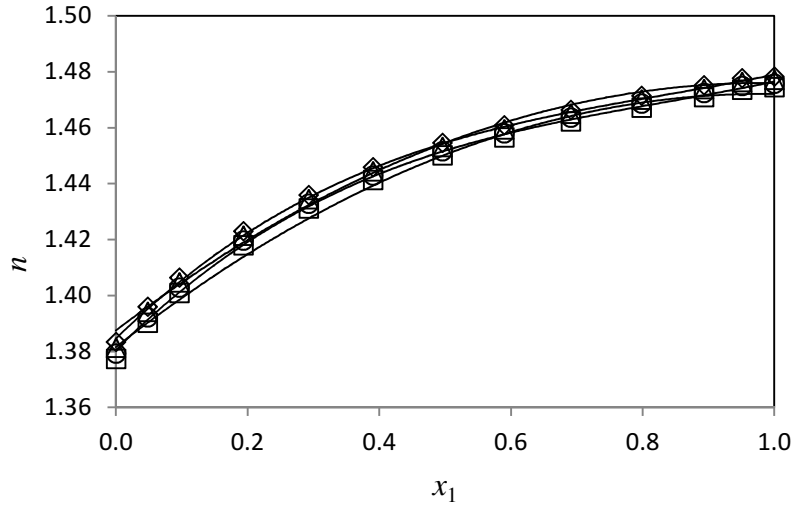

Figure 6.9 Refractive index, n, of the binary mixture plotted against mole fraction x_1 of IL at T = (298.15 to 313.15) K. ◊, T = 298.15 K; Δ, T = 303.15 K; ○, T = 308.15 K; and □, T = 313.15 K. For the binary mixture {[BMIM]$^+$[MeSO$_4$]$^-$ (x_1) + 1-Propanol (x_2)}. The solid lines represent the corresponding prediction by L-L approximation.

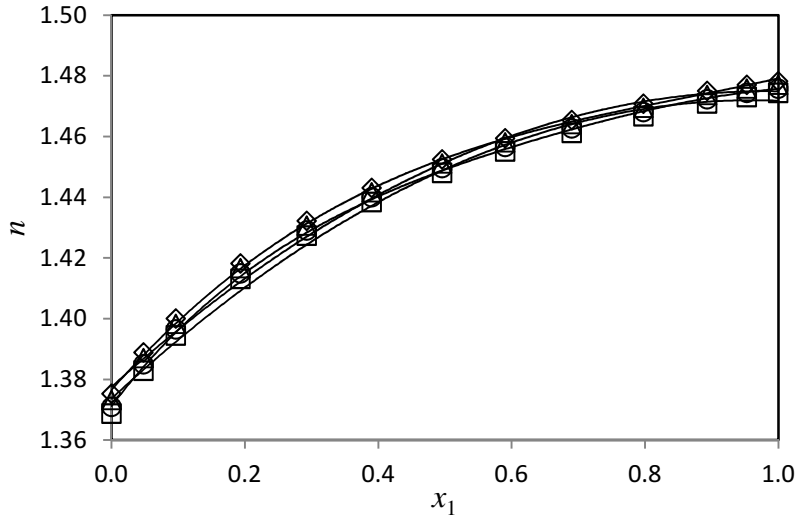

Figure 6.10 Refractive index, n, of the binary mixture plotted against mole fraction x_1 of IL at T = (298.15 to 313.15) K. ◊, T = 298.15 K; Δ, T = 303.15 K; ○, T = 308.15 K; and □, T = 313.15 K. For the binary mixture {[BMIM]$^+$[MeSO$_4$]$^-$ (x_1)+ 2-Propanol (x_2)}. The solid lines represent the corresponding prediction by L-L approximation.

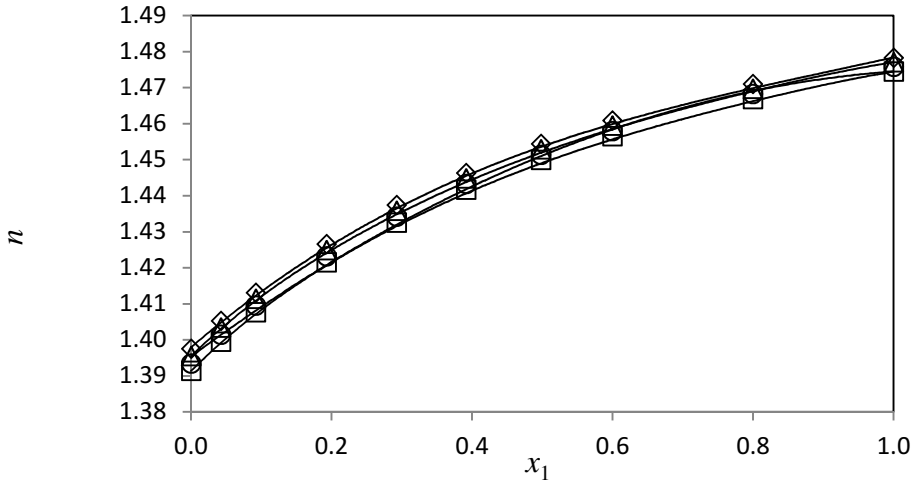

Figure 6.11 Refractive index, n, of the binary mixture plotted against mole fraction x_1 of IL at T = (298.15 to 313.15) K. ◊, T = 298.15 K; Δ, T = 303.15 K; ○, T = 308.15 K; and □, T = 313.15 K. For the binary mixture {[BMIM]$^+$[MeSO$_4$]$^-$ (x_1) + 1-Butanol (x_2)}. The solid lines represent the corresponding prediction by L-L approximation.

Table 6.4 Root Mean Square Deviation, RMSD, between the experimental and the predicted refractive index for the binary mixtures at *T* = (298.15, 303.15, 308.15, and 313.15) K.

Property	*T* / K			
	298.15	303.15	308.15	313.15
	Root Mean Square Deviation			
	($[BMIM]^+[MeSO_4]^-$ + Methanol)			
n	0.00037	0.00051	0.00042	0.00037
	($[BMIM]^+[MeSO_4]^-$ + 1-Propanol)			
n	0.00064	0.00061	0.00058	0.00056
	($[BMIM]^+[MeSO_4]^-$ + 2-Propanol)			
n	0.00059	0.00060	0.00058	0.00058
	($[BMIM]^+[MeSO_4]^-$ + 1-Butanol)			
n	0.00072	0.00068	0.00068	0.00069

Figures 5.10-5.13 show the refractive index deviations for the four studied binary mixtures. The value of Δn increases in the order 1-butanol < 1-propanol < 2-propanol < methanol. The refractive index deviation decreases with an increase in the chain length of the alcohols. However secondary alcohols have higher refractive index deviation than the primary alcohol.

CHAPTER 7

CONCLUSION

Excess molar volume V_m^E, excess isentropic compressibility κ_S^E, refractive index deviation Δn, and molar refraction for ($[BMIM]^+[MeSO_4]^-$ + methanol, or 1-propanol, or 2-propanol, or 1-butanol) have been calculated from the density, speed of sound, and refractive index respectively, at $T =$ (298.15, 303.15, 308.15, and 313.15) K over the whole range of concentrations. For all the systems studied V_m^E and κ_S^E are negative and V_m^E decrease slightly when the temperature increases. The negative V_m^E and κ_S^E for these mixtures are due to ion-dipole interactions and/or packing effects between the alcohol and the IL. V_m^E increase in the order: methanol > 2-propanol > 1-propanol > 1-butanol showing that V_m^E is a function of the composition, chain length and position of the hydroxyl group on the alcohol. The refractive index deviation at T = (298.15, 303.15, 308.15, and 313.15) K is positive over the whole composition range. The Redlich-Kister smoothing equation was used to fit the V_m^E, κ_S^E, and Δn data. The Lorentz-Lorenz equation was used to correlate the volumetric property and predict the density or the refractive index of the binary mixtures of ionic liquid and alcohols. The Lorentz-Lorenz approximation gives poor correlation for the excess molar volume for the mixtures ($[BMIM]^+[MeSO_4]^-$ + methanol, or 1-propanol, or 2-propanol, or 1-butanol) and better predicts density or refractive index.

CHAPTER 8

RECOMMENDATIONS

The deviation of the speed of sound from ideality can be calculated using sound velocity mixing rules and prediction of the refractive index for binary mixtures should be done. Deviations of the speed of sound from the ideal values, u^{D}, are thus obtained by subtraction, $u^{\mathrm{D}} = u - u^{\mathrm{id}}$. u^{id} can be calculated from:

$$u^{\mathrm{id}} = V^{\mathrm{id}} \left(M^{\mathrm{id}} \cdot K_{\mathrm{s}}^{\mathrm{id}} \right)^{1/2} \tag{8.1}$$

where V^{id}, M^{id}, and $K_{\mathrm{s}}^{\mathrm{id}}$ are molar volume, molar mass, and molar isentropic compressibility of the ideal mixture (Zorębski and Deć 2012).

Several mixing rules have been proposed to calculate mixture sound velocity from pure component data (Parades *et al.* 2012).

$$u^{1/3}\mathrm{V} = \sum_{i=1}^{2} x_i u_i^{1/3} \mathrm{V}_i \therefore u = \left(\sum_{i=1}^{2} x_i u_i^{1/3} \mathrm{V}_i \Big/ \mathrm{V} \right)^3 \tag{8.2}$$

$$u = \left(\sum_{i=1}^{2} \Phi_i u_i^{1/3} \right)^3 \tag{8.3}$$

$$\kappa_{\mathrm{s}} = \sum_{i=1}^{2} \Phi_i \kappa_{\mathrm{s},i} \therefore u = \left(\rho \sum_{i=1}^{2} \Phi_i \kappa_{\mathrm{s},i} \right)^{-1/2} \tag{8.3}$$

Where u is the sound velocity, V is molar volume, ϕ is the volume fraction, κ_s is the isentropic compressibility, x is the mole fraction and ρ is the density of the mixture.

These mixing rules can be used to calculate the speed of sound for the binary mixtures.

Prediction of refractive indices of binary mixtures is essential for the determination of composition of binary liquid mixtures. The most widely used theoretical rules for predicting refractivity of binary liquid mixtures are due to Weiner, Heller and Gladstone-Dale (Mehra 2003).

The experimental work can be extended to ternary systems.

REFERENCES

Abdulagatov I.M. , Tekin A. , Safarov J. , Shahverdiyev A., Hassel E. *High-pressure densities and derived volumetric properties (excess, apparent, and partial molar volumes) of binary mixtures of {methanol (1) + $[BMIM]^+[BF_4]^-$ (2)}*, J. Chem. Thermodyn. 40, **2008**, 1386-1401.

Alvarez V.H., Mattedi S., Martin-Pastor M., Aznar M., Iglesias M. *Thermophysical properties of binary mixtures of {ionic liquid 2-hydroxy ethylammonium acetate + (water, methanol, or ethanol)}*, J. Chem. Thermodyn. 43 (7), **2011**, 997-1010.

Andreatta A.E., Arce A., Rodil E., Soto A. *Physical Properties of Binary and Ternary Mixtures of Ethyl Acetate, Ethanol, and 1-Octyl-3-methyl-imidazolium Bis(trifluoromethylsulfonyl)imide at 298.15 K*, J. Chem. Eng. Data 54 (3), **2009**, 1022-1028.

Arce A., Martínez-Ageitos J., Rodil E., Soto A. *Thermophysical properties for1-butanol + ethanol + 2-methoxy-2-methylbutane ternary system,* Fluid Phase Equilib. 187-188, **2001**, 155-169.

Arce A., Rodil E., Soto A. *Physical and Excess Properties for Binary Mixtures of 1-Methyl-3-Octylimidazolium Tetrafluoroborate, $[OMIM]^+[BF_4]^-$, Ionic Liquid with Different Alcohols***,** J. Solution Chem. 35(1), **2006**, 63-78.

Armand M., Endres F., MacFarlane D.R., Ohno H., Scrosati B. *Ionic-liquid materials for the electrochemical challenges of the future*, Nature Materials. 8, **2009**, 621 – 629.

Azevedo R., Szydlowski J., Pires P.F., Esperança J.M.S.S., Guedes H.J.R., Rebelo L.P.N. *novel non-intrusive microcell for sound-speed measurements in liquids. Speed of sound and thermodynamic properties of 2-propanone at pressures up to 160 MPa*, J. Chem. Thermodyn. 36, **2004**, 211-222.

Battino R. *Volume changes on mixing for binary mixtures of liquids*, Chemical Reviews 71 (5), **1971**, 5-45.

Beath L.A., Neill S.P.O`, Williamson A.G. *Thermodynamics of ether solutions II.Volumes of mixing of ethers with carbon tetrachloride and with chloroform at* 25^0 *C*, J. Chem. Thermodyn. 1 (3), **1969**, 293-300.

Bhujrajh P., Deenadayalu, N. *Liquid Densities and Excess Molar Volumes for Binary Systems (Ionic Liquids + Methanol or Water) at 298.15, 303.15 and 313.15 K, and at Atmospheric Pressure,* J. Solution Chem. 36, **2007**, 631–642.

Blandamer M.J. *Introduction to Chemical Ultrasonics*, *London, New York,* Academic Press, 1973, Series : Physical Chemistry; V 28.

Bottomly G.A., Scott R.L. *A grease – free continuous dilution dilatometer; excess volumes for benzene + carbon tetrachloride*, J. Chem. Thermodyn. 6 (10), **1974**, 973-981.

Brocos P., Piñeiro Á., Bravo R., Amigo A. *Thermodynamics of Mixtures Involving Some Linear or Cyclic Ketones and Cyclic Ethers. 1. Systems Containing Tetrahydrofuran*, J. Chem. Eng. Data 47 (2), **2002**, 351–358.

Brocos P., Piñeiro Á., Bravo R., Amigo A. *Refractive indices, molar volumes and molar refractions of binary liquid mixtures: concepts and correlations*, Phys. Chem. Chem. Phys. 5, **2003**, 550-557.

Calvar N., Gómez E., González B., Domínguez Á. *Experimental Determination, Correlation, and Prediction of Physical Properties of the Ternary Mixtures Ethanol + Water with 1-Octyl-3-methylimidazolium Chloride and 1-Ethyl-3-methylimidazolium Ethylsulfate at 298.15 K,* J. Chem. Eng. Data 52, **2007**, 2529–2535.

Cerdeirina C.A., Tovar C.A., Troncoso J., Carballo E., Roman L. *Excess volumes and excess heat capacities of nitromethane + (1-propanol or 2-propanol)*, Fluid Phase Equilib. 157, **1999**, 93-102.

Chum H.L., Koch V.R., Miller L.L., Osteryoung R.A. *Electrochemical scrutiny of organometallic iron complexes and hexamethylbenzene in a room temperature molten salt*, J. Am. Chem. Soc. 97 (11), **1975**, 3264-3265.

Crosthwaite J.M., Muldoon M.J., Dixon J.K., Anderson J.L., Brennecke J.F. *Phase transition and decomposition temperatures, heat capacities and viscosities of pyridinium ionic liquids*, J. Chem. Thermodyn. 37, **2005**, 559-568.

Deenadayalu N., Sen S., Sibiya P. N. *Application of the PFV EoS correlation to excess molar volumes of (1-ethyl-3-methylimidazolium ethylsulfate + alkanols) at different temperatures*, J. Chem. Thermodyn. 41, **2009**, 538-548.

Domanska U., Pobudkowska A., Wisniewska A. *Solubility and Excess Molar Properties of 1,3-Dimethylimidazolium Methylsulfate, or 1-Butyl-3-Methylimidazolium Methylsulfate, or 1-Butyl-3-Methylimidazolium Octylsulfate Ionic Liquids with n-Alkanes and Alcohols: Analysis in Terms of the PFP and FBT Models*, J. Solution Chem. 35 (3), **2006**, 311-334.

Domańska U., Królikowski M., Paduszyński K. *Phase equilibria study of the binary systems (N-butyl-3-methylpyridinium tosylate ionic liquid + an alcohol),* J. Chem. Thermodyn. 41, **2009,** 932-938.

Earle M.J., Seddon K.R. *Ionic liquids. Green solvents for the future,* Pure Appl. Chem. 72 (7), **2000,** 1391-1398.

Feng R., Zhao D., Guo Y. *Revisiting Characteristics of Ionic Liquids: A Review for Further Application Development*, Journal of Environmental Protection 1, **2010,** 95-104.

Frank F., Reid D.S.,; Water in Crystalline Hydrates Aqueous Solutions of Simple Non Electrolytes, 2, **1973**, 323-380.

Fermeglia M., Torriano G. *Density, Viscosity, and Refractive Index for Binary Systems of n-C16 and Four Nonlinear Alkanes at 298.15 K*, J. Chem. Eng. Data 44 (5), **1999**, 965–969.

Fort D.A., Swatloski R.P., Moyna P., Rogers R.D., Moyna G. *Use of ionic liquids in the study of fruit ripening by high-resolution ^{13}C NMR spectroscopy: 'green' solvents meet green bananas,* Chem. Commun. **2006**, 714-716.

Franks F., Smith H. T. *Apparent molal volumes and expansibilities of electrolytes in dilute aqueous solution,* Trans. Faraday Soc. 63, **1967**, 2586-2598.

Fletcher S.I., Sillars F.B., Hudson N.E., Hall P.J. *Physical Properties of Selected Ionic Liquids for Use as Electrolytes and Other Industrial Applications*, J. Chem. Eng. Data 55, **2010**, 778–782.

Gabriel S., Weiner J. *Ueber einige Abkömmlinge des Propylamins,* European Journal of Inorganic Chemistry 21 (2), **1888,** 2669–2679.

Gale R.J., Osteryoung R.A. *Potentiometric investigation of dialuminum heptachloride formation in aluminium chloride-1-butylpyridinium chloride mixtures*, Inorg. Chem. 18 (6), **1979**, 1603-1605.

García-Miaja G., Troncoso J., Romaní L. Excess *properties for binary systems ionic liquid + ethanol: Experimental results and theoretical description using the ERAS model,* Fluid Phase Equilib. 274, **2008**, 59-67.

García-Mardones M., Pérez-Gregorio V., Guerrero H., Bandrés I., Lafuente C. *Thermodynamic study of binary mixtures containing 1-butylpyridinium tetrafluoroborate and methanol, or ethanol,* J. Chem. Thermodyn. 42, **2010**, 1500–1505.

García-Mardones M., Barrós A., Bandrés I., Artigas H., Lafuente C. *Thermodynamic properties of binary mixtures combining two pyridinium-based ionic liquids and two alkanols,* J. Chem. Thermodyn. 51, **2012**, 17–24.

Giridhar P., Venkatesan K.A., Srinivasan T. G., Rao P.R.V. *Electrochemical behaviour of uranium(VI) in 1-butyl-3-methylimidazolium chloride and thermal characterization of uranium oxide deposit*, Electrochim. Acta 52 (9), **2007**, 3006-3012.

Gołdon A., Dąbrowska K., Hofman T. *Densities and Excess Volumes of the 1,3- Dimethylimidazolium Methylsulfate + Methanol System at Temperatures from (313.15 to 333.15) K and Pressures from (0.1 to 25) MPa,* J. Chem. Eng. Data 52 (5), **2007**, 1830–1837.

González B., Calvar N., Gómez E., Dominguez Á. *Physical properties of the ternary system (ethanol + water + 1-butyl-3-methylimidazolium methylsulphate) and its binary mixtures at several temperatures*, J. Chem. Thermodyn. 40, **2008**, 1274-1281.

González E.J., Domínguez Á, Macedo E.A. *Excess properties of binary mixtures containing 1-hexyl-3-methylimidazolium bis(trifluoromethylsulfonyl)imide ionic liquid and polar organic compounds,*
J. Chem. Thermodyn**. 2012**.

González E. J., Alonso L., Domínguez Á. *Physical Properties of Binary Mixtures of the Ionic Liquid 1-Methyl-3-octylimidazolium Chloride with Methanol, Ethanol, and 1-Propanol at T = (298.15, 313.15, and 328.15) K and at P = 0.1 MPa*, J. Chem. Eng. Data 51, **2006**, 1446-1452.

González E.J., González B., Calvar N., Domínguez Á. *Physical Properties of Binary Mixtures of the Ionic Liquid 1-Ethyl-3-methylimidazolium Ethyl Sulfate with Several Alcohols at T = (298.15, 313.15, and 328.15) K and Atmospheric Pressure*, J. Chem. Eng. Data 52 (5), **2007**, 1641-1648.

González B., Calvar N., Gómez E., Domínguez I., Domínguez Á. *Synthesis and Physical Properties of 1-Ethylpyridinium Ethylsulfate and its Binary Mixtures with Ethanol and 1-Propanol at Several Temperatures*, J. Chem. Eng. Data 54 (4), **2009**, 1353-1358.

Govender U. P. *Thermodynamics of liquid mixtures: experimental & theoretical studies on the thermo chemical & volumetric behaviour of some liquid & liquid mixtures*, PhD thesis, UKZN, Durban, 2-6, **1996**.

Handa Y. P., Benson G. C. *Volume changes on mixing two liquids: A review of the experimental techniques and the literature data*, Fluid Phase Equilibr. 3 (2-3), **1979**, 185-249.

Hasan M, Hiray A.P., Kadam U.B., Shirude D. F., Kurhe K. J., Sawant A. B. *Densities, Sound Speed, and IR Studies of (Methanol + 1-Acetoxybutane) and (Methanol + 1,1-Dimethylethyl Ester) at (298.15, 303.15, 308.15, and 313.15) K,* J. Chem. Eng. Data 55, **2010**, 535–538.

Heintz A., Klasen D., Lehmann J. K. *Excess Molar Volumes and Viscosities of Binary Mixtures of Methanol and the Ionic Liquid 4-Methyl-N-butylpyridinium Tetrafluoroborate at 25, 40, and 50°C,* J. Solution Chem. 31 (6), **2002**, 467-476.

Hofman T., Goldon A., Nevines A., Letcher T. *Densities, excess volumes, isobaric expansivity, and isothermal compressibility of the (1-ethyl-3-methylimidazoliumethylsulfate + methanol) system at temperatures (283.15 to 333.15) K and pressures from (0.1 to 35) MPa*, J. Chem. Thermodyn. 40, **2008**, 580-591.

Hoiland H. *Partial Molar Volumes of Biochemical Model Compounds in Aqueous Solution*, Thermodynamic Data for Biochemistry and Biotechnology **1986,** 17-44.

Iglesias-Otero M.A., Troncoso J., Carballo E., Romanı´ L. *Density and refractive index in mixtures of ionic liquids and organic solvents: Correlations and predictions*, J. Chem. Thermodyn. 40, **2008**, 949–956.

Jiménez E., Casas H., Segade L., Franjo C. *Surface Tensions, Refractive Indexes and Excess Molar Volumes of Hexane + 1-Alkanol Mixtures at 298.15 K*, J. Chem. Eng. Data 45 (5), **2000**, 862–866.

Johnson K.E. *What's an Ionic Liquid*? The Electrochemical Society, Interface spring **2007.**

Karkamkar A., Aardahl C., Autrey T. *Recent Developments on Hydrogen Release from Ammonia Borane*, Material Matters. 2 (2), **2007**, 6-9.

Keyes D.B., Hildebrand J.H. *A study of the system aniline-hexane*, J. Am. Chem. Soc., 39 (10), **1917**, 2126–2137.

Kumaran M.K., McGlashan M.L. *An improved dilution dialometer for measurements of excess volumes*, J. Chem. Thermodyn. 9 (3), **1977**, 259-267.

Kurnia K., Mutalib M. I., Murugesan T., Ariwahjoedi B. *Physicochemical Properties of Binary Mixtures of the Protic Ionic Liquid Bis(2-hydroxyethyl)methylammonium Formate with Methanol, Ethanol, and 1-Propanol*, J. Solution Chem. 40, **2011**, 818-831.

Lapkin A.A., Plucinski P.K., Cutler M. *Comparative Assessment of Technologies for Extraction of Artemisinin*, J. Nat. Prod. 69 (11), **2006**, 1653-1664.

Li Y., Ye H., Zeng P., Qi F. *Volumetric Properties of Binary Mixtures of the Ionic Liquid 1-Butyl-3-Methylimidazolium Tetrafluoroborate with Aniline*, J. Solution Chem. 39, **2010**, 219-230.

Lorentz H.A. "*The theory of electrons and its application to the phenomena of light and radiant heat*", 2nd ed. Dover publications, New York, **1953**.

Lorentz L. "*Ueber die refraktionsconstante*" Wied. Ann. 11, **1880**, 70-103.

MacFarlane D.R., Golding J., Forsyth S., Forsyth M., Deacon G.B. *Low viscosity ionic liquids based on organic salts of the dicyanamide anion*, Chem. Commun. 16, **2001,** 1430-1431.

Marchetti A., Tassi L., Ulrici A., Vaccari G., Sanna G. *Refractive indices of binary mixtures of (1,2-dichloroethane + 2-chloroethanol) at various temperatures*, J. Chem. Thermodyn. 31, **1999**, 647–660.

Marino G., Piñeiro M.M., Iglesias M., Orge B., Tojo J. *Temperature Dependence of Binary Mixing Properties for Acetone, Methanol, and Linear Aliphatic Alkanes (C_6−C_8)*, J. Chem. Eng. Data 46 (3), **2001**, 728–734.

Marsh K.N. *Thermodynamics of liquid mixtures*, Annu. Rep. Prog. Chem., Sect. C: Phys. Chem., Chapter 4**,** 77, **1980**, 101-120**.**

Marsh K. N. *Thermodynamics of liquid mixtures*, Annu. Rep. Prog. Chem., Sect. C: Phys. Chem. Chapter 7. 81, **1984**, 209-245.

Mehra R. *Application of refractive index mixing rules in binary systems of hexadecane and heptadecane with n-alkanols at different temperatures*, Proc. Indian Acad. Sci. (Chem. Sci.), 115 (2), **2003**, 147–154.

Millero F. J. *Molal volumes of electrolytes*, Chem. Rev. 71 (2), **1971**, 147–176.

Millero F. J. *Review of the Experimental and Analytical Methods for the Determination of the Pressure-Volume-Temperature Properties of Electrolytes,* American Chemical Society, chapter 31, **1980**, 581-622.

Missen R.W. *Use of Term "Excess Function*", Ind. Eng. Chem. Fundamen. 8 (1), **1969**, 81-84.

Mokhtarani B., Sharifi A., Mortaheb H. R., Mirzaei M., Mafi M., Sadeghian F. *Densities and Viscosities of Pure 1-Methyl-3-octylimidazolium Nitrate and Its Binary Mixtures with Alcohols at Several Temperatures*, J. Chem. Eng. Data 55 (9), **2010**, 3901–3908.

Mosteiro L., Mascato E., Cominges B.E., Iglesias T.P., Legido J.L. *Density, speed of sound, refractive index and dielectric permittivity of (diethyl carbonate+ n-decane) at several temperatures*, J. Chem. Thermodyn. 33, **2001**, 787–801.

Najdanovic-Visak V., Esperança J. M. S. S., Rebelo L. P. N., Da Ponte M. N., Guedes H. J. R., Seddon K. R., Szydlowski J. *Phase behavior of room temperature ionic liquid solutions: an unusually large co-solvent effect in (water + ethanol)*, Phys. Chem. Chem. Phys. 4, **2002**, 1701-1703.

Nath J., Mishra S. K. *Relative permittivities and refractive indices of binary mixtures of cyclohexanone with dichloromethane, trichloromethane,1,2-dichloroethane, trichloroethene and cyclohexane at T = 303.15 K*, Fluid Phase Equilibr. 145, **1998**, 89–97.

Nevines J.A. *Thermodynamics of nonelectrolytes liquid mixtures*, PhD thesis, UKZN, Durban, 78-80, 1997.

Pal A., Singh W. *Excess molar volumes and excess partial molar volumes of {x$CH_3O(CH_2)_2OH$ + (1 −x) $H(CH_2)_v O(CH_2)_2O (CH_2)_2OH$}, (v= 1, 2, and 4) at the temperature 298.15 K*, J. Chem. Thermodyn. 28, **1996**, 227-232.

Pal A., Singh W. *Excess molar volumes and excess partial molar volumes of {x$C_6H_5CH_3$+ (1−x)H(CH_2)v (OCH_2CH_2)$_3$OH} (v= 1,2, and 4) at the temperature 298.15 K*, J. Chem. Thermodyn. 28, **1996**, 717-722.

Paredes M.L.L., Reis R.A., Silva A.A., Santos R.N.G., Santos G.J., Ribeiro M.H.A., Ximango P.B. *Densities, sound velocities, and refractive indexes of (tetralin + n-decane) and thermodynamic modeling by Prigogine–Flory–Patterson model*, J. Chem. Thermodyn. 45, 2012, 35–42.

Pereiro A. B., Tojo E., Rodrı´guez A., Canosa J., Tojo J. *Properties of ionic liquid HMIMPF_6 with carbonates, ketones and alkyl acetates*, J. Chem. Thermodyn. 38, **2006**, 651-661.

Pereiro A.B., Rodríguez A. *Study on the phase behaviour and thermodynamic properties of ionic liquids containing imidazolium cation with ethanol at several temperatures*, J. Chem. Thermodyn. 39, **2007**, 978-989.

Pereiro A.B., Rodríguez A. *Thermodynamic Properties of Ionic Liquids in Organic Solvents from (293.15 to303.15) K*, J. Chem. Eng. Data 52 (2), **2007**, 600–608.

Pereiro A.B., Verdía P., Tojo E., Rodríguez,A. *Physical Properties of 1-Butyl-3-methylimidazolium Methyl Sulfate as a Function of Temperature,* J. Chem. Eng. Data 52 (2), **2007**, 377–380.

Pflug H.D., Benson G.C. *Molar excess volumes of binary n-alcohol systems at 25 °C*, Canadian Journal of Chemistry, 46 (2), **1968**, 287-294.

Plechkova N.V., Seddon K.R. *Applications of ionic liquids in the chemical industry*, Chem. Soc. Rev. 37, **2008**, 123-150.

Rao Ch. J., Venkatesan K.A., Nagarajan K., Srinivasan T.G. *Dissolution of uranium oxides and electrochemical behavior of U(VI) in task specific ionic liquid*, Radiochim. Acta. 96 (7), **2008**, 403-409.

Rao Ch. J., Venkatesan K.A., Nagarajan K., Srinivasan T.G., Rao P.R.V. *Electrochemical behaviour of europium (III) in N-butyl-N-methylpyrrolidinium bis(trifluoromethylsulfonyl)imide*, Electrochim. Acta. 54 (20), **2009**, 4718-4725.

Rao Ch. J., Venkatesan K.A., Nagarajan K., Srinivasan T.G., Rao P.R.V. *Electrodeposition of metallic uranium at near ambient conditions from room temperature ionic liquid*, Journal of Nuclear Materials. 408 (1), **2011**, 25-29.

Rebelo L.P.N., Najdanovic-Visak V., Visak Z.P., Nunes da Ponte M., Szydlowski J., Cerdeiriña C.A., Troncoso J., Romaní L., Esperança J.M.S.S., Guedes H.J.R., De Sousa H.C. *A detailed thermodynamic analysis of $[BMIM]^+[BF_4]^-$ + water as a case study to model ionic liquid aqueous solutions,* Green Chem**.** 6, **2004**, 369-381.

Redhi G.G. *Thermodynamics of liquid mixtures containing carboxylic acids*, PhD thesis, UKZN, Durban, **2003**, 6-16.

Redlich O., Kister A.T. *Algebraic Representation of Thermodynamic Properties and the Classification of Solutions*, Ind. Eng. Chem. 40, **1948**, 345–348.

Ritzoulis G., Fidantsi A. *Relative Permittivities, Refractive Indices, and Densities for the Binary Mixtures N,N -Dimethylacetamide with Methanol, Ethanol, 1-Butanol, and 2-Propanol at 298.15 K*, J. Chem. Eng. Data 45 (2), **2000**, 207–209.

Rodriguez A., Canosa J., Tojo J. *Density, Refractive Index, and Speed of Sound of Binary Mixtures (Diethyl Carbonate + Alcohols) at Several Temperatures*, J. Chem. Eng. Data 46, **2001**, 1506–1515.

Seddon K.R., Stark A., Torres M.J. *Influence of chloride, water, and organic solvents on the physical properties of ionic liquids*, Pure Appl. Chem, 72, **2000**, 1391-1398.

Shao D., Lu X., Fang W., Guo Y., Xu L. *Densities and Viscosities for Binary Mixtures of the Ionic Liquid N-Ethyl Piperazinium Propionate with n-Alcohols at Several Temperatures*, J. Chem. Eng. Data **2012**.

Sibiya P.N., Deenadayalu N. *Excess molar volumes and isentropic compressibility of binary systems{trioctylmethylammonium bis(trifluoromethysulfonyl)imide + methanol or ethanol or 1-propanol} at different temperatures,* J. Chem. Thermodyn. 40, 2008, 1041-1045.

Sibiya P.N. *Excess molar volumes, Partial molar volumes and isentropic compressibilities of binary systems (ionic liquid + alkanol)*, M.Tech thesis, DUT, Durban, 2008.

Sibiya P.N., Deenadayalu N. *Excess molar volumes and partial molar volumes of binary systems (ionic liquid + methanol or ethanol or 1-propanol) at T = (298.15, 303.15 and 313.15) K*, S. Afr. J. Chem. 62, **2009,** 20-25.

Smith G.P., Dworkin A.S., Pagni R.M., Zingg S.P. *Broensted superacidity of hydrochloric acid in a liquid chloroaluminate. Aluminum chloride - 1-ethyl-3-methyl-1H-imidazolium chloride (55.O m/o AlCl3)*, J. Am. Chem. Soc. 111 (2), **1989**, 525–530.

Solanki S., Hooda N., Sharma V.K. *Topological investigations of binary mixtures containing ionic liquid 1-ethyl-3-methylimidazolium tetrafluoroborate and pyridine or isomeric picolines,* J. Chem. Thermodyn. 56, **2013**, 123–135.

Stoimenovski J., MacFarlane D.R., Bica K., Rogers R.D. *Crystalline vs. Ionic Liquid Salt Forms of Active Pharmaceutical Ingredients: A Position Paper*, Pharmaceutical Research, 27 (4), **2010,** 521-526.

Stokes R. H., Marsh K. N. *Solutions of Nonelectrolytes*, J. Chem. Thermodyn. 23, **1972**, 65-92.

Swatloski R.P., Spear S.K., Holbrey J.D., Rogers R.D. *Dissolution of Cellulose with Ionic Liquids*, J. Am. Chem. Soc. 124 (18), **2002**, 4974–4975.

Tu Chein-Hsiun, Lee Shu-Lien, Peng I-Hung. *Excess Volumes and Viscosities of Binary Mixtures of Aliphatic Alcohols (C_1−C_4) with Nitromethane*, J. Chem. Eng. Data 46 (1), **2001**, 151–155.

Vercher E., Orchillés A.V., Miguel P.J., Martínez-Andreu A. *Volumetric and Ultrasonic Studies of 1-Ethyl-3-methylimidazolium Trifluoromethanesulfonate Ionic Liquid with Methanol, Ethanol, 1-Propanol, and Water at Several Temperatures*, J. Chem. Eng. Data 52, **2007**, 1468-1482.

Vercher E., Llopis F. J., González-Alfaro M. V., Martínez-Andreu A. *Density, Speed of Sound, and Refractive Index of 1-Ethyl-3-methylimidazolium Trifluoromethanesulfonate with Acetone, Methyl Acetate, and Ethyl Acetate at temperatures from (278.15 to 328.15) K*, J. Chem. Eng. Data 55 (3), **2010**, 1377–1388.

Vercher E., Orchillés A.V., Llopis F.J., González-Alfaro V., Martínez-Andreu A. *Ultrasonic and Volumetric Properties of 1-Ethyl-3-methylimidazoliumTrifluoromethanesulfonate Ionic Liquid with 2-Propanol or Tetrahydrofuran at Several Temperatures*, J. Chem. Eng. Data 56, 2011, 4633–4642.

Walas S.M. *Phase Equilibria in Chemical Engineering*, Butterworths, Stoneham, MA, **1985.**

Walden P. *from Wikipedia,* Bull. Acad. Sci. St. Petersburg 8, **1914,** 405-422.

Weyershausenand B., Lehmann K. *Industrial application of ionic liquids as performance additives*, Green. Chem. 7, **2005,** 15–19.

Wilkes J.S., Levisky J.A., Wilson R.A., Hussey C.L. *Dialkylimidazolium chloroaluminate melts: a new class of room-temperature ionic liquids for electrochemistry, spectroscopy and synthesis*, Inorg, 21 (3), **1982**, 1263–1264.

Wilkes J.S., Zaworotko M.J. *Air and water stable 1-ethyl-3-methylimidazolium based ionic liquids*, J. Chem.Soc., Chem. Commun. **1992**, 965-967.

Wood S.E., Brusie J.P. *The Volume of Mixing and the Thermodynamic Functions of Benzene-Carbon Tetrachloride Mixture*, J. Am. Chem. Soc. 65, 1**943**, 1891.

Wu B., Reddy R.G., Rogers R.D. *Novel Ionic Liquid Thermal Storage for Solar Thermal Electric Power Systems,* Proceedings of the International Solar Energy Conference, **2001**, April 21-25.

Urzhumov, Yaroslav A.*"Sub-wavelength Electromagnetic Phenomena in Plasmonic and Polaritonic Nanostructures: from Optical Magnetism to Super-resolution*". The University of Texas at Austin (**2007**).

Yao H., Zhang S., Wang J., Zhou Q., Dong H., Zhang X. *Densities and Viscosities of the Binary Mixtures of 1-Ethyl-3-methylimidazolium Bis(trifluoromethylsulfonyl)imide withN-Methyl-2-pyrrolidone or Ethanol at T = (293.15 to 323.15) K*. J. Chem. Eng. Data **2012.**

Yu Z., Gao H., Wang H. , Chen L. *Densities, Viscosities, and Refractive Properties of the Binary Mixtures of the Amino Acid Ionic Liquid $[BMIM]^+[Ala]^-$ with Methanol or Benzylalcohol at T = (298.15 to 313.15) K*, J. Chem. Eng. Data 56 (6), **2011**, 2877-2883.

Zorębski E., Geppert-Rybczyńska M. *Thermodynamic and transport properties of (1-Butanol + 1,4-Butanediol) at temperatures from (298.15 to 318.15) K*, J. Chem. Thermodyn. 42, **2010**, 409–418.

Zafarani-Moattar M.T., Sadeghia R., Sarmad S. *Measurement and modeling of densities and sound velocities of the systems {poly(propylene glycol) + methanol, +Ethanol, +1-propanol, +2-propanol and +1-butanol} at T = 298.15 K*, J. Chem. Thermodyn. 38, **2006**, 257–263.

Zafarani-Moattar M.T., Shekaari H. *Volumetric and Speed of Sound of Ionic Liquid, 1-Butyl-3-methylimidazolium Hexafluorophosphate with Acetonitrile and Methanol at T = (298.15 to 318.15) K*, J. Chem. Eng. Data 50, **2005**, 1694-1699.

Zafarani-Moattar M.T., Shekaari H. *Application of Prigogine–Flory–Patterson theory to excess molar volume and speed of sound of 1-n-butyl-3-methylimidazolium hexafluorophosphate or 1-n-butyl-3-methylimidazolium tetrafluoroborate in methanol and acetonitrile,* J. Chem. Thermodyn. 38, **2006**, 1377-1384.

Zafarani-Moattar M.T., Majdan-Cegincara R. *Viscosity, Density, Speed of Sound, and Refractive Index of Binary Mixtures of Organic Solvent + Ionic Liquid, 1-Butyl-3-methylimidazolium Hexafluorophosphate at 298.15 K*, J. Chem. Eng. Data 52 (6), **2007**, 2359–2364.

Zhong Y., Wang H., Diao K. *Densities and excess volumes of binary mixtures of the ionic liquid1-butyl-3-methylimidazolium hexafluorophosphate with aromatic compound at T = (298.15 to 313.15) K*, J. Chem. Thermodyn. 39, **2007,** 291-296.

Zorębski E., Deć E. *Speeds of sound and isentropic compressibilities for binary mixtures of 1,2-ethanediol with 1-butanol, 1-hexanol, or 1-octanol in the temperature range from 293.15 to 313.15 K*, J. Mol. Liq. 168, **2012**, 61–68.

APPENDIX

Article Published:

Densities, speeds of sound, and refractive indices for binary mixtures of 1-butyl-3-methylimidazolium methyl sulphate ionic liquid with alcohols at T = (298.15, 303.15, 308.15, and 313.15) K. *J. Chemical Thermodynamics,* **2013,** 57, 238-247.

Sangeeta Singh, Martin Aznar and Nirmala Deenadayalu.